Report DOT-HS-031-2-419

DUMMY HEAD MECHANICAL IMPEDANCE TESTS

Prepared for:
National Highway Traffic Safety Administration
U.S. Department of Transportation
Nassif Building, 7th and E Streets, S.W.
Washington, D.C. 20590

Final Report for Period:
31 May 1972 - 13 August 1972

13 August 1972

Richard L. Stalnaker
James H. McElhaney

Highway Safety Research Institute
The University of Michigan
Ann Arbor, Michigan 48105

1. Report No.	2. Government Accession No.	3. Recipient's Catalog No.

4. Title and Subtitle	5. Report Date
Dummy Head Mechanical Impedance Tests	13 August 1972
	6. Performing Organization Code
7. Author(s) R. L. Stalnaker and J. H. McElhaney	8. Performing Organization Report No. Bio-M-24
9. Performing Organization Name and Address Highway Safety Research Institute The University of Michigan Huron Parkway and Baxter Road Ann Arbor, Michigan 48105	10. Work Unit No.
	11. Contract or Grant No. DOT-HS-031-2-419
12. Sponsoring Agency Name and Address National Highway Traffic Safety Administration U.S. Department of Transportation Nassif Building, 7th and E Streets, S.W. Washington, D.C. 20590	13. Type of Report and Period Covered Final Report 31 May 1972 - 13 August 1972
	14. Sponsoring Agency Code

15. Supplementary Notes

16. Abstract

Specifications are being developed for anthropomorphic dummies to be used in testing motor vehicles and equipment for compliance with the various motor vehicle safety standards. It is highly desirable that the dummy respond, in a realistic, human-like fashion in vehicle crash test. The purpose of this testing program was to determine the mechanical impedance characteristics of a number of developmental dummy heads and to correlate the data with existing mechanical impedance data for human cadaver heads.

Four dummy heads were mounted on an electromagnetic shaker and properly instrumented to obtain the following information over a frequency range of 30-5000 Hz:

a. Driving point impedance (DPI) and acceleration at each of the following points.
   1. forehead
   2. side of the head
   3. back of the head
b. Transfer point impedance (TPI) and acceleration at the center of gravity (CG) of the head and at a point on the skull, opposite the driving point.

The mechanical impedance and acceleration were recorded at 11 locations on each head. The DPI of each dummy head in each direction was compared to the DPI of fresh unembalmed cadavers tested in a similar manner.

17. Key Words	18. Distribution Statement

19. Security Classif.(of this report)	20. Security Classif.(of this page)	21. No. of Pages	22. Price

Form DOT F 1700.7 (8-69)

TABLE OF CONTENTS

LEGEND

LEGEND (Cont'd.)

LEGEND (Cont'd.)

Figure A-40 DHMZ-3 T.P.I. at Point Opposite D.P., Driving Point - Frontal

Figure A-41 DHMZ-3 Acceleration at Point Opposite D.P., Driving Point - Frontal

Figure A-42 DHMZ-3 D.P.I. - Occipital

Figure A-43 DHMZ-3 T.P.I. at C.G., Driving Point - Occipital

Figure A-44 DHMZ-3 Acceleration at C.G., Driving Point - Occipital

Figure A-45 DHMZ-3 T.P.I. at Point Opposite D.P., Driving Point - Occipital

Figure A-46 DHMZ-3 Acceleration at Point Opposite D.P., Driving Point - Occipital

Figure A-47 DHMZ-3 D.P.I. - Parietal

Figure A-48 DHMZ-3 T.P.I. at C.G., Driving Point - Parietal

Figure A-49 DHMZ-3 Acceleration at C.G., Driving Point - Parietal

Figure A-50 DHMZ-3 T.P.I. at Point Opposite D.P., Driving Point - Parietal

Figure A-51 DHMZ-3 Acceleration at Point Opposite D.P., Driving Point - Parietal

Figure A-52 DHMZ-4 D.P.I. - Frontal (Acceleration at D.P. - 5 g's)

Figure A-53 DHMZ-4 D.P.I. - Frontal (Acceleration at D.P. - 10 g's)

Figure A-54 DHMZ-4 D.P.I. - Frontal (Acceleration at D.P. - 20 g's)

Figure A-55 DHMZ-4 T.P.I. at C.G., Driving Point - Frontal

Figure A-56 DHMZ-4 Acceleration at C.G., Driving Point - Frontal

Figure A-57 DHMZ-4 T.P.I. at Point Opposite D.P., Driving Point - Frontal

Figure A-58 DHMZ-4 Acceleration at Point Opposite D.P. Driving Point - Frontal

Figure A-59 DHMZ-4 D.P.I. - Occipital

Figure A-60 DHMZ-4 T.P.I. at C.G., Driving Point - Occipital

Figure A-61 DHMZ-4 Acceleration at C.G., Driving Point - Occipital

Figure A-62 DHMZ-4 T.P.I. at Point Opposite D.P., Driving Point - Occipital

Figure A-63 DHMZ-4 Acceleration at Point Opposite D.P., Driving Point - Occipital

Figure A-64 DHMZ-4 D.P.I. - Parietal

LEGEND (Cont'd.)

NOMENCLATURE

a = acceleration, in/sec^2

c = damping constant, lb-sec/in.

f = force, lb.

i = $\sqrt{-1}$

k = spring constant, lb/in.

m = mass, slugs

t = time, sec.

v = velocity, in/sec.

x = displacement, in.

z = mechanical impedance, lb-sec/in.

Φ = phase angle, degree

ω = frequency, radians/sec.

ω_n = undamped natural frequency, radians/sec.

Subscripts

k - reference to spring

c - reference to damping

m - reference to mass

o - peak value of sine wave

ACKNOWLEDGMENT

This research program was carried out by the staff of the Biosciences Division of the Highway Safety Research Institute, The University of Michigan. The authors would like to thank Mr. Stan Backaitis for his suggestions, co-operation and support. We also would like to thank Messrs. Dinesh Mohan, Glenn Myers and Steven Fisher for their efforts and time in the preparation of all the graphs and figures in this report.

1. INTRODUCTION

In analyzing various sled and car crash data, it has become apparent that a serious problem exists in terms of test reproducibility. It is axiomatic in the experimental sciences that a valid test must yield reproducible results, and do so in more than one laboratory. Careful consideration of the elements of these sled and car crash tests identified the crash dummy as a major contributor to the difficulties in test repeatability. The accelerometers mounted in the head of current model dummies measure not only the gross whole-body motion, but also react to both local deformation and internal component interactions. Thus, the head accelerometers respond to the vibration of the lightly-damped cast aluminum head. To document these effects in the head, the driving-point impedance, transfer-point impedance, and acceleration frequency response of dummy heads were compared. The impedance was chosen as the appropriate dynamic test because on one plot of the results, the change in effective mass, stiffness, and damping can be shown as they vary with frequency (in this case from 30-5000 hertz). Additionally, the location of the resonance and antiresonance frequencies may be determined from the same data. The response of the head to the compliance test conditions will depend upon the characteristics of these impedance properties.

2. METHODS

The response of a system to a sinusoidally varying force depends on the instantaneous values of the mass, stiffness, and damping. The response may be described in terms of displacement, velocity, or acceleration, but a description in terms of mechanical impedance (the ratio of applied force to velocity, pounds-seconds per inch [lb-sec/in]) offers several advantages.[1,2]

A body exhibiting high impedance brings to mind massiveness, stiffness, and small motion; conversely, low impedance suggests lightness, springness, and large motion. Such qualitative statements are, however, apt to be misleading. The correct view may be formed only by considering the quantitative relationship with frequency. As the frequency with which the energy is impressed changes, there is a change of both magnitude and phase of the resulting motion. The resistive and reactive components of impedance are complicated functions of frequency and they tend to alternate in their dominance of the system response. This latter action leads to an apparent change of weight, the system responding alternatively as a mass or as a spring as the frequency is varied through the resonances and antiresonances. This type of response leads in turn to a great change in the degree of isolation for the components within the system and is, therefore, of importance in determining the lumped parameters of a "Black Box System."[3,4]

If a linear mechanical system is harmonically excited by a force

$$f = |f_o| e^{i\omega t} \tag{1}$$

which results in a velocity response

$$v = |v_o| e^{i(\omega t - \phi)} \tag{2}$$

where ϕ is the phase angle between the velocity and force (with the force as the reference), the driving-point mechanical impedance (DPI) based on

the force and velocity (measured at the point of force application) is

$$z = \frac{|f_o|e^{i\omega t}}{|v_o|e^{i(\omega t-\phi)}} \tag{3}$$

$$z = \frac{|f_o|}{|v_o|}e^{i\phi} \tag{4}$$

$$z = |z_o|e^{i\phi} \tag{5}$$

The ratio of the driving force to the velocity at another point in the system may be expressed as the transfer-point impedance (TPI).

There are several methods available for determining impedance analytically. The use of the Laplace Transform is perhaps the most powerful method. An operational method developed by Firestone[5] for analyzing lumped-parameter systems is also useful in many cases. This technique will be presented briefly.

The impedance for the three simple elements- spring, dash-pot, and mass - will be obtained. These elements will be combined to form a simple system, and driving-point impedance expression for this system will be obtained. We know from harmonic motion

$$v = i\omega x \tag{6}$$

$$a = i\omega v \tag{7}$$

Now consider a simple spring. By definition the spring constant k is

FIGURE 1. PURE SPRING

$$k = \frac{f}{x} \tag{8}$$

Subsituting for x in terms of velocity

$$k = \frac{f\omega i}{v} \tag{9}$$

The impedance z_k looking into a weightless spring restrained at the opposite end is

$$z_k = \frac{f}{v} = \frac{k}{i\omega} - i\frac{k}{\omega} \tag{10}$$

Spring impedance decreases as frequency increases, and the force vector leads the velocity vector by 90 degrees.

By definition the damping constant c for a viscous damper is

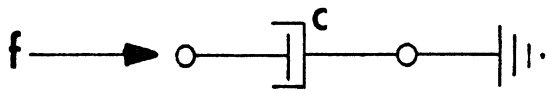

FIGURE 2. PURE DAMPER

$$c = \frac{f}{v} \tag{11}$$

The impedance z_c of a weightless viscous damper attached at the opposite end is

$$z_c = \frac{f}{v} = c \tag{12}$$

Damper impedance is independent of frequency, and force is in phase with velocity.

The impedance of a simple mass can be found from Newton's Third Law,

FIGURE 3. PURE MASS

$$f = ma \tag{13}$$

Substituting for a in terms of v

$$f = mi\omega v \tag{14}$$

The impedance z_m of a free mass is

$$z_m = \frac{f}{v} = i\omega m \tag{15}$$

Mass impedance increases as frequency increases, and the force vector lags the velocity vector by 90 degrees.

The impedances of the three ideal elements (mass, spring, and damper) are functions of frequency. It is convenient to plot impedance data on graph

paper with Logarithmic impedance and frequency scales. The individual ideal elements (mass, spring, and damper) are plotted on log-log paper in Figure 4.

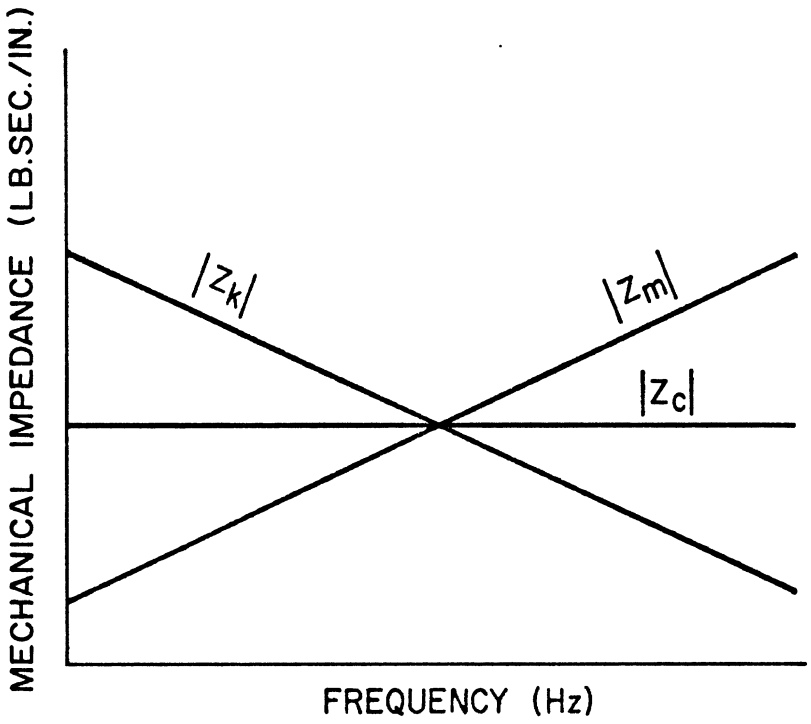

FIGURE 4. PLOT OF IDEAL ELEMENTS ON LOG-LOG PAPER.

The mechanical impedance and acceleration were measured at four separate locations on four dummy heads furnished by the government. These four dummy heads were assigned test numbers, and are shown in Figure 5.

The location of each driving point was specified in the following manner.

1. Forehead - Two inches below the top of the skull in the midsaggital plane.
2. Back of Head - Two inches below the top of the skull in the midsaggital plane.

Old Alderson Head

DHMZ-1

New Alderson Head

DHMZ-2

Old Sierra Head

DHMZ-3

New Sierra Head

DHMZ-4

FIGURE 5. HEADS USED IN MECHANICAL IMPEDANCE TEST.

3. Side of Head - Three inches below the top of the skull and 4.25 inches forward of the back of the skull.

The vibrational characteristics measured on each head were:

Phase 1. Driving-point impedance and acceleration at each driving point.

Phase 2. Transfer-point impedance and acceleration at the center of gravity in the direction of the sinusoidal input.

Phase 3. Transfer-point impedance and acceleration at a point opposite to the driving point.

Phase 4. Driving-point impedance at two different acceleration inputs than used for Phases 1 through 3.

The skin was removed from each head and the skull blocked up on a milling machine, with the neck plate used as a base. All driving points and accelerometer mounting points on the skull were laid out and milled to provide flat surfaces parallel to, or perpendicular to, the medial plane. This was to insure that loading occurred along the appropriate axis. Holes were drilled perpendicular to these surfaces to allow the accelerometer or loading fixture to be bolted on.

A rigid, specially designed mounting block was fabricated to fasten the accelerometers to the neck plate and to locate them at the center of gravity of the head. This device allowed the accelerometers to be directed along the appropriate axes.

The skin was replaced and the accelerometers mounted, with particular care taken to align the accelerometers at the center of gravity as given in SAE Recommended Practice J963. The head was weighed and the location of the C.G. measured. Weight was added to the head until it weighed 10.2 lb. A one-pound weight was mounted where the neck fastens to the skull and the

ballast weight was moved around until the CG was in accordance with J963. The one-pound neck weight was removed and the head was then mounted on a GM rubber neck. This head and neck system was then fastened to a Sierra 50th percentile dummy. All heads were set-up and tested in this configuration.

The tests were carried out on a 300-pound Model 20 Unholtz-Dickie electromagnetic shaker. The shaker was automatically controlled by a Spectral Dynamics Model 105B amplitude servo/monitor, at a constant 5 G's peak for the standard runs and 10 and 20 G's peak respectively for Phase 4. The frequency range investigated for all tests was 30-5000 hertz.

A Spectral Dynamics, automatic mechanical impedance analyzer system was used for all recording. This impedance computer coupled with a X-Y-Y' plotter converted the force-time and acceleration-time information into phase and impedance versus frequency plots as well as acceleration frequency plots (Figure 6). The mechanical impedance-measuring head used in these tests was made up of an Unholtz-Dickie Model 75D21 accelerometer, flat to 5000 hertz and capable of resolving a fraction of a G, and a Kistler Model 904A load washer which is flat to 50,000 hertz and will resolve 0.05 pounds. This impedance head and the head connector were calibrated and found to have a mass-like impedance over the frequency range of interest. The Unholtz-Dickie Model 75D21 was also used to measure all of the remote accelerations.

These tests were carried out in the following manner. The dummy with the test head mounted was strapped to an adjustable table. The dummy head was then rigidly fastened to the shaker at the forehead attachment point. The driving point impedance was recorded for three constant input accelerations: 5, 10, and 20 G's peak. The transfer point impedance and acceleration at the center of gravity and at the point opposite the driving point

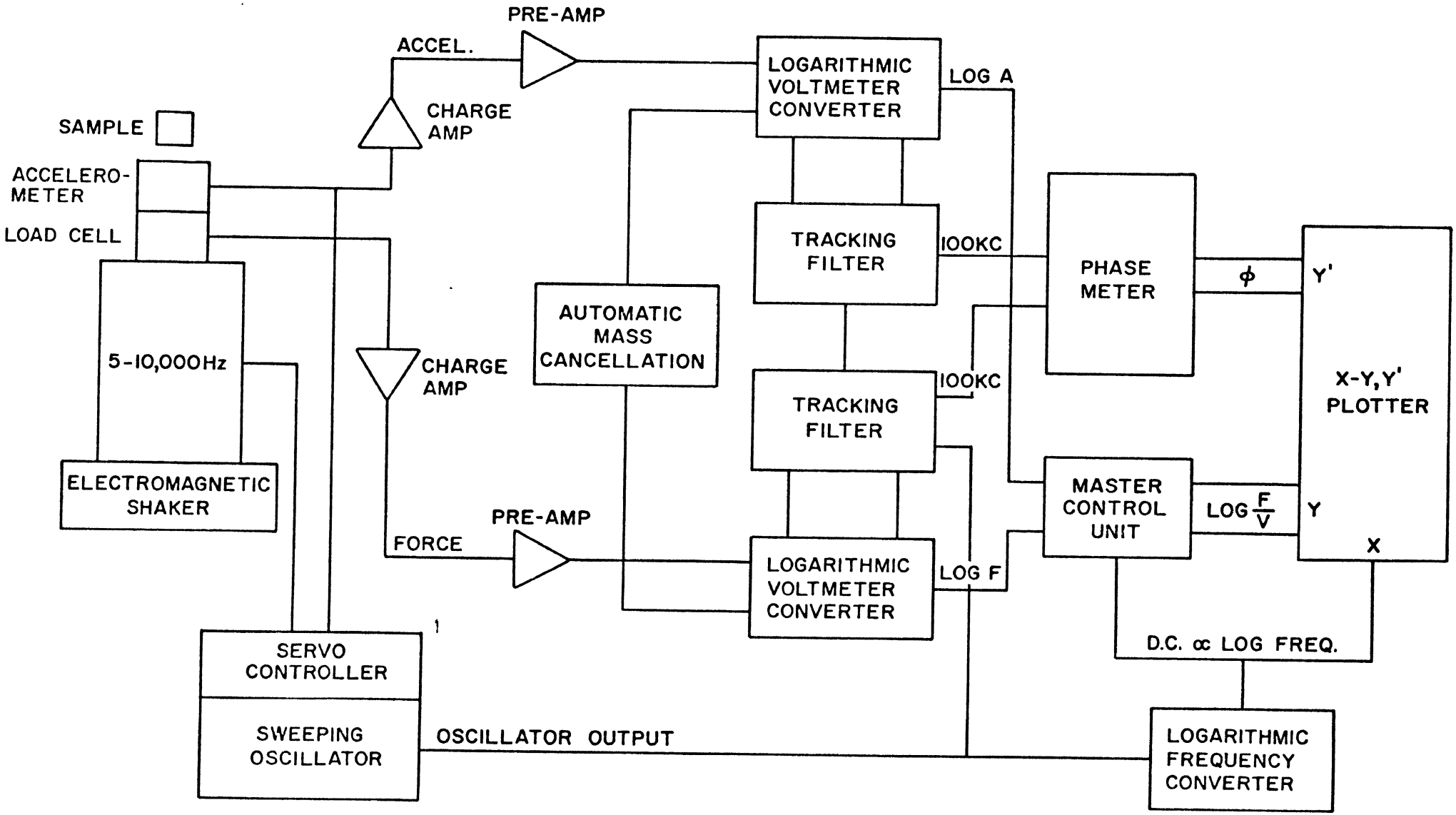

FIGURE 6. AUTOMATIC IMPEDANCE MEASURING SYSTEM.

were then recorded. All of the transfer point impedances were made with a constant input of 5 G's peak at the driving point. The forehead attachment was then disconnected from the shaker and the head turned and reconnected to the side attachment point. The DPI was recorded as well as the TPI and acceleration at the CG and at the point opposite the driver point for a 5 G peak driving-point input. This same procedure was repeated for the back of the head. Each dummy head was tested in this same manner. (Figure 7).

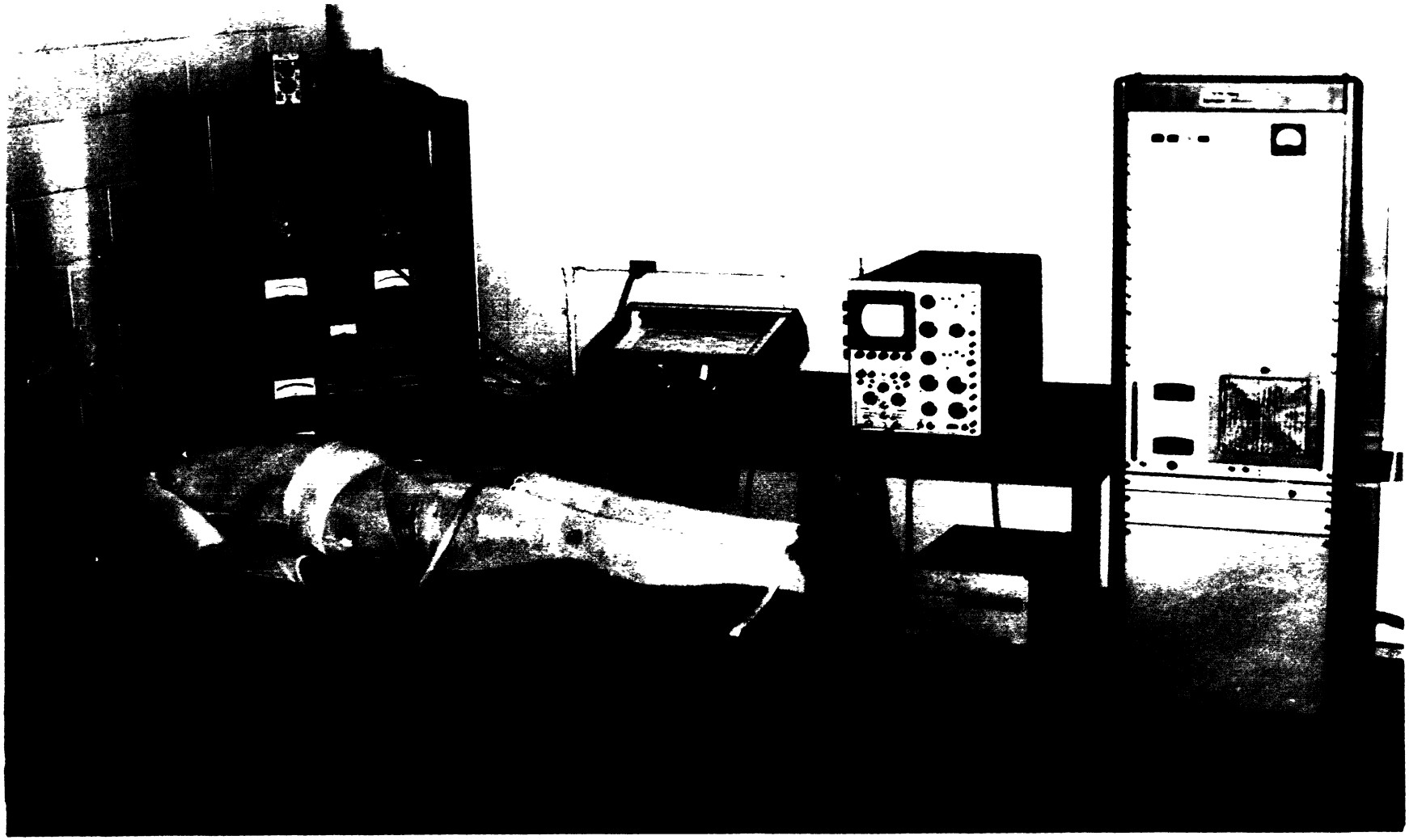

FIGURE 7. MECHANICAL IMPEDANCE TEST SET-UP.

3. RESULTS

The mechanical impedance and acceleration (as functions of frequency) of the dummy heads are given in Appendix A. Curves are presented for each driving point and for each accelerometer position. Each dummy head was exposed to 5, 10 and 20 G's peak input at the forehead. There was no dependency evident between the input acceleration level and driving-point mechanical impedance up to an acceleration level of 20 G's.

The driving-point mechanical impedance of each dummy head is compared to the driving-point mechanical impedance of fresh cadaver heads (with bodies attached) tested in a similar manner. The results of these comparisons are listed on Table 1 and shown in Figures 8, 9 and 10. All of the dummy heads were found to be very much stiffer than the human head, resulting in much higher resonant frequency in the dummy heads. The damping was considerably higher in the cadaver than in the dummy heads, except for the new Alderson head (DHMZ-2). The small resonance spike at approximately 50 hertz is the resonance effect of the head-neck-body system. The many spurious high frequency resonances are due to the head ballast weights, the occiput plate, and the head-neck coupling mechanism. To further ascertain the origin of the spurious resonances' spikes, the dummy heads were stripped to the skull, and the driving-point impedance again determined for the front of the head. The results of these tests are shown in Figure 11. These tests show that the metal heads have many more resonances and antiresonances than do the wooden (DHMZ-4) and the ceramic (DHMZ-2) heads.

The transfer-point impedance for the opposite side of the head will in general not exhibit an antiresonance before the first resonance (i.e., at a frequency below that of the lowest resonance frequency). This is due to the

TABLE 1. HEAD IMPEDANCE TEST SUMMARY

Test	Driving Point				Center of Gravity				Point Opposite D.P.		Comments
	Resonance*		Antiresonance		Resonance		Antiresonance		Resonance		
	Freq Hz	Imped lb/in/sec	Freq Hz	Imped lb/in/sec	Freq Hz	Imped lb/in/sec	Freq Hz	Imped lb/in/sec	Freq Hz	Imped lb/in/sec	
DHMZ-1:											
Frontal	3200	3.5	950	1250	3200	20.0	-	-	3200	10.0	Large antiresonance peak at C.G. after head resonance.
Parietal	3000	5.0	670	900	3000	5.0	1500	1800	2100	70.0	
Occipital	2300	5.0	670	450	2300	4.5	1800	900	2300	35.0	Two equal antiresonance peaks at 500 and 670 Hz at D.P.
DHMZ-2:											
Frontal	1750	8.0	800	120	1600	10.0	-	-	1650	25.0	
Parietal	1500	3.0	380	100	1900	7.0	1350	800	1500	19.0	
Occipital	550	16.0	300	48	-	-	-	-	-	-	No major identifiable resonance or antiresonance at C.G.
DHMZ-3:											
Frontal	2900	7.5	730	600	1150	16.0	-	-	2800	11.0	
Parietal	1750	2.0	450	750	1600	2.0	-	-	1650	8.0	
Occipital	2600	10.0	775	460	1100	14.0	-	-	2500	50.0	Three antiresonance peaks before resonance.
DHMZ-4:											
Frontal	1650	2.7	450	360	1250	11.0	-	-	1650	6.5	Large antiresonance peak at C.G. after head resonance.
Parietal	1650	3.4	470	300	1350	20.0	-	-	1650	20.0	
Occipital	1200	3.8	410	250	1200	7.5	-	-	1200	11.0	
Human†											
Frontal	820	2.7	320	70	-	-	-	-	-	-	
Parietal	770	2.2	240	30	-	-	-	-	-	-	
Occipital	600	4.8	230	55	-	-	-	-	-	-	

*All values are for the first resonance and antiresonance
†Values are means from a band of data

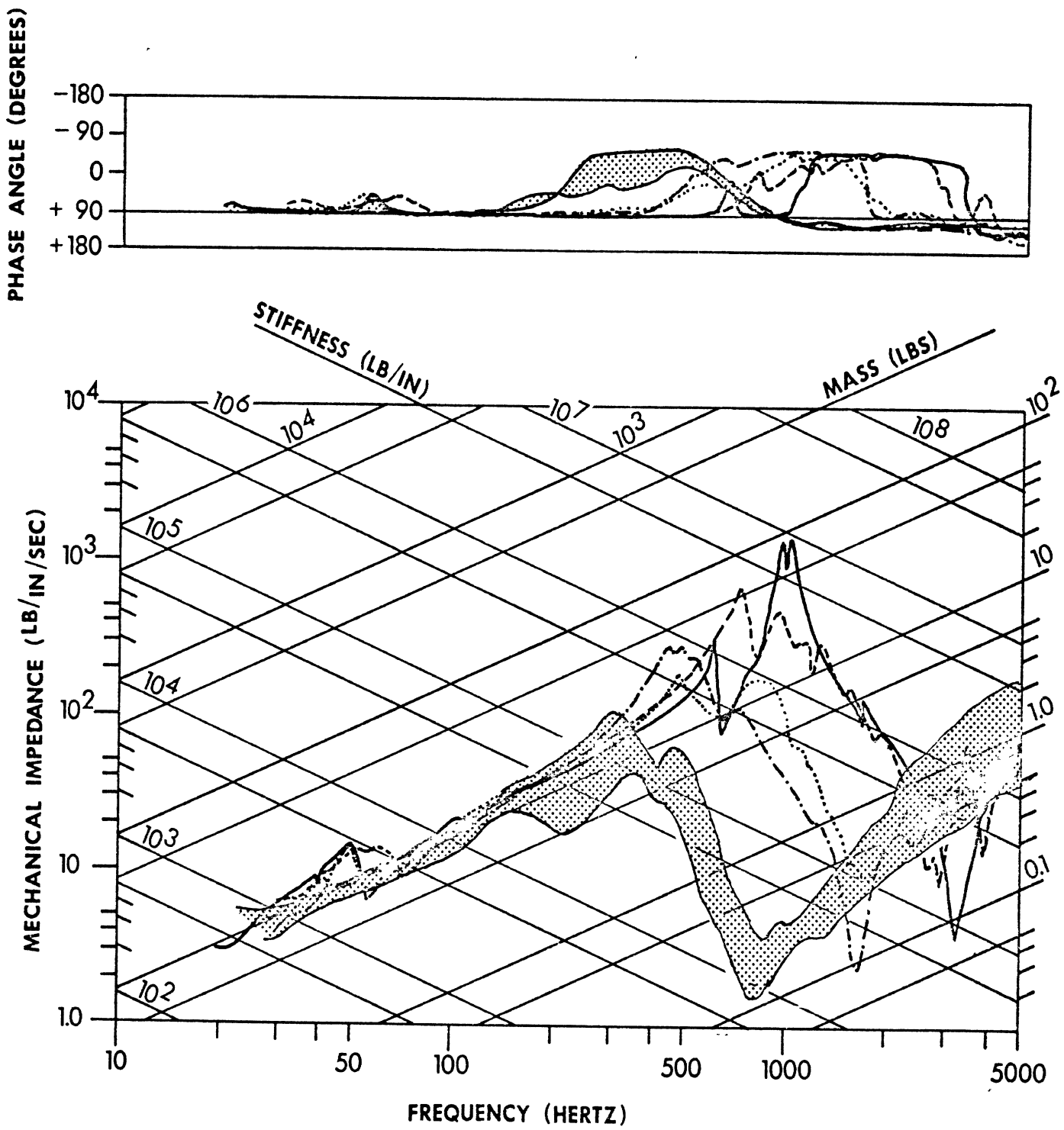

Mechanical Impedance of Heads — Frontal

Figure 8.

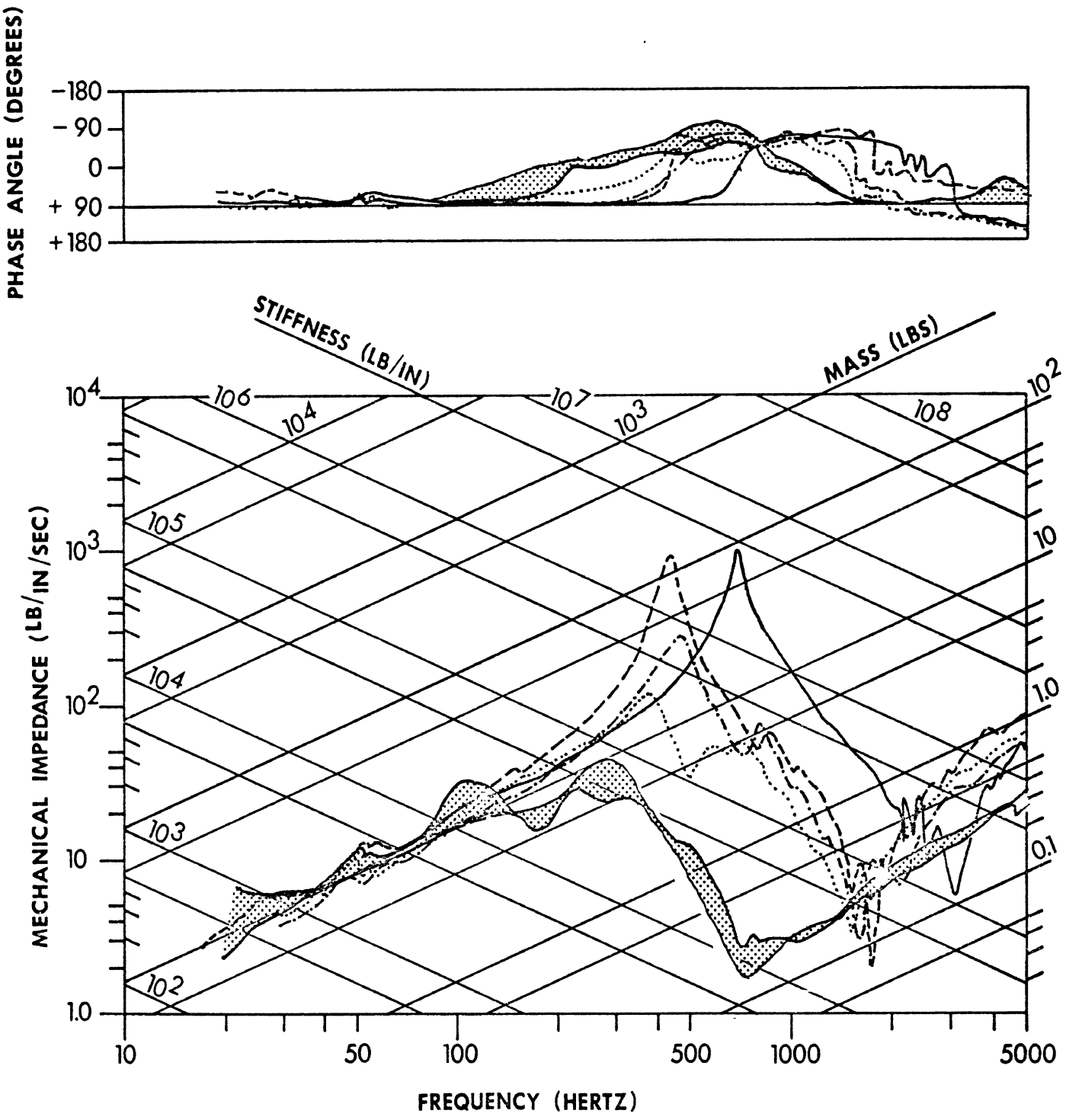

Mechanical Impedance of Heads — Parietal

Figure 9.

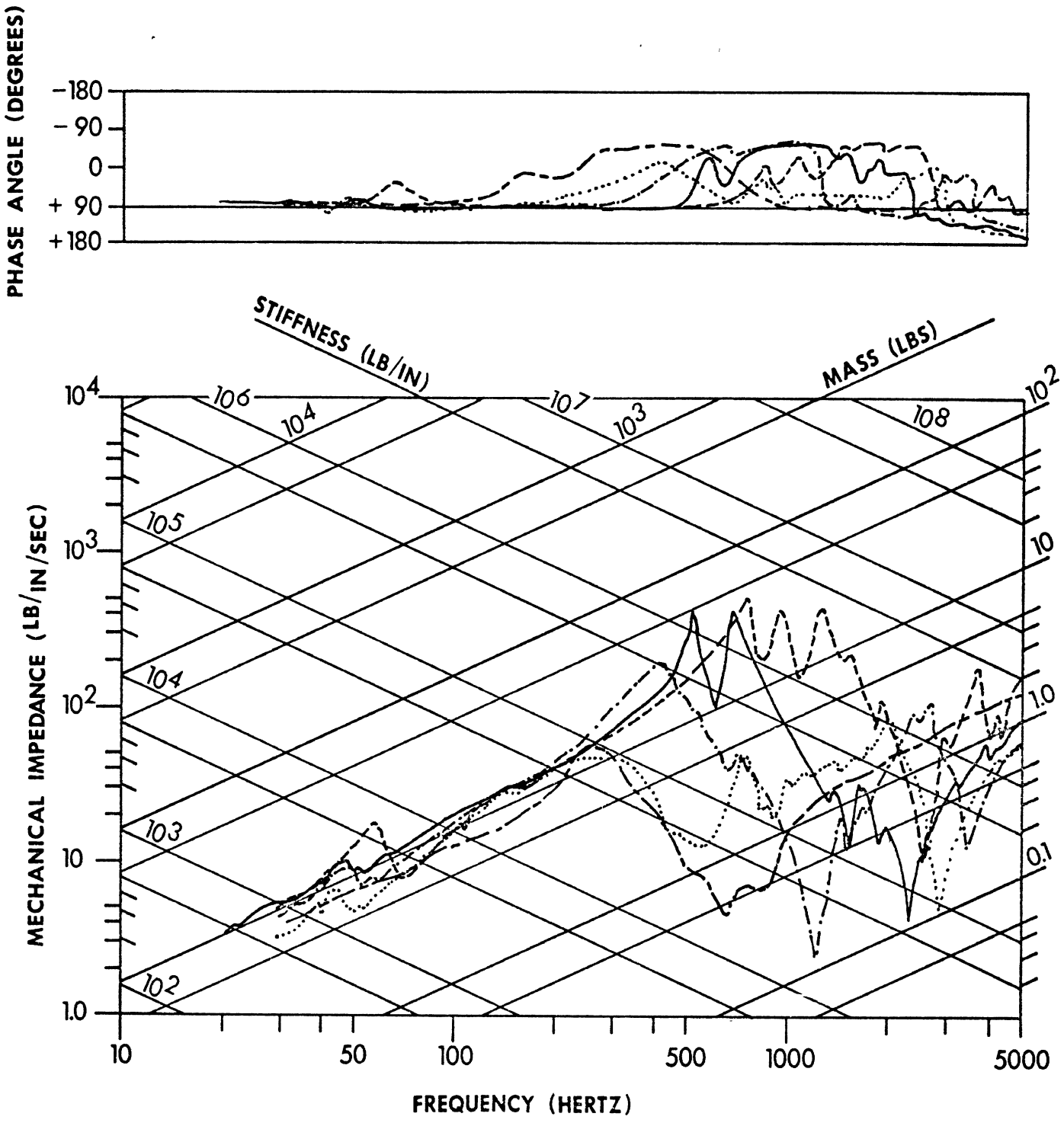

Mechanical Impedance of Heads — Occipital

Figure 10.

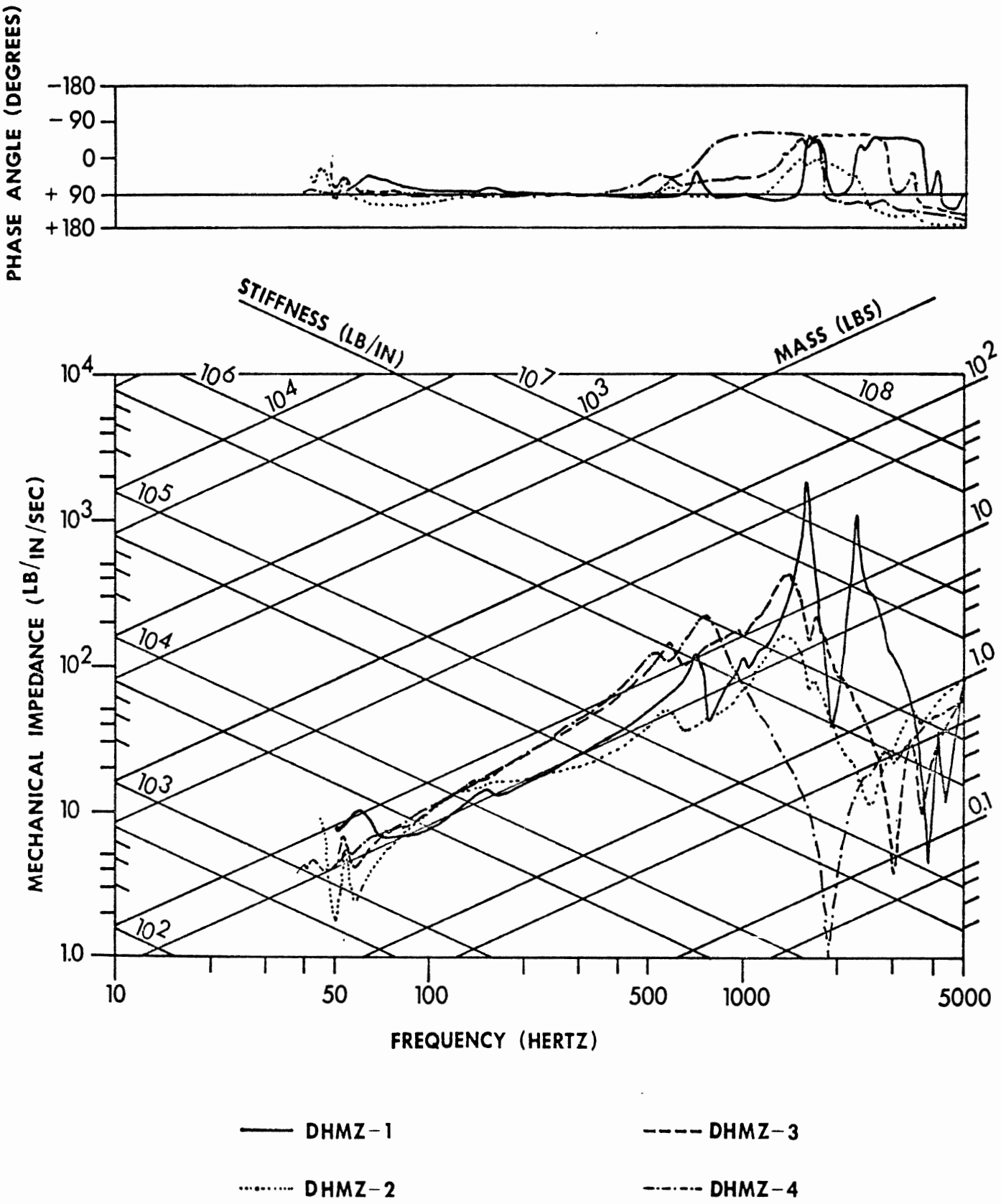

Mechanical Impedance of Dummy Heads Only — Frontal

Figure 11.

phase relationship between the velocity of the skull at the transfer point and the force at that driving point. The force is in phase with the velocity and therefore the impedance will not reflect the increase in force that is recorded by the DPI. Any antiresonances before the skull resonances at the opposite side will have been caused by other parts of the dummy head system being excited.

The transfer-point impedance for the CG can be of any form depending upon how and where the accelerometer is mounted to the skull. The CG was approximately 1.5 to 2.5 inches from the driving point so that some angular motion as well as linear motion was recorded by the transfer accelerometer. For these tests the neck and the accelerometers were fastened to the same plate in the head. Mounting the accelerometers in this fashion allowed the body motion to be monitored, resulting from head-neck-body coupling.

4. CONCLUSIONS

The mechanical impedance approach to analyzing the frequency response of a structure was found to work very well in the dummy heads. The apparent mass, stiffness, and damping of each dummy head (as a function of frequency) were clearly evident and their values were found to be repeatable. The values of these parameters for each dummy head were compared to those of the cadaver and to one another. The conclusions from these tests and comparisons are given below:

1. All dummy heads were found to be linear in the acceleration range of 5 to 20 G's peak.
2. All of the dummy heads except one were damped less than the cadaver heads. DHMZ-2 (new Alderson head) appeared to have approximately the same damping as the human head.
3. All of the dummy heads were stiffer than the human head by approximately an order of magnitude.
4. Each head behaved as a multi-degree of freedom system because of the ballast weights, skull cap, types of bolt fasteners, and the shape of the head.
5. Mounting the accelerometers to the plate where the dummy's head and neck were joined resulted in acceleration readings which included effects of the head-neck system, as well as effects of the head alone.

5. REFERENCES

1. Roberts, V. L., V. R. Hodgson and L. M. Thomas "Fluid Pressure Gradients Caused by Impact to the Human Skull," ASME 66-HUF-1, 1966.

2. Chenea, P. E. "On the Application of the Impedance Method to Continuous Systems," J. Applied Mechanics, 1953.

3. Churcia, A. H. "Mobility and Impedance Concepts," J. Machine Design, 1960.

4. Franke, E. K. "Mechanical Impedance Measurements of the Human Body Surface," USAF Technical Report No. 6469, 1951.

5. Harris, C. M. and C. E. Crede "Shock Vibration Handbook," McGraw-Hill Book Company, Inc., New York, Vol. 1, Chapter 25, 1961.

APPENDIX A

TEST RESULTS

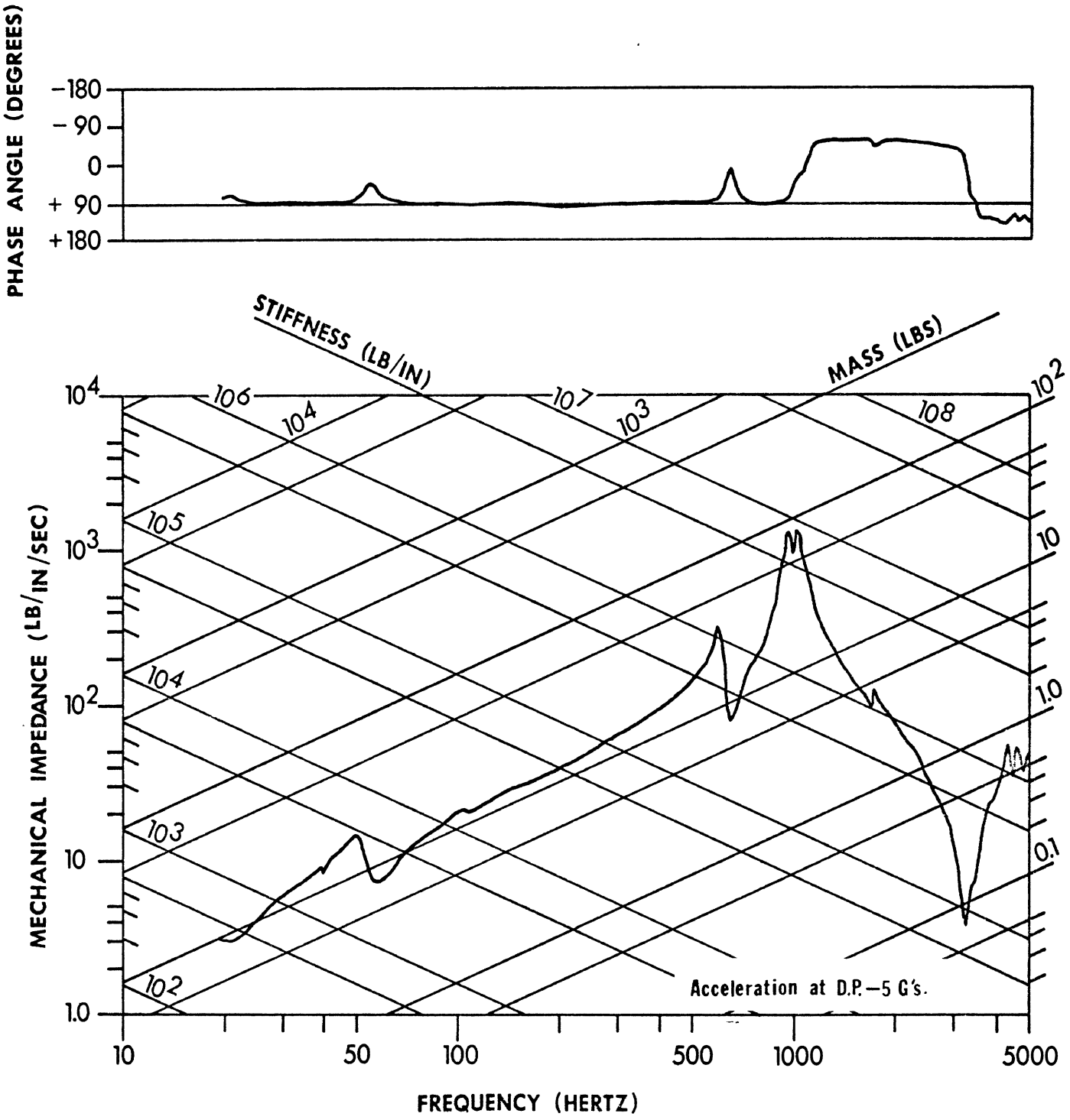

DRIVING POINT:	FRONTAL ☒	D.P.I.	☒
	OCCIPITAL ☐	T.P.I. (CENTER OF GRAVITY)	☐
	PARIETAL ☐	T.P.I. (POINT OPPOSITE D.P.)	☐

Test DHMZ-1 Dummy Head Mechanical Impedance

Figure A-1

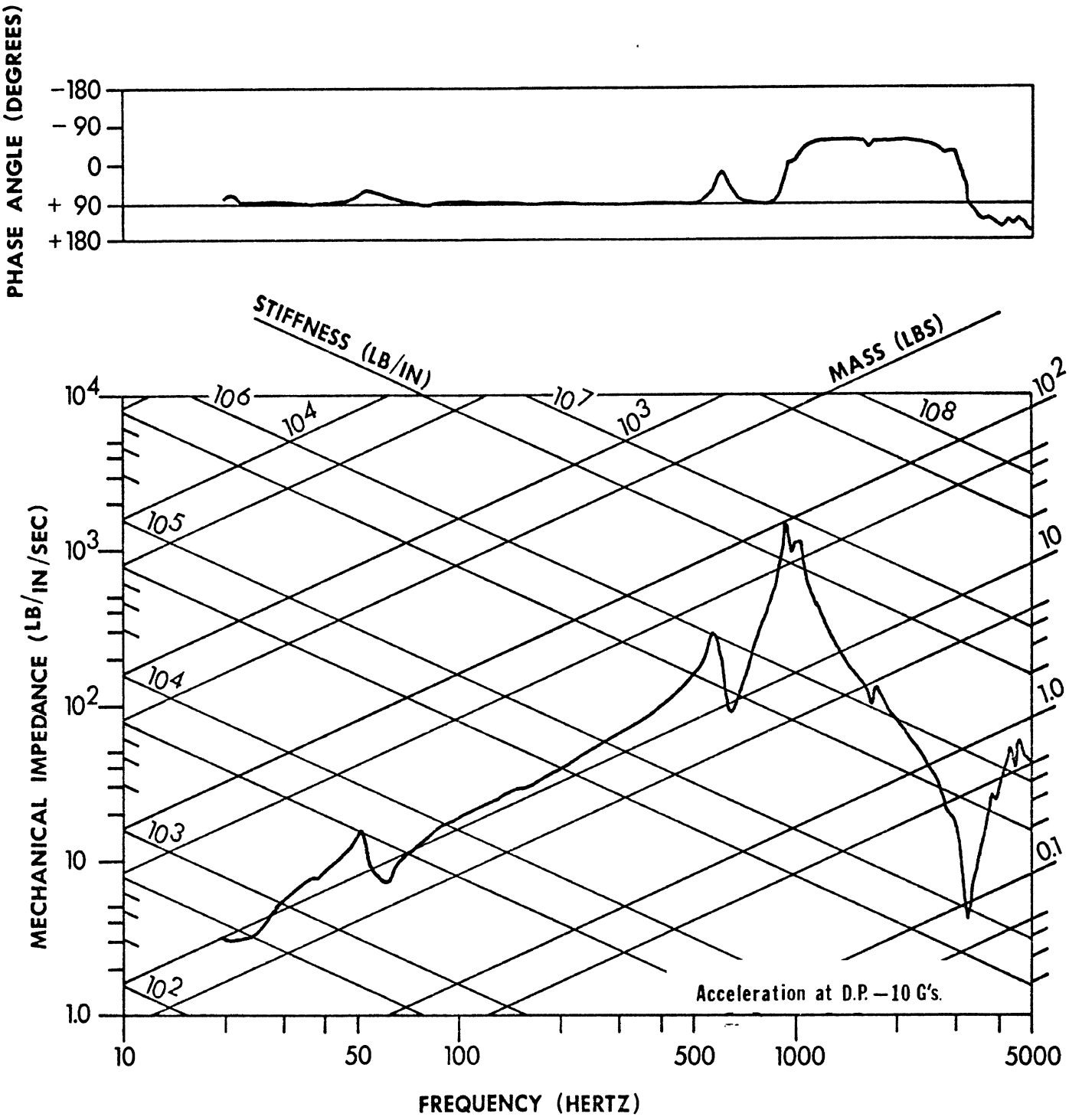

DRIVING POINT:	FRONTAL	☒	D.P.I.	☒
	OCCIPITAL	☐	T.P.I. (CENTER OF GRAVITY)	☐
	PARIETAL	☐	T.P.I. (POINT OPPOSITE D.P.)	☐

Test DHMZ-1 Dummy Head Mechanical Impedance

Figure A-2

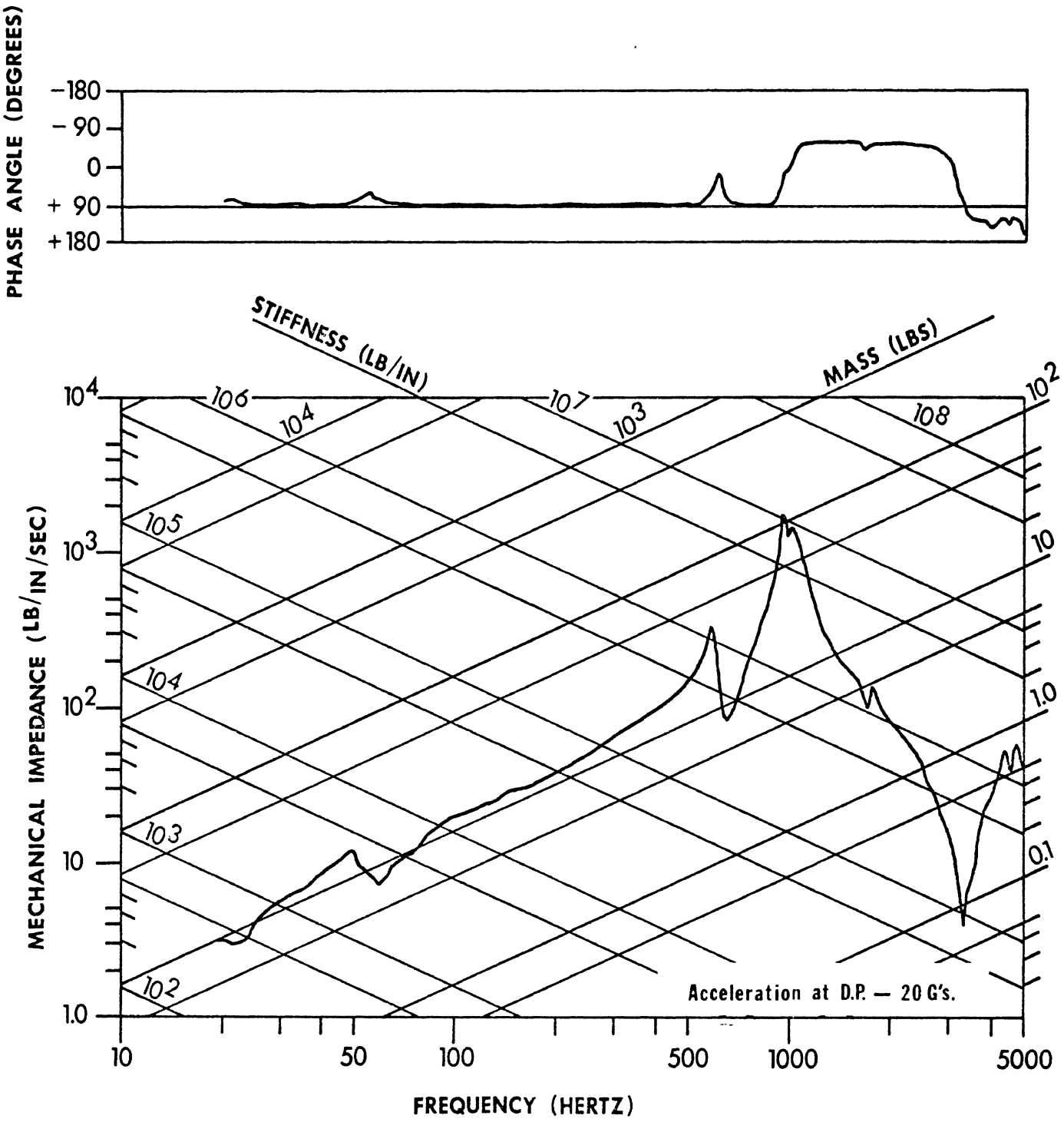

DRIVING POINT: FRONTAL ☒ D.P.I. ☒

OCCIPITAL ☐ T.P.I. (CENTER OF GRAVITY) ☐

PARIETAL ☐ T.P.I. (POINT OPPOSITE D.P.) ☐

Test DHMZ-1 Dummy Head Mechanical Impedance

Figure A-3

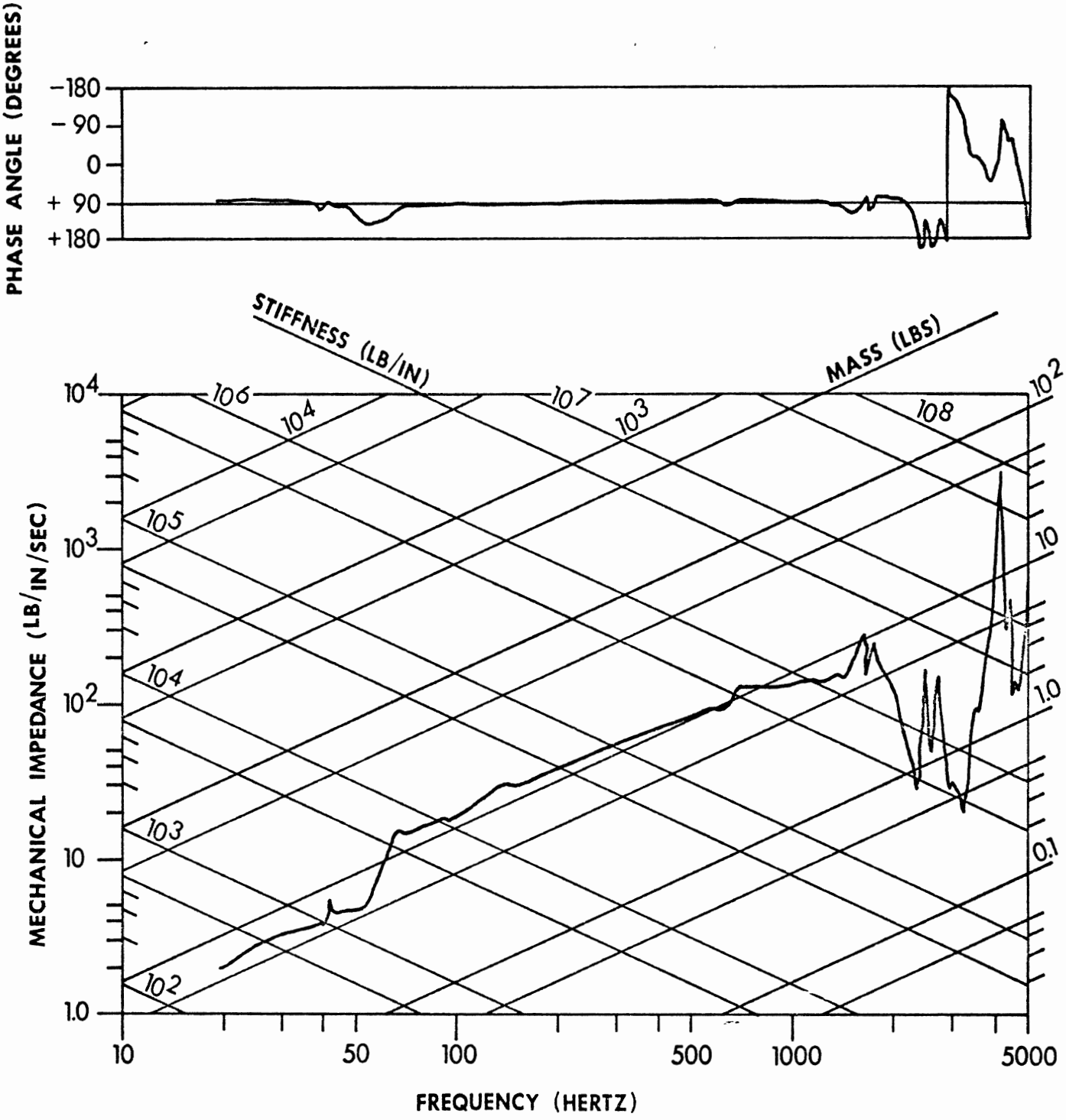

DRIVING POINT: FRONTAL ☒ D.P.I. ☐

OCCIPITAL ☐ T.P.I. (CENTER OF GRAVITY) ☒

PARIETAL ☐ T.P.I. (POINT OPPOSITE D.P.) ☐

Test DHMZ-1 Dummy Head Mechanical Impedance

Figure A-4

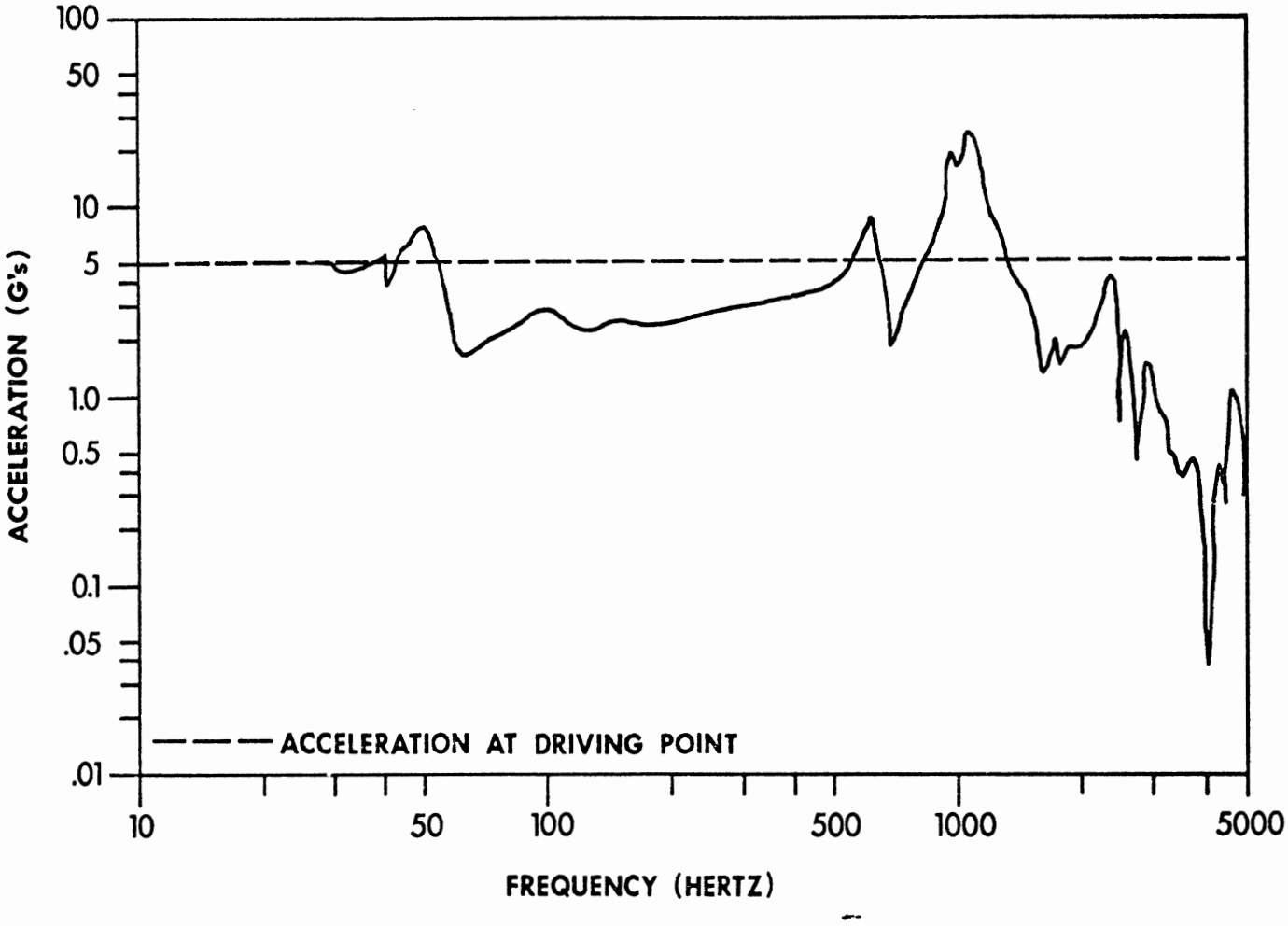

DRIVING POINT: FRONTAL ☒
OCCIPITAL ☐
PARIETAL ☐

TRANSFER POINT ACCELERATION:
CENTER OF GRAVITY ☒
POINT OPPOSITE D.P. ☐

Test DHMZ-1 Dummy Head Accelerations

Figure A-5

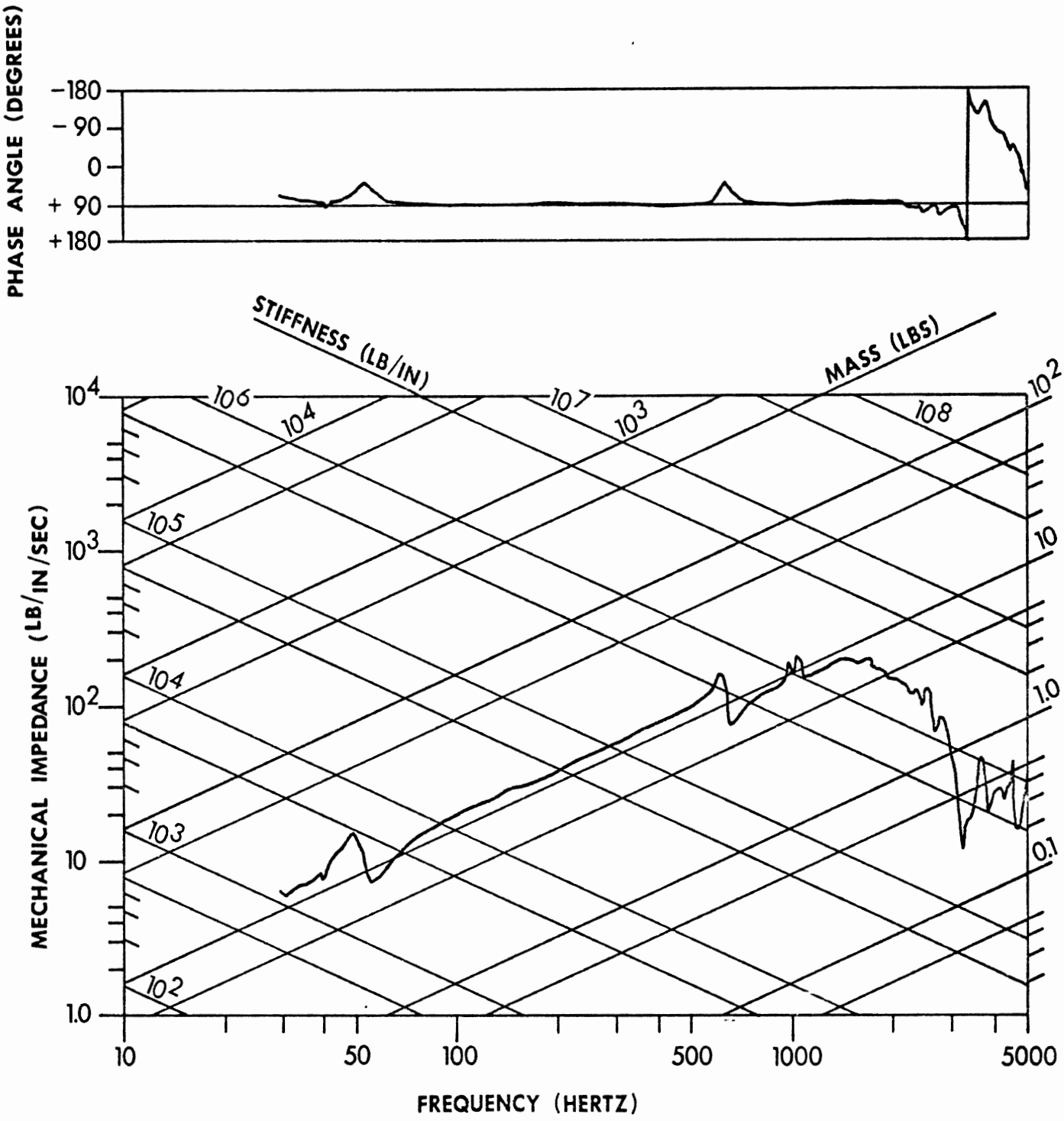

DRIVING POINT:	FRONTAL ☒	D.P.I.	☐
	OCCIPITAL ☐	T.P.I. (CENTER OF GRAVITY)	☐
	PARIETAL ☐	T.P.I. (POINT OPPOSITE D.P.)	☒

Test DHMZ-1 Dummy Head Mechanical Impedance

Figure A-6

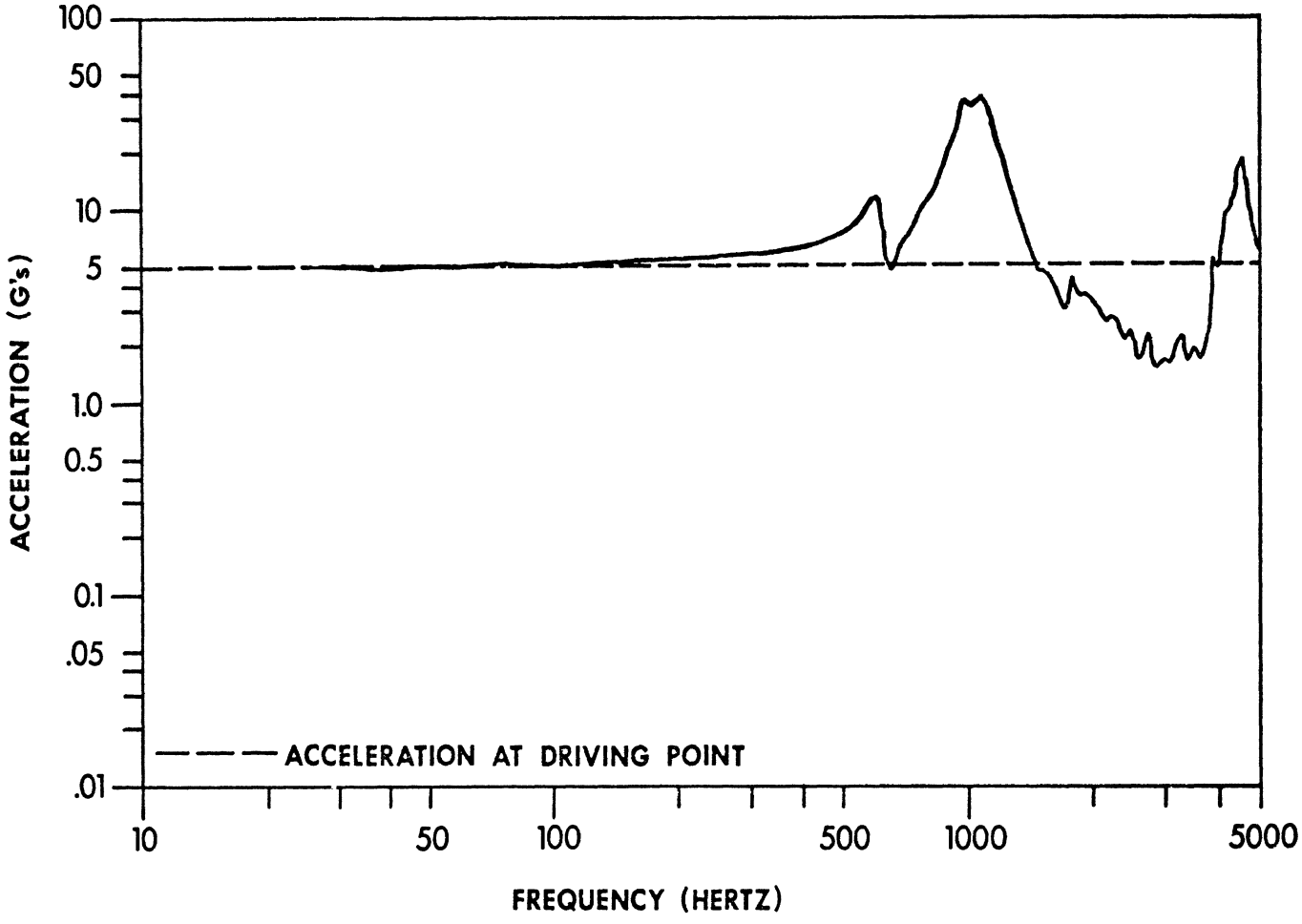

DRIVING POINT: FRONTAL ☒ OCCIPITAL ☐ PARIETAL ☐

TRANSFER POINT ACCELERATION: CENTER OF GRAVITY ☐ POINT OPPOSITE D.P. ☒

Test DHMZ-1 Dummy Head Accelerations

Figure A-7

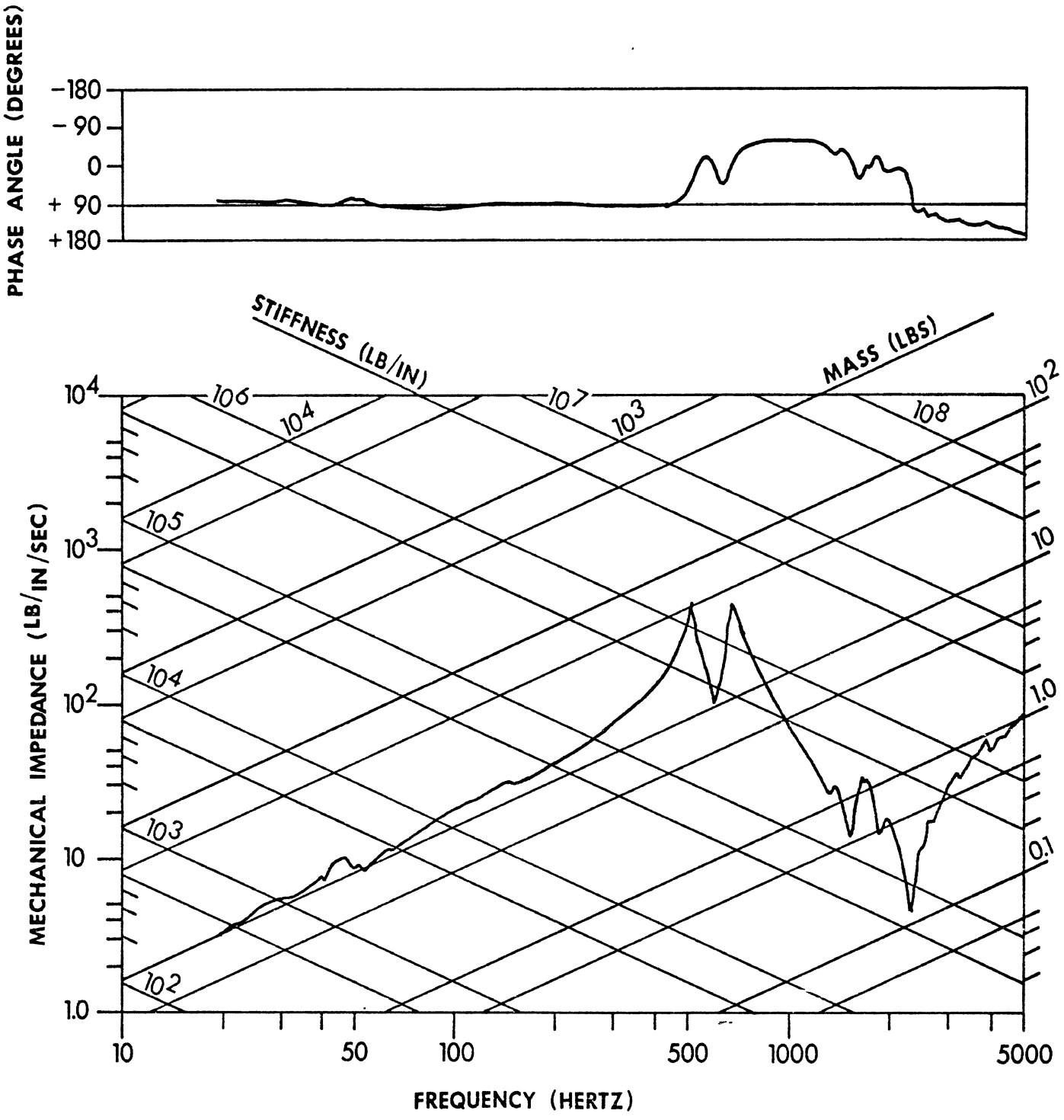

DRIVING POINT: FRONTAL ☐ D.P.I. ☒

OCCIPITAL ☒ T.P.I. (CENTER OF GRAVITY) ☐

PARIETAL ☐ T.P.I. (POINT OPPOSITE D.P.) ☐

Test DHMZ-1 Dummy Head Mechanical Impedance

Figure A-8

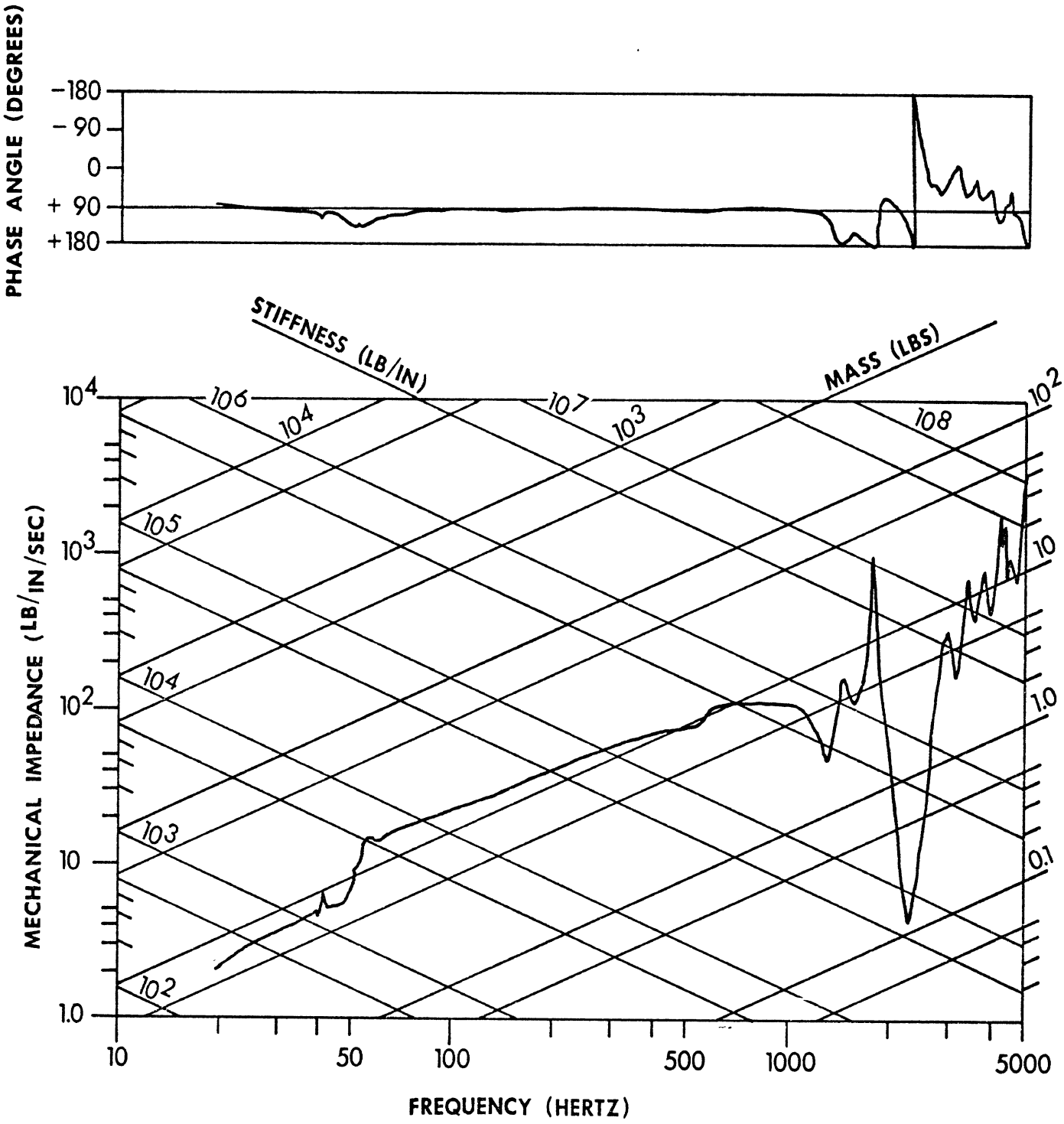

DRIVING POINT: FRONTAL ☐ D.P.I. ☐

OCCIPITAL ☒ T.P.I. (CENTER OF GRAVITY) ☒

PARIETAL ☐ T.P.I. (POINT OPPOSITE D.P.) ☐

Test DHMZ-1 Dummy Head Mechanical Impedance

Figure A-9

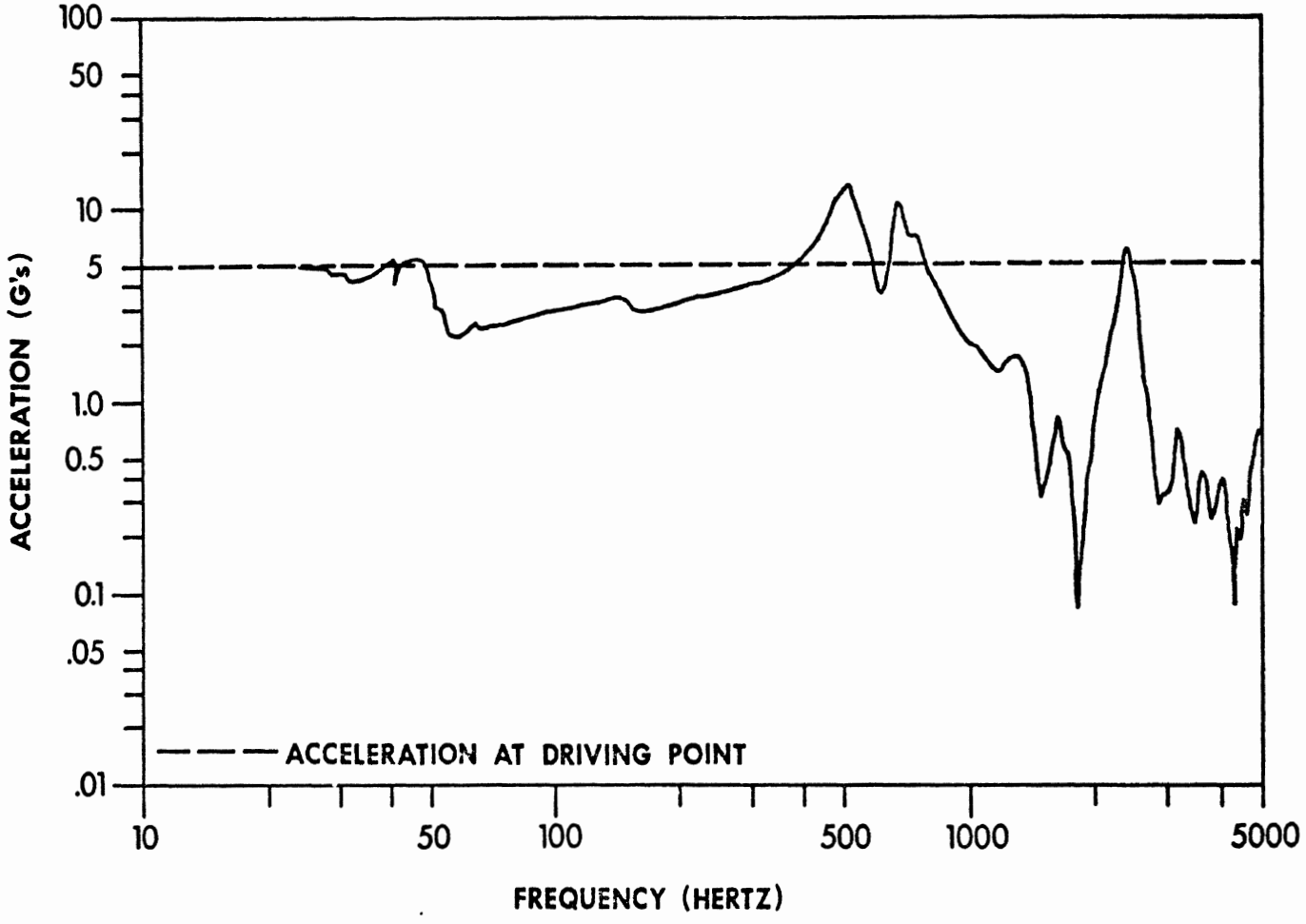

DRIVING POINT: FRONTAL ☐ OCCIPITAL ☒ PARIETAL ☐

TRANSFER POINT ACCELERATION: CENTER OF GRAVITY ☒ POINT OPPOSITE D.P. ☐

Test DHMZ-1 Dummy Head Accelerations

Figure A-10

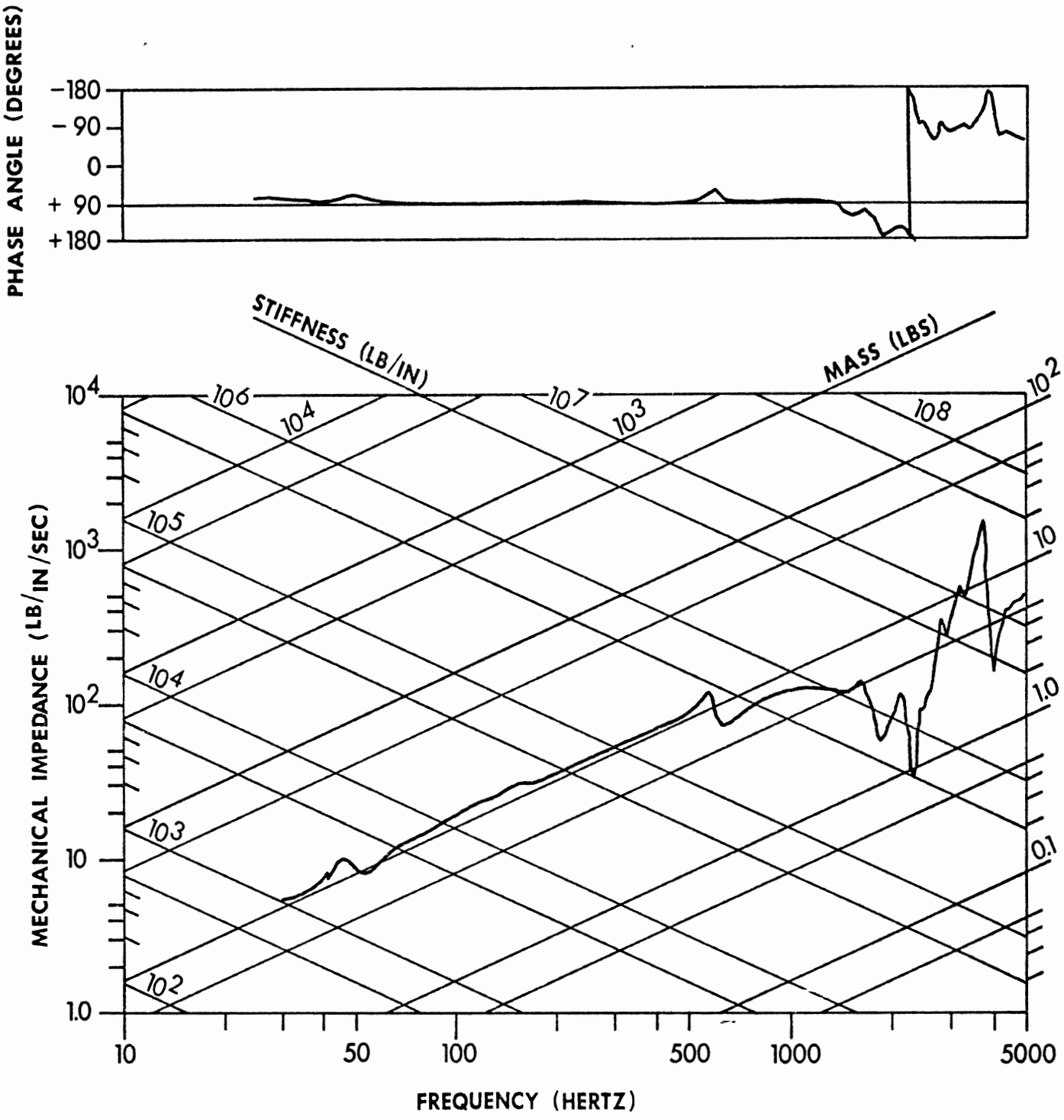

DRIVING POINT:

FRONTAL	☐	D.P.I.	☐
OCCIPITAL	☒	T.P.I. (CENTER OF GRAVITY)	☐
PARIETAL	☐	T.P.I. (POINT OPPOSITE D.P.)	☒

Test DHMZ-1 Dummy Head Mechanical Impedance

Figure A-11

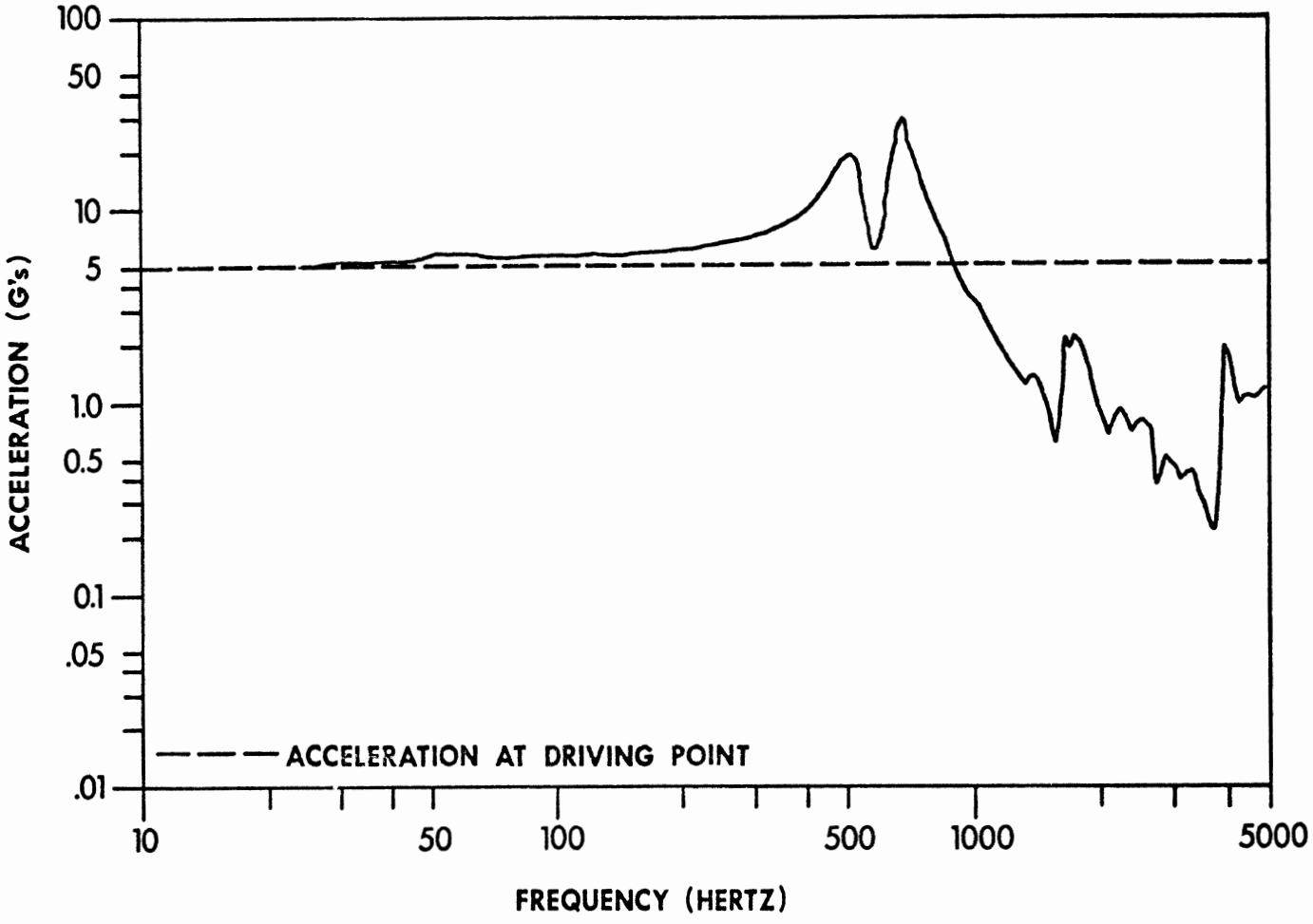

DRIVING POINT: FRONTAL ☐
OCCIPITAL ☒
PARIETAL ☐

TRANSFER POINT ACCELERATION:
CENTER OF GRAVITY ☐
POINT OPPOSITE D.P. ☒

Test DHMZ-1 Dummy Head Accelerations

Figure A-12

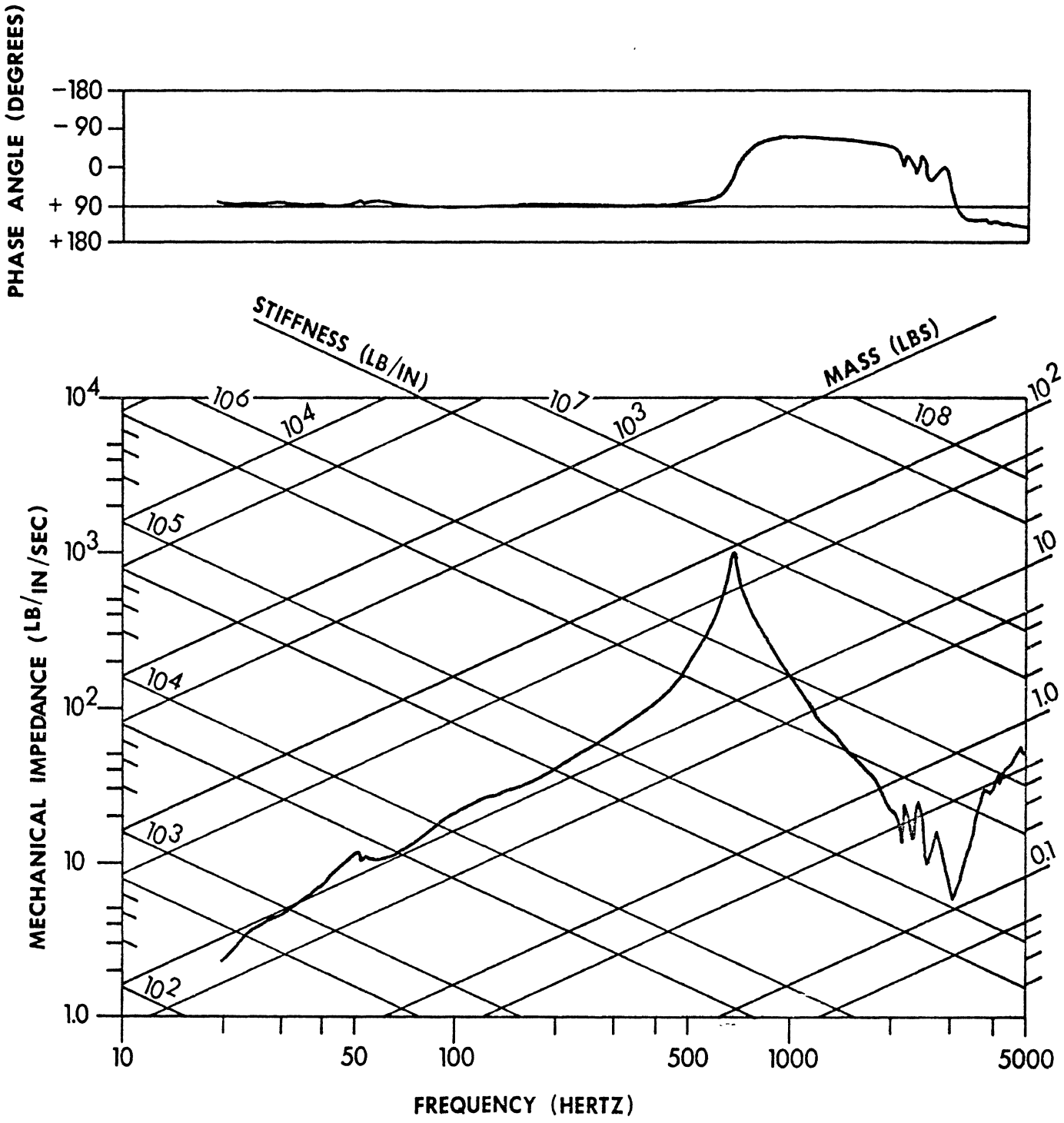

DRIVING POINT: FRONTAL ☐ D.P.I. ☒

OCCIPITAL ☐ T.P.I. (CENTER OF GRAVITY) ☐

PARIETAL ☒ T.P.I. (POINT OPPOSITE D.P.) ☐

Test DHMZ-1 Dummy Head Mechanical Impedance

Figure A-13

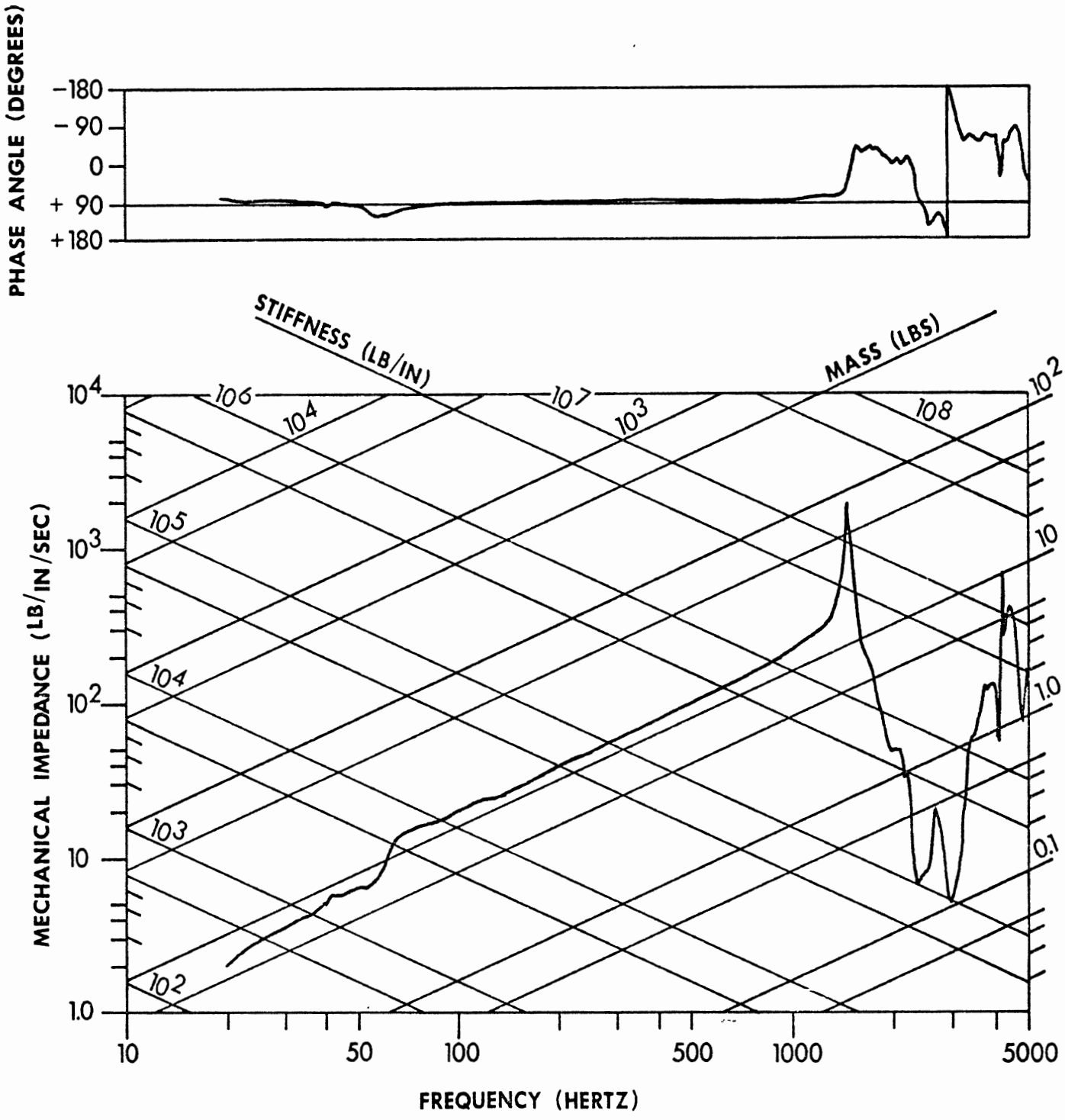

DRIVING POINT: FRONTAL ☐ D.P.I. ☐

OCCIPITAL ☐ T.P.I. (CENTER OF GRAVITY) ☒

PARIETAL ☒ T.P.I. (POINT OPPOSITE D.P.) ☐

Test DHMZ-1 Dummy Head Mechanical Impedance

Figure A-14

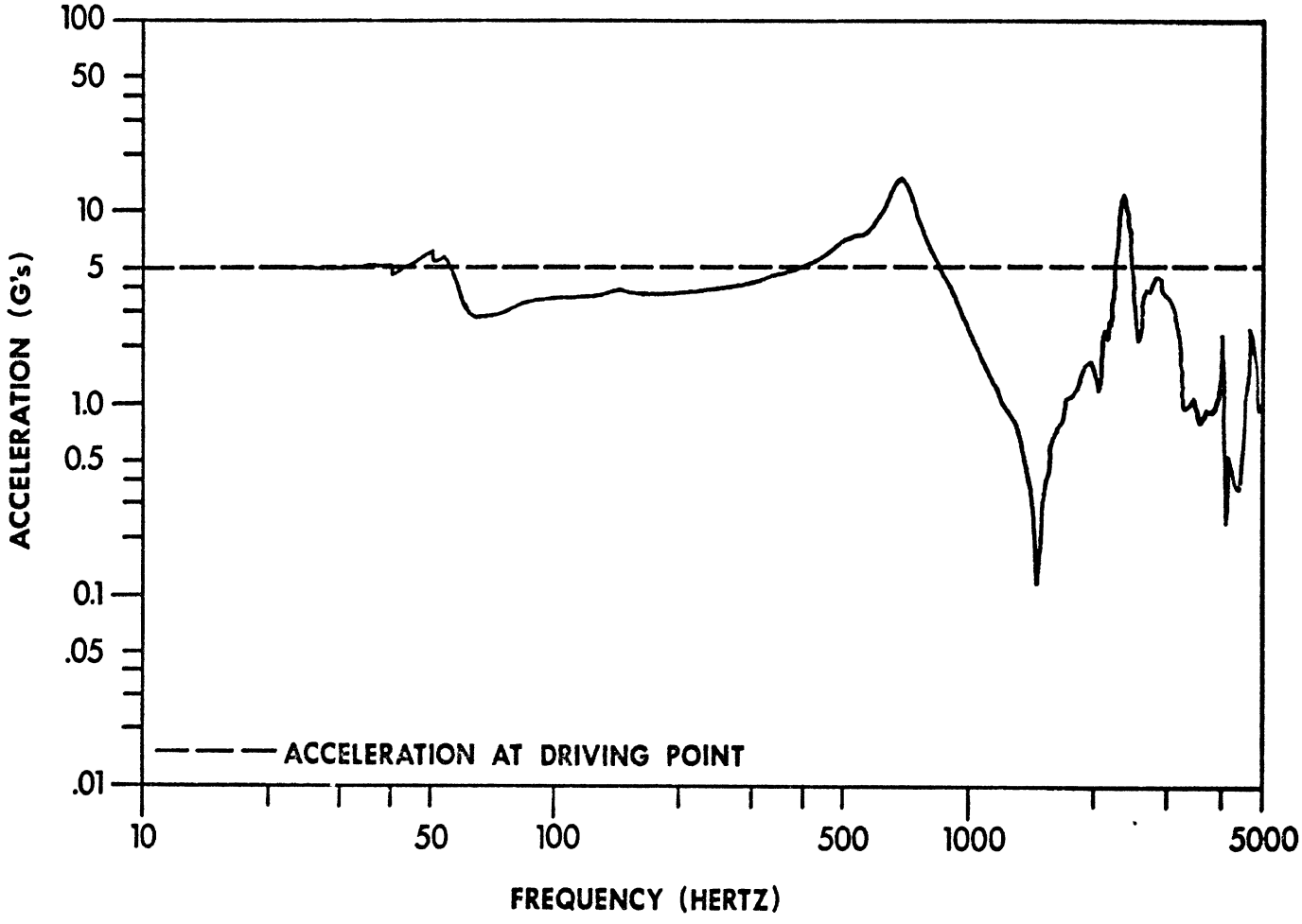

DRIVING POINT: FRONTAL ☐
OCCIPITAL ☐
PARIETAL ☒

TRANSFER POINT ACCELERATION:
CENTER OF GRAVITY ☒
POINT OPPOSITE D.P. ☐

Test DHMZ-1 Dummy Head Accelerations

Figure A-15

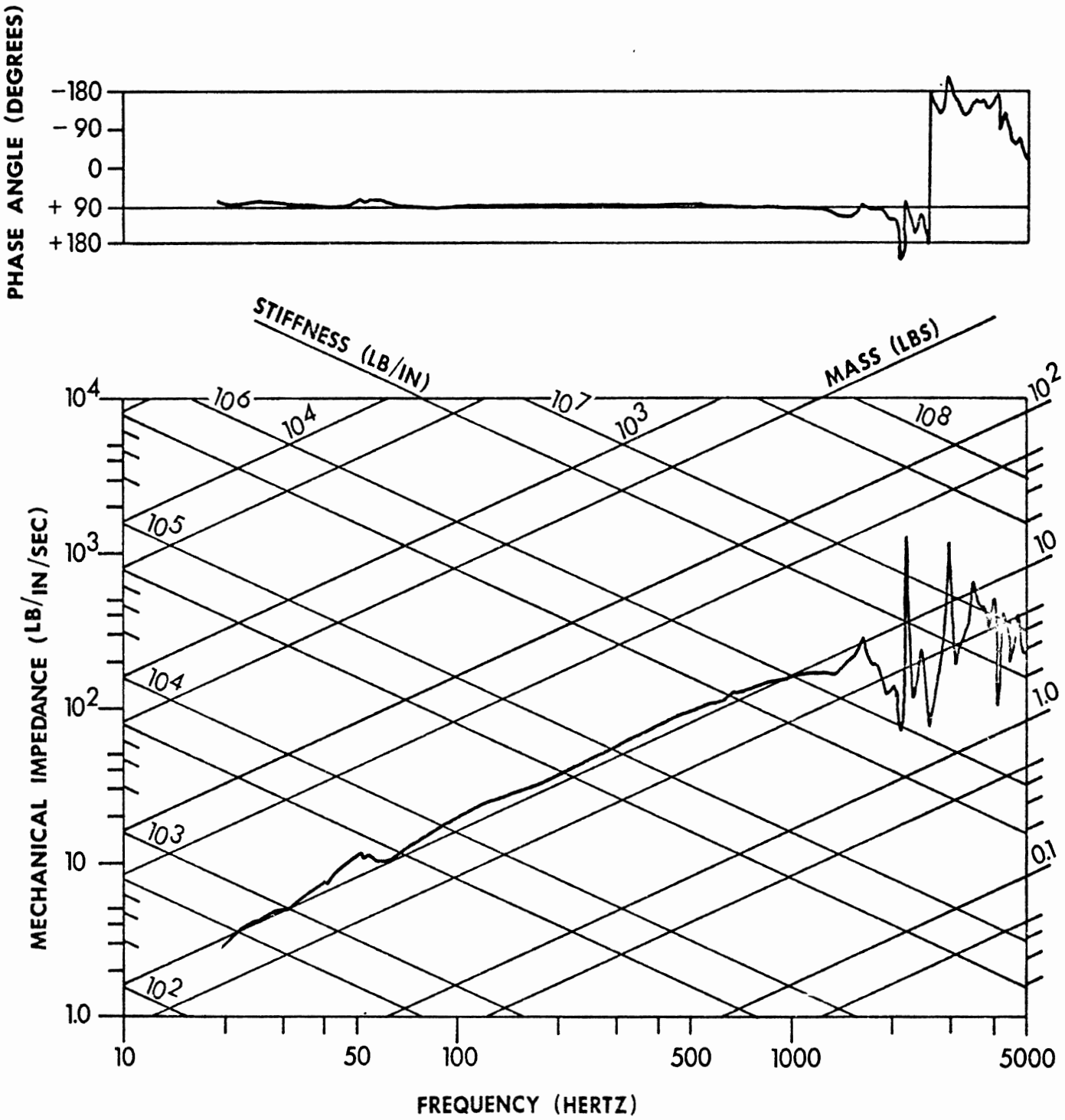

DRIVING POINT: FRONTAL ☐ D.P.I. ☐

OCCIPITAL ☐ T.P.I. (CENTER OF GRAVITY) ☐

PARIETAL ☒ T.P.I. (POINT OPPOSITE D.P.) ☒

Test DHMZ-1 Dummy Head Mechanical Impedance

Figure A-16

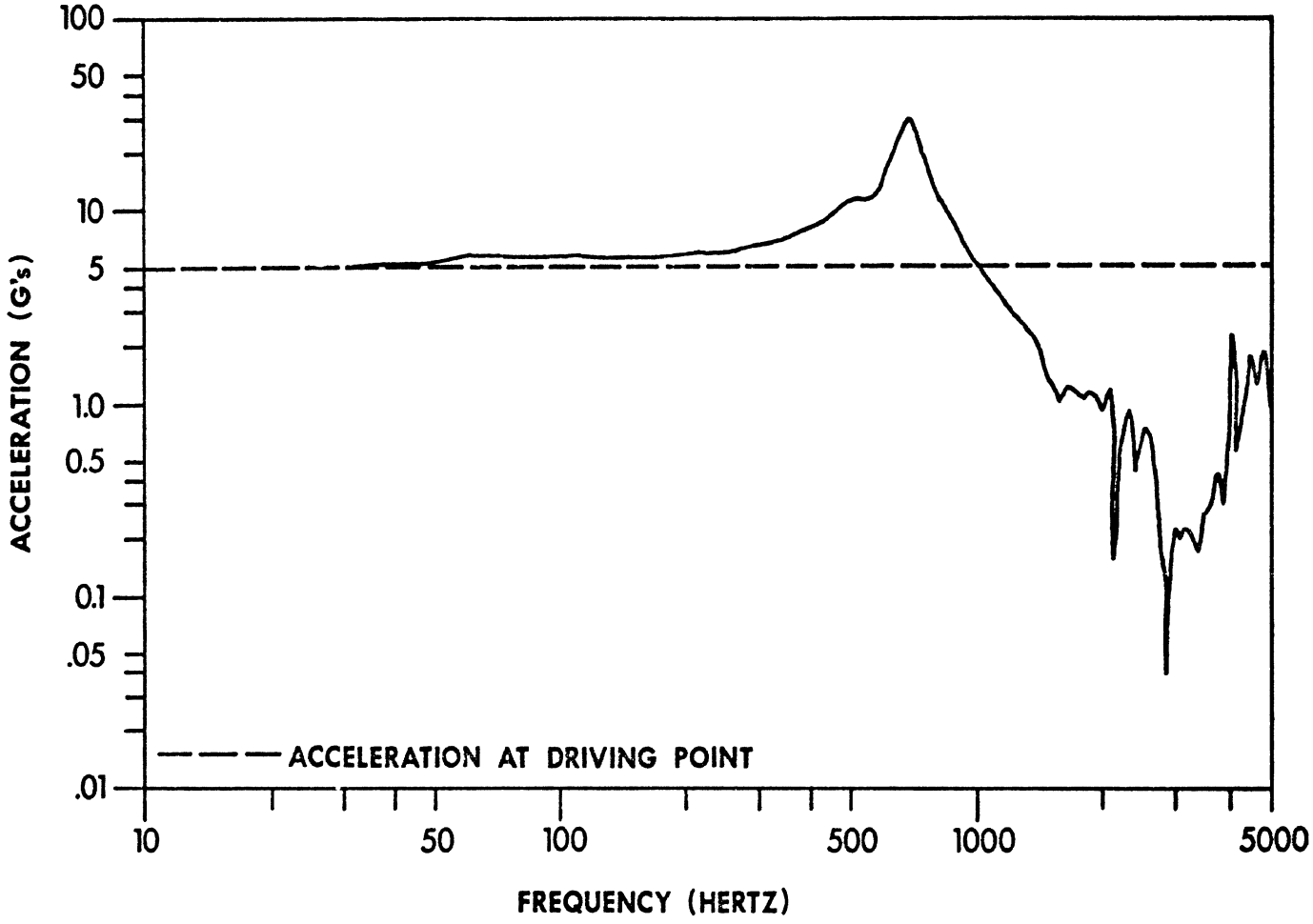

DRIVING POINT: FRONTAL ☐
OCCIPITAL ☐
PARIETAL ☒

TRANSFER POINT ACCELERATION:
CENTER OF GRAVITY ☐
POINT OPPOSITE D.P. ☒

Test DHMZ-1 Dummy Head Accelerations

Figure A-17

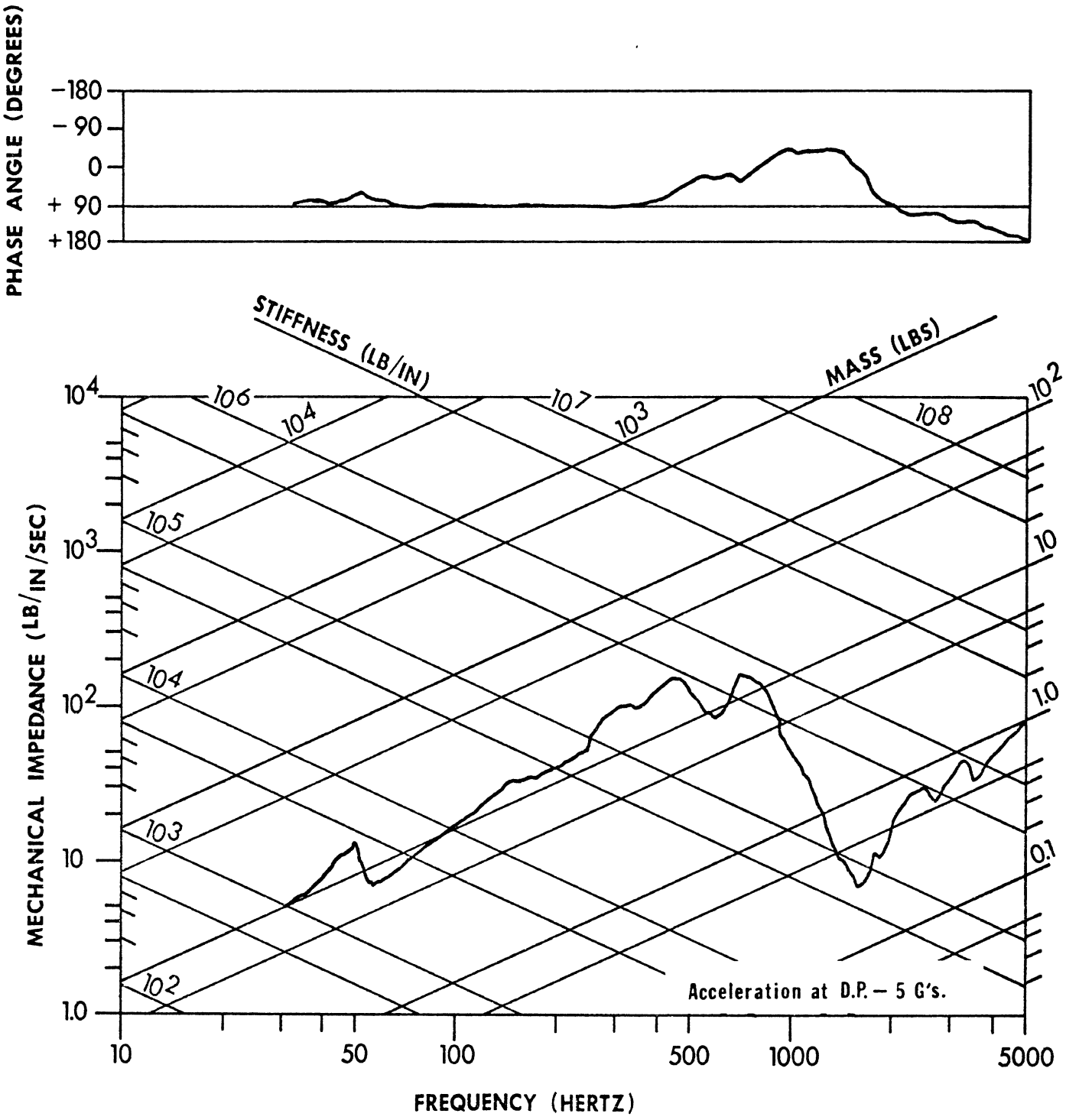

DRIVING POINT: FRONTAL ☒ D.P.I. ☒

OCCIPITAL ☐ T.P.I. (CENTER OF GRAVITY) ☐

PARIETAL ☐ T.P.I. (POINT OPPOSITE D.P.) ☐

Test DHMZ-2 Dummy Head Mechanical Impedance

Figure A-18

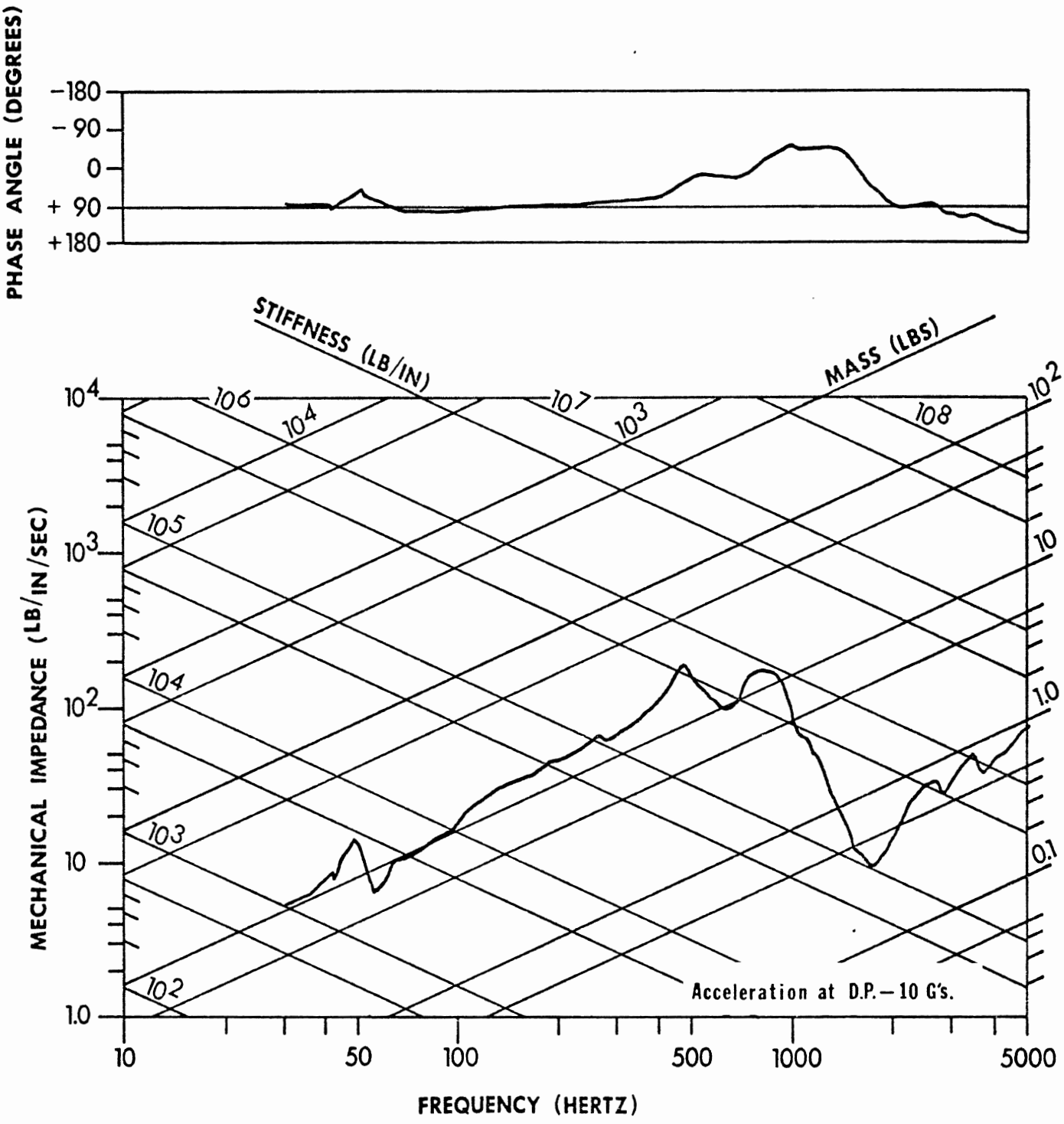

DRIVING POINT: FRONTAL ☒ D.P.I. ☒

OCCIPITAL ☐ T.P.I. (CENTER OF GRAVITY) ☐

PARIETAL ☐ T.P.I. (POINT OPPOSITE D.P.) ☐

Test DHMZ-2 Dummy Head Mechanical Impedance

Figure A-19

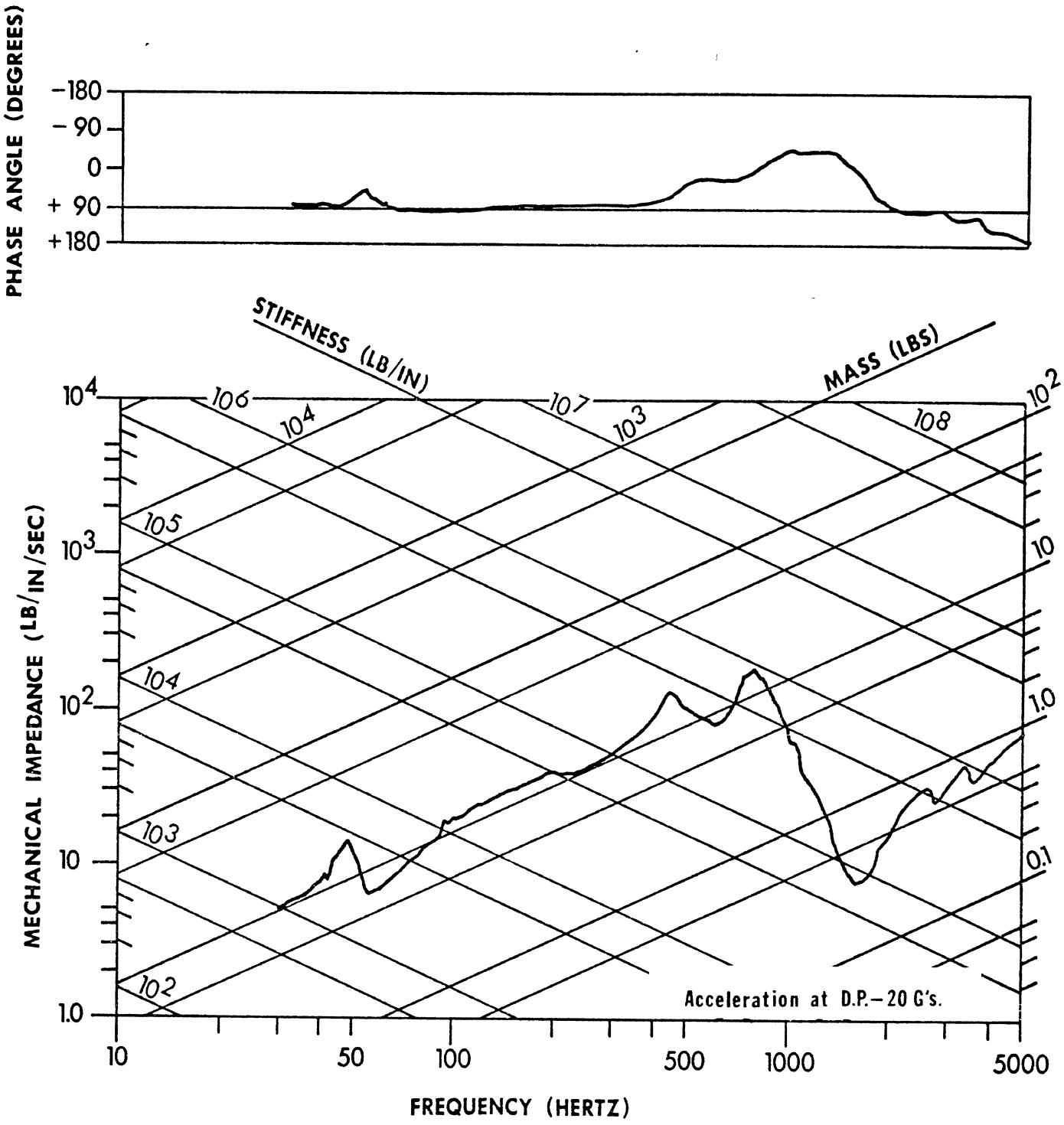

DRIVING POINT: FRONTAL ☒ D.P.I. ☒

OCCIPITAL ☐ T.P.I. (CENTER OF GRAVITY) ☐

PARIETAL ☐ T.P.I. (POINT OPPOSITE D.P.) ☐

Test DHMZ-2 Dummy Head Mechanical Impedance

Figure A-20

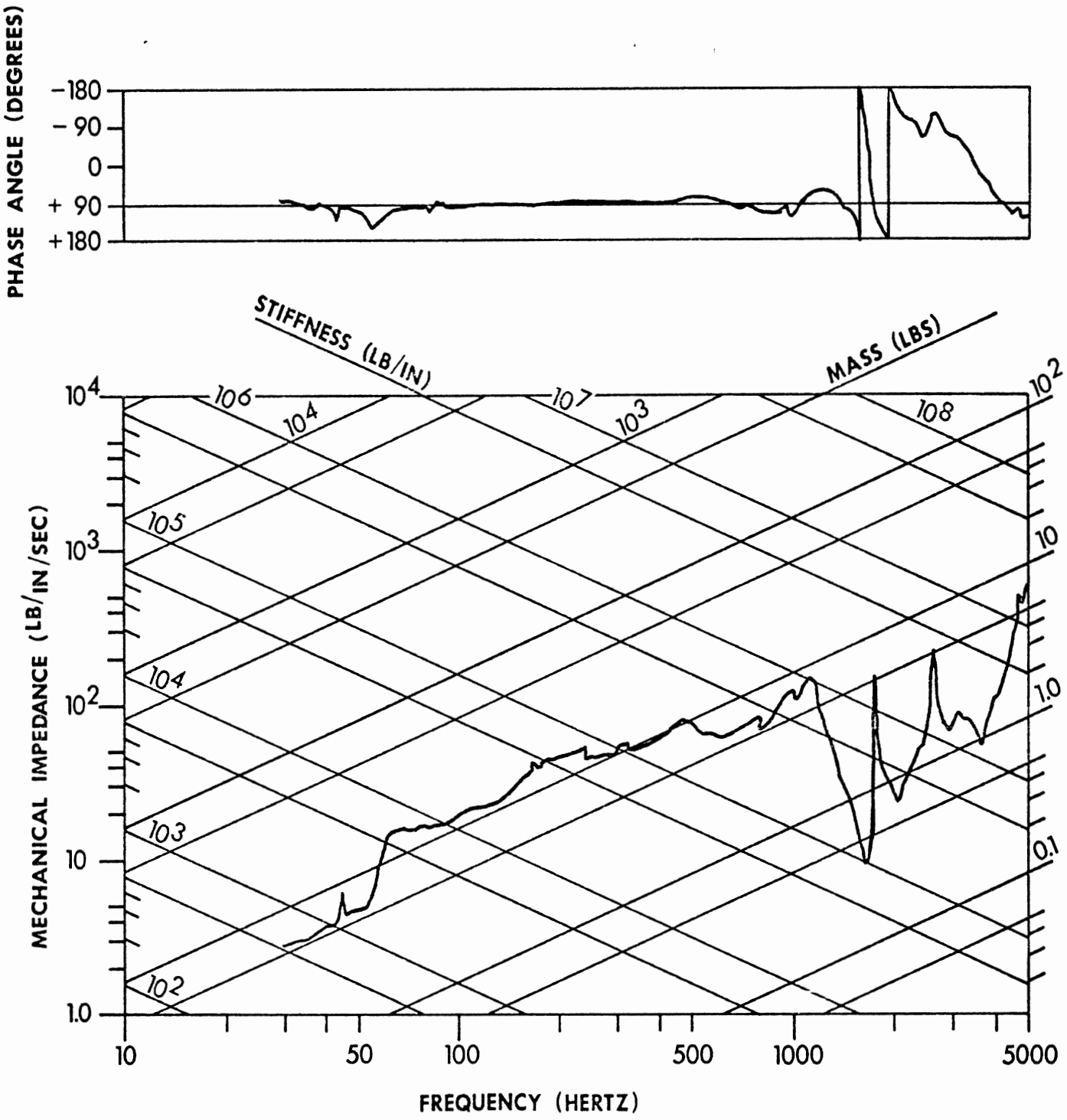

DRIVING POINT: FRONTAL ☒ D.P.I. ☐

OCCIPITAL ☐ T.P.I. (CENTER OF GRAVITY) ☒

PARIETAL ☐ T.P.I. (POINT OPPOSITE D.P.) ☐

Test DHMZ-2 Dummy Head Mechanical Impedance

Figure A-21

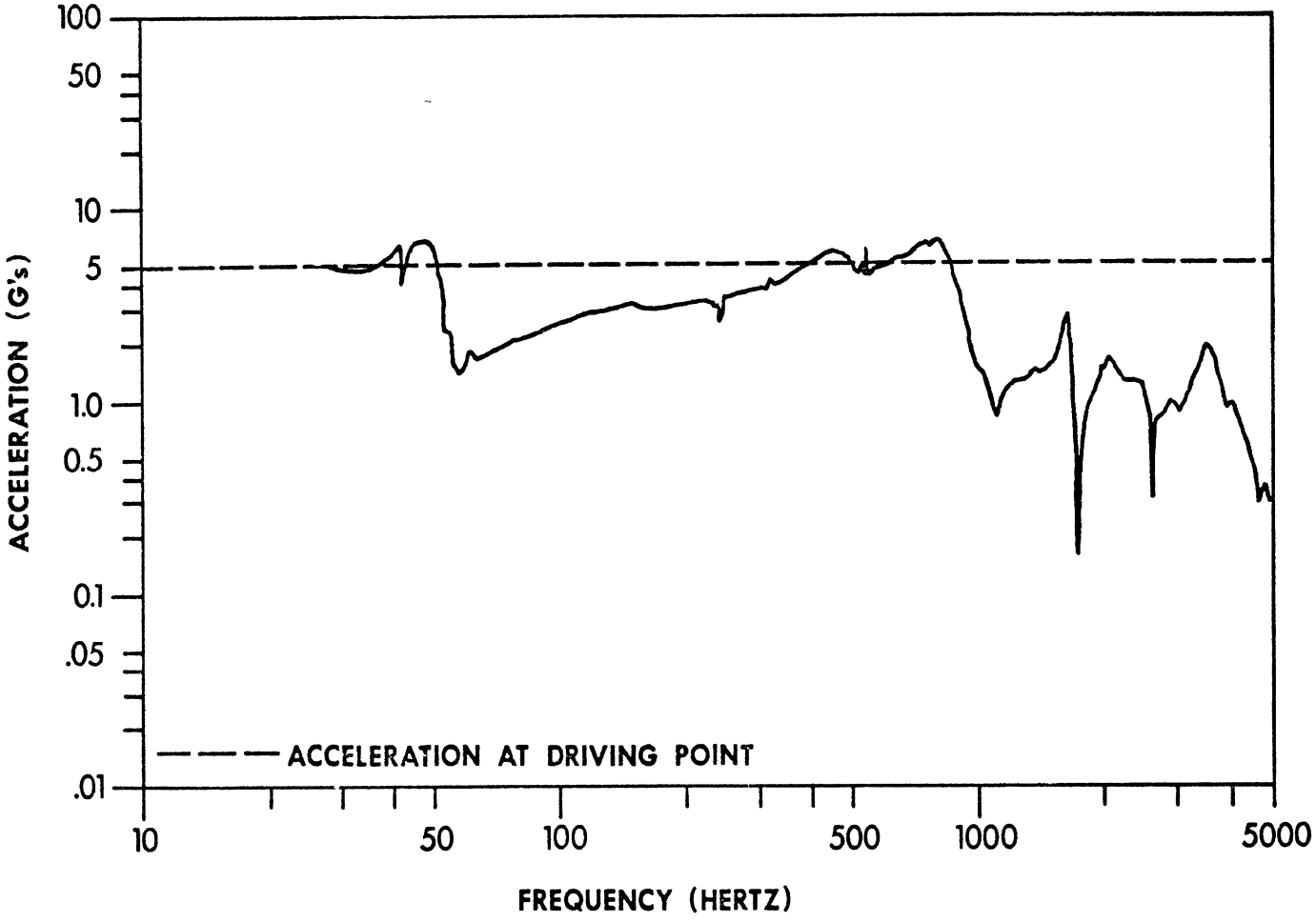

DRIVING POINT: FRONTAL ☒
OCCIPITAL ☐
PARIETAL ☐

TRANSFER POINT ACCELERATION:
CENTER OF GRAVITY ☒
POINT OPPOSITE D.P. ☐

Test DHMZ-2 Dummy Head Accelerations

Figure A-22

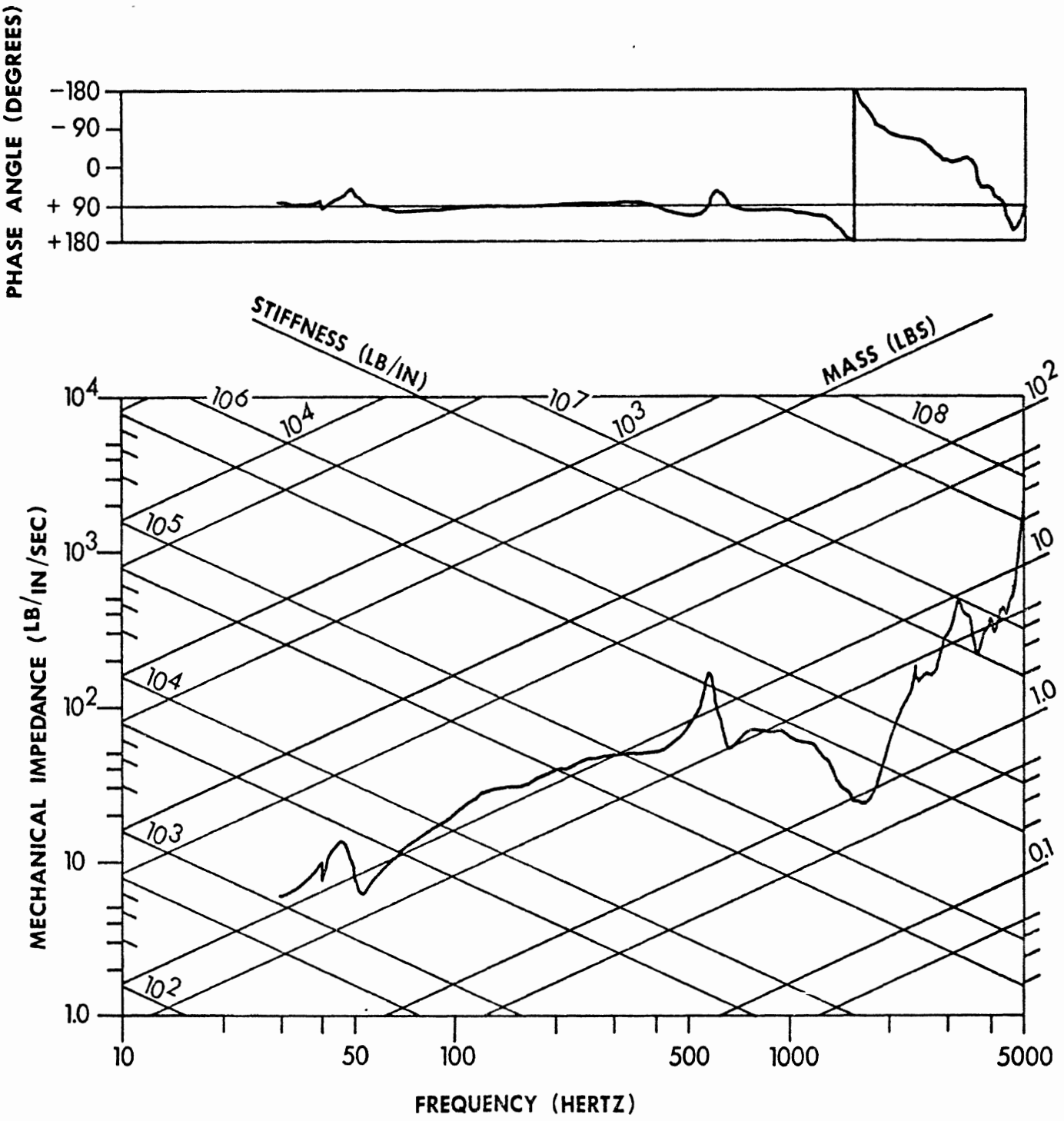

DRIVING POINT: FRONTAL ☒ D.P.I. ☐

OCCIPITAL ☐ T.P.I. (CENTER OF GRAVITY) ☐

PARIETAL ☐ T.P.I. (POINT OPPOSITE D.P.) ☒

Test DHMZ-2 Dummy Head Mechanical Impedance

Figure A-23

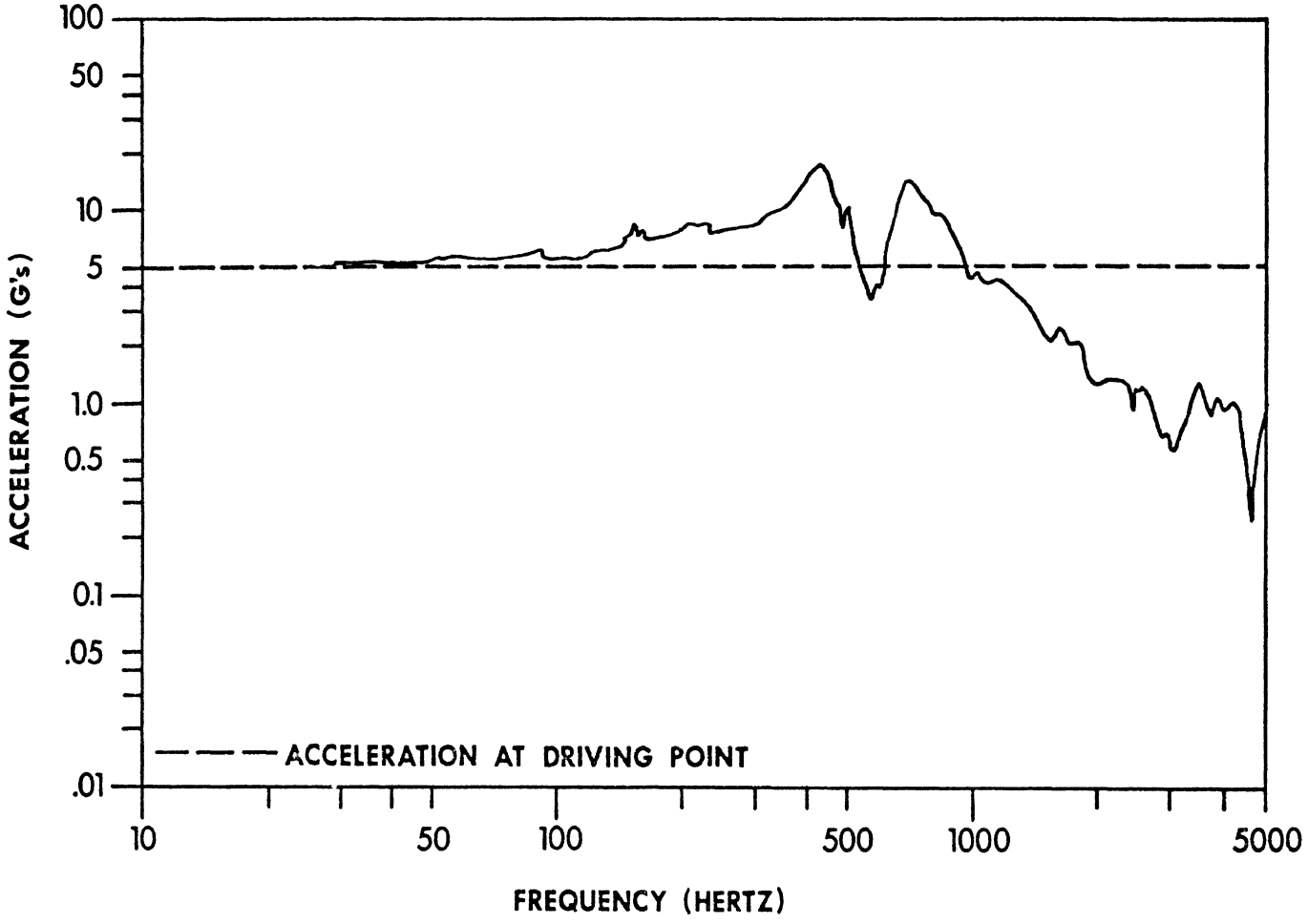

DRIVING POINT: FRONTAL ☒
OCCIPITAL ☐
PARIETAL ☐

TRANSFER POINT ACCELERATION:
CENTER OF GRAVITY ☐
POINT OPPOSITE D.P. ☒

Test DHMZ-2 Dummy Head Accelerations

Figure A-24

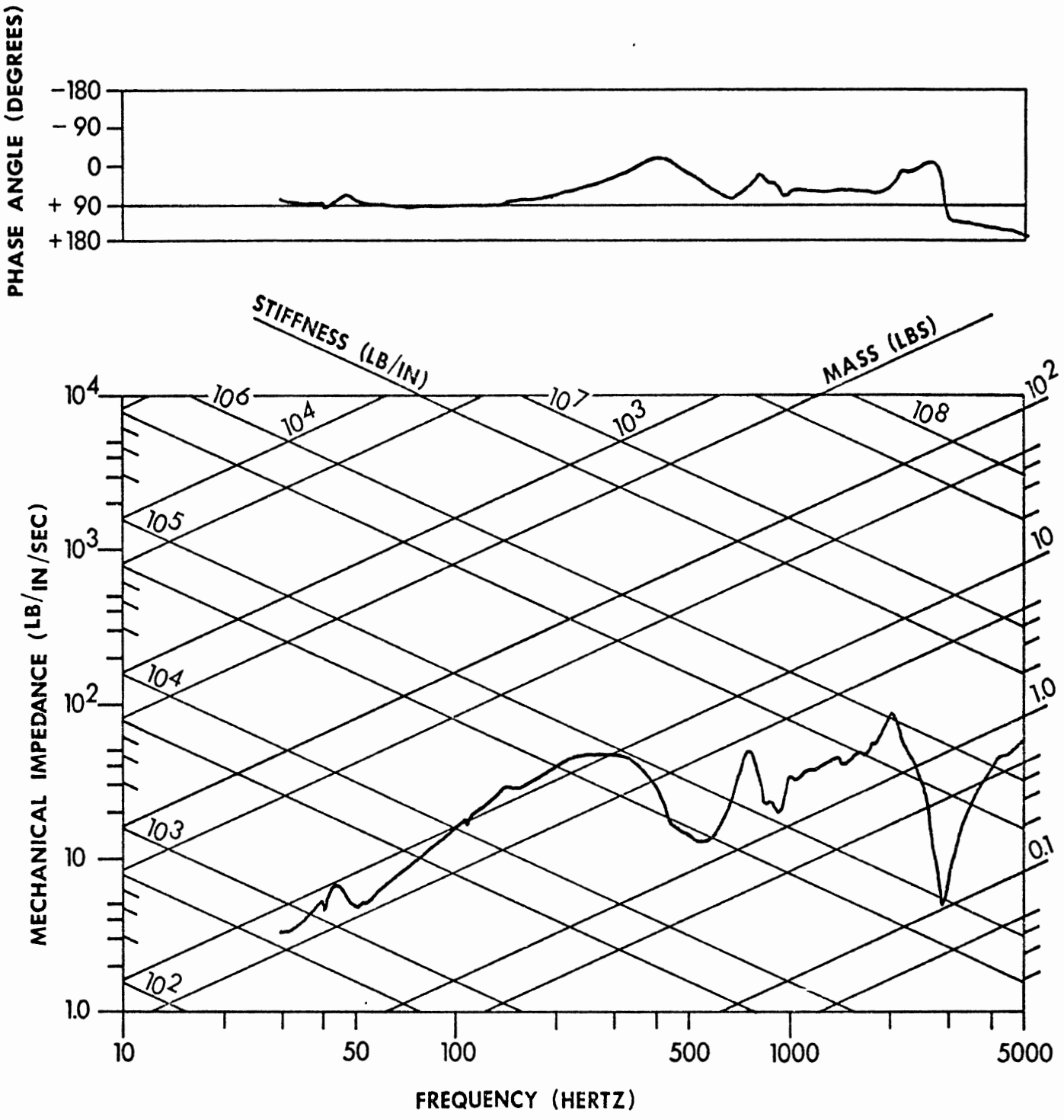

DRIVING POINT: FRONTAL ☐ D.P.I. ☒

OCCIPITAL ☒ T.P.I. (CENTER OF GRAVITY) ☐

PARIETAL ☐ T.P.I. (POINT OPPOSITE D.P.) ☐

Test DHMZ-2 Dummy Head Mechanical Impedance

Figure A-25

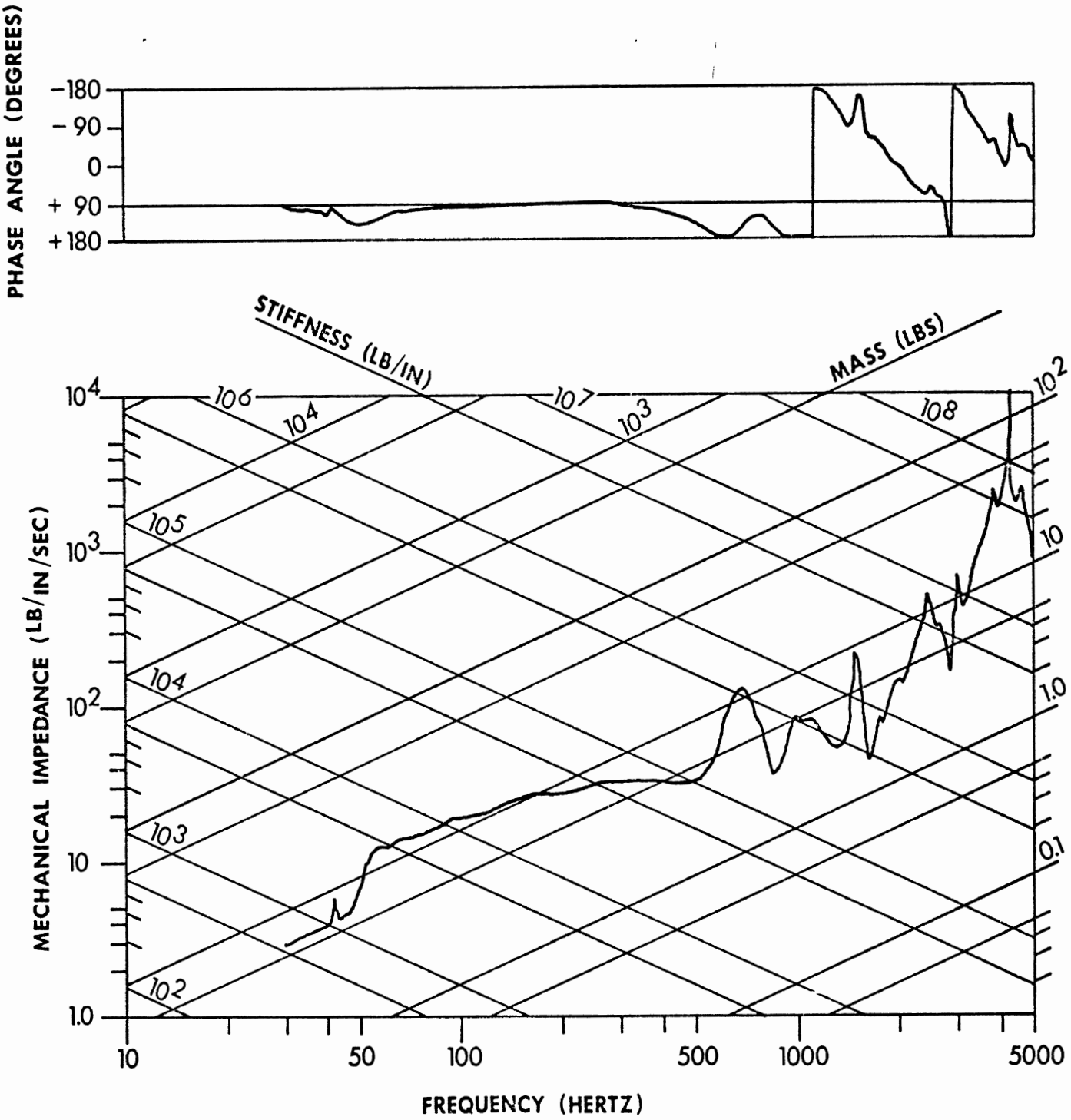

Test DHMZ-2 Dummy Head Mechanical Impedance

Figure A-26

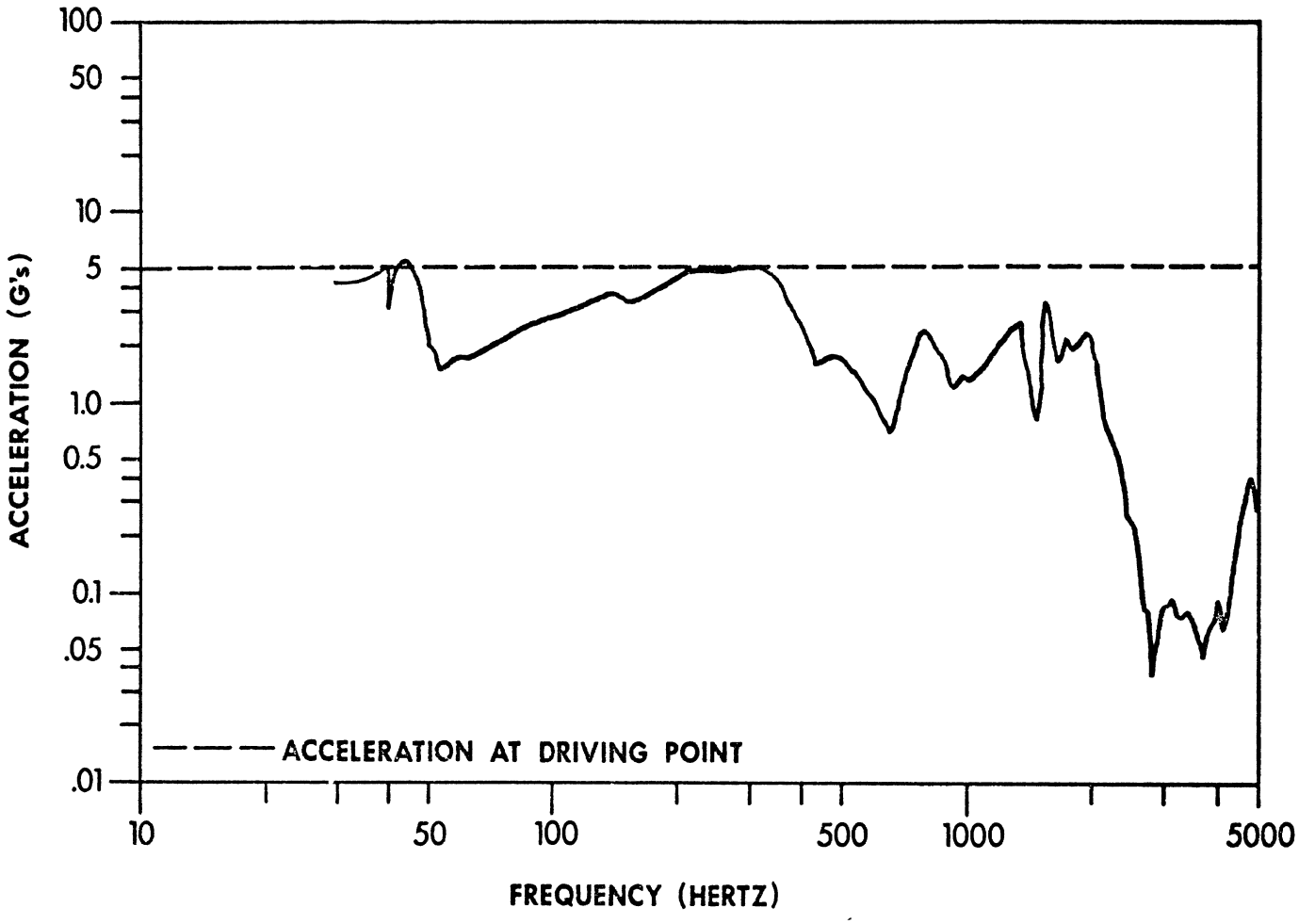

DRIVING POINT: FRONTAL ☐
OCCIPITAL ☒
PARIETAL ☐

TRANSFER POINT ACCELERATION:
CENTER OF GRAVITY ☒
POINT OPPOSITE D.P. ☐

Test DHMZ-2 Dummy Head Accelerations

Figure A-27

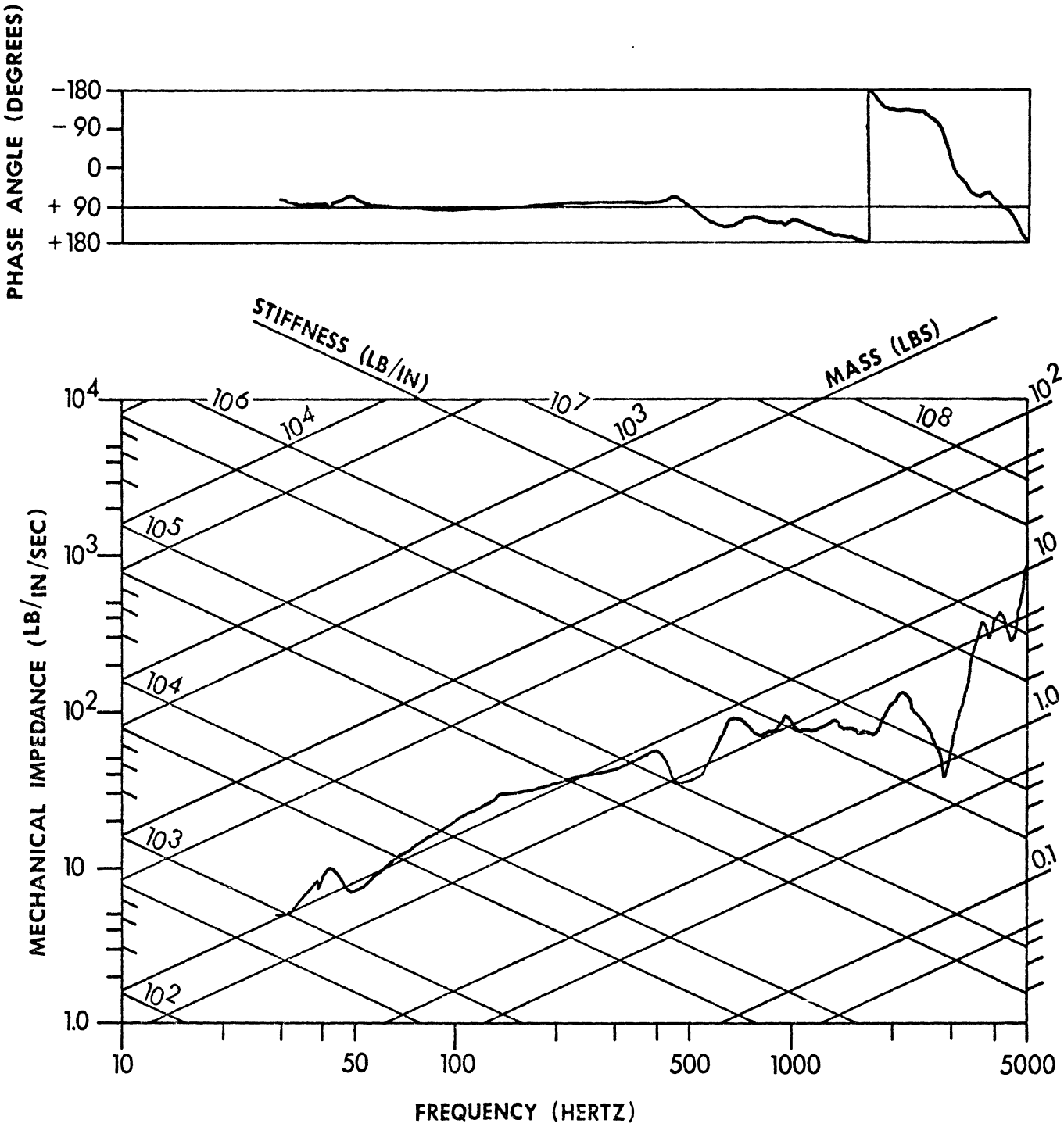

DRIVING POINT: FRONTAL ☐ D.P.I. ☐

OCCIPITAL ☒ T.P.I. (CENTER OF GRAVITY) ☐

PARIETAL ☐ T.P.I. (POINT OPPOSITE D.P.) ☒

Test DHMZ-2 Dummy Head Mechanical Impedance

Figure A-28

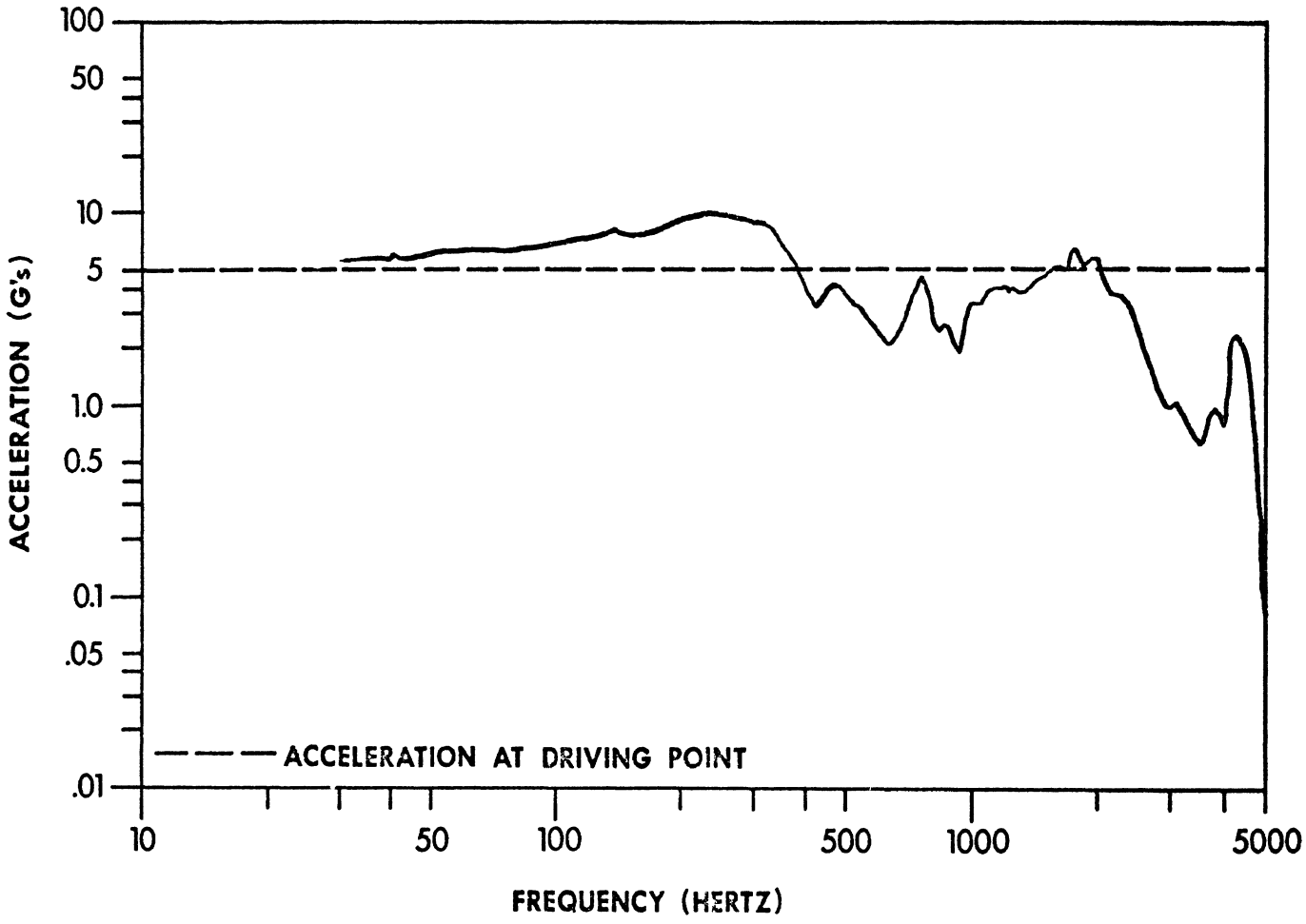

DRIVING POINT: FRONTAL ☐
OCCIPITAL ☒
PARIETAL ☐

TRANSFER POINT ACCELERATION:
CENTER OF GRAVITY ☐
POINT OPPOSITE D.P. ☒

Test DHMZ-2 Dummy Head Accelerations

Figure A-29

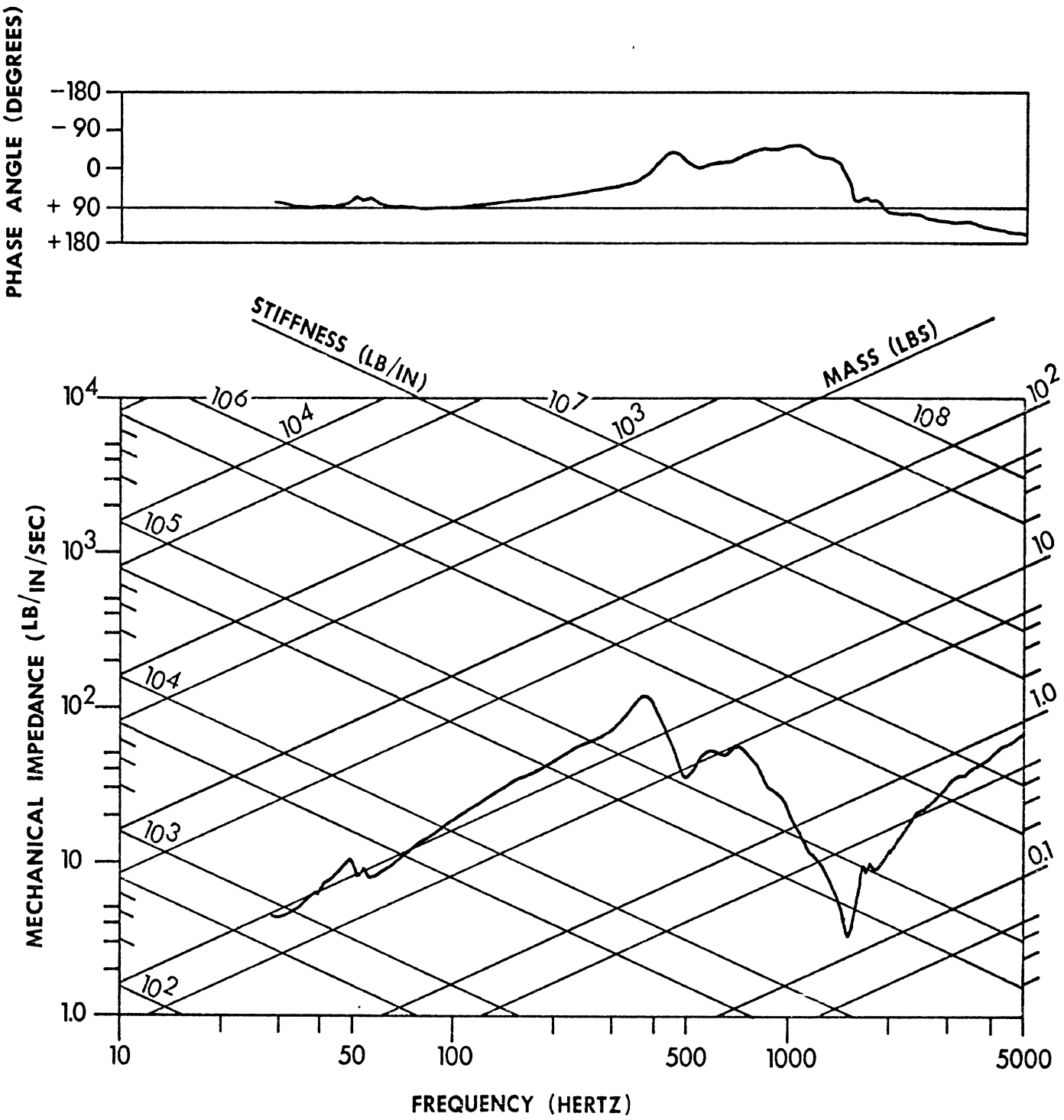

DRIVING POINT:	FRONTAL ☐	D.P.I.	☒
	OCCIPITAL ☐	T.P.I. (CENTER OF GRAVITY)	☐
	PARIETAL ☒	T.P.I. (POINT OPPOSITE D.P.)	☐

Test DHMZ-2 Dummy Head Mechanical Impedance

Figure A-30

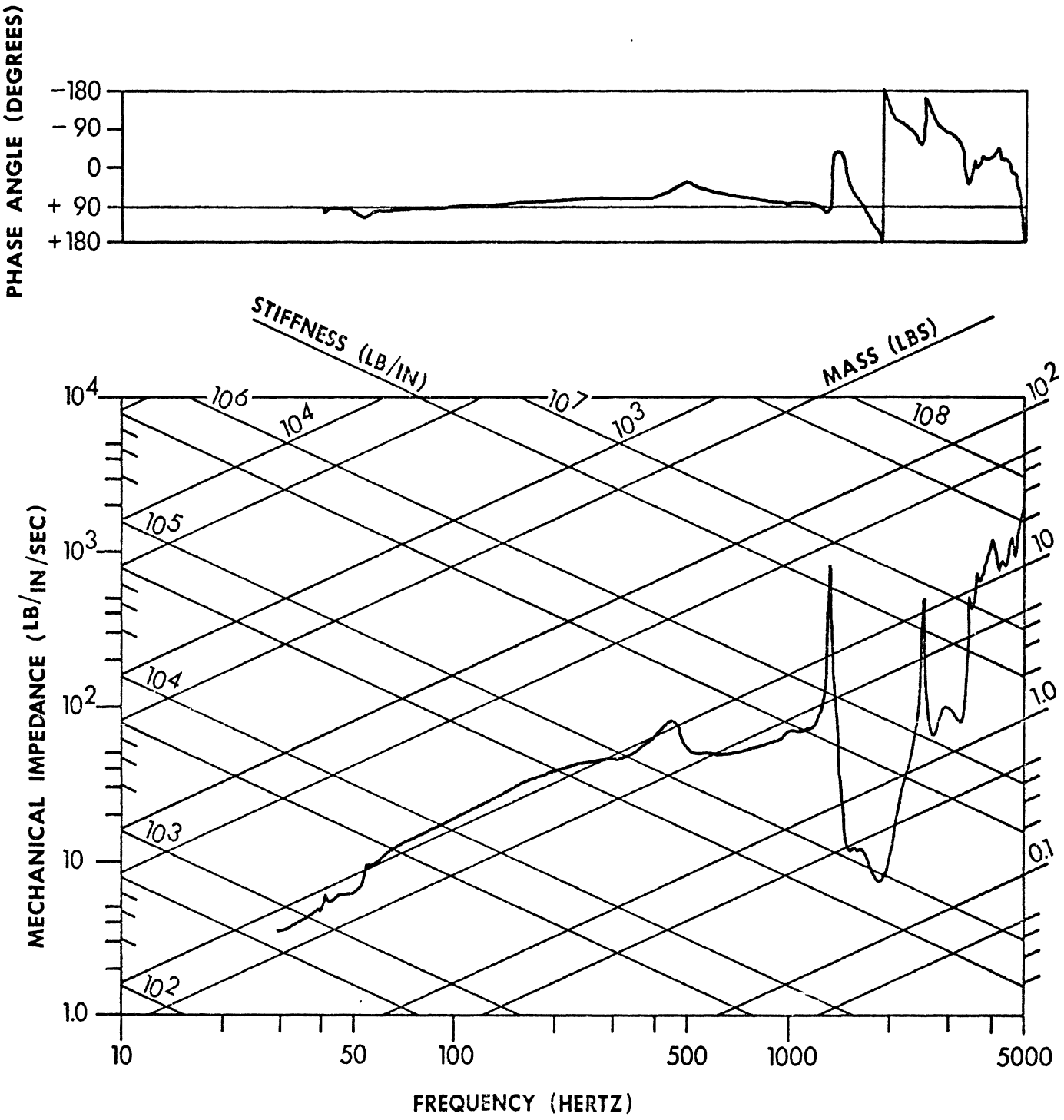

DRIVING POINT: FRONTAL ☐ D.P.I. ☐

OCCIPITAL ☐ T.P.I. (CENTER OF GRAVITY) ☒

PARIETAL ☒ T.P.I. (POINT OPPOSITE D.P.) ☐

Test DHMZ-2 Dummy Head Mechanical Impedance

Figure A-31

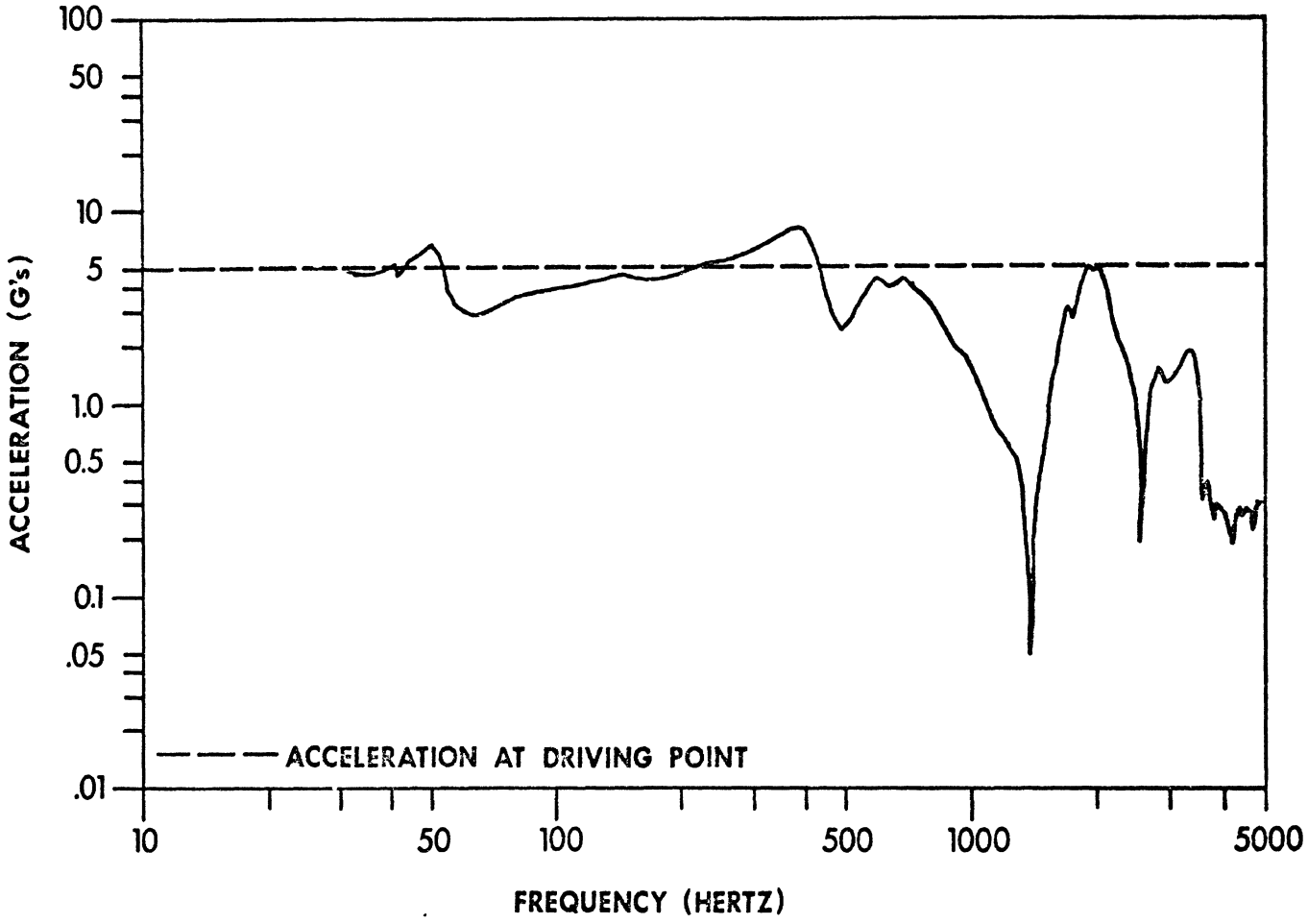

DRIVING POINT: FRONTAL ☐ OCCIPITAL ☐ PARIETAL ☒

TRANSFER POINT ACCELERATION: CENTER OF GRAVITY ☒ POINT OPPOSITE D.P. ☐

Test DHMZ-2 Dummy Head Accelerations

Figure A-32

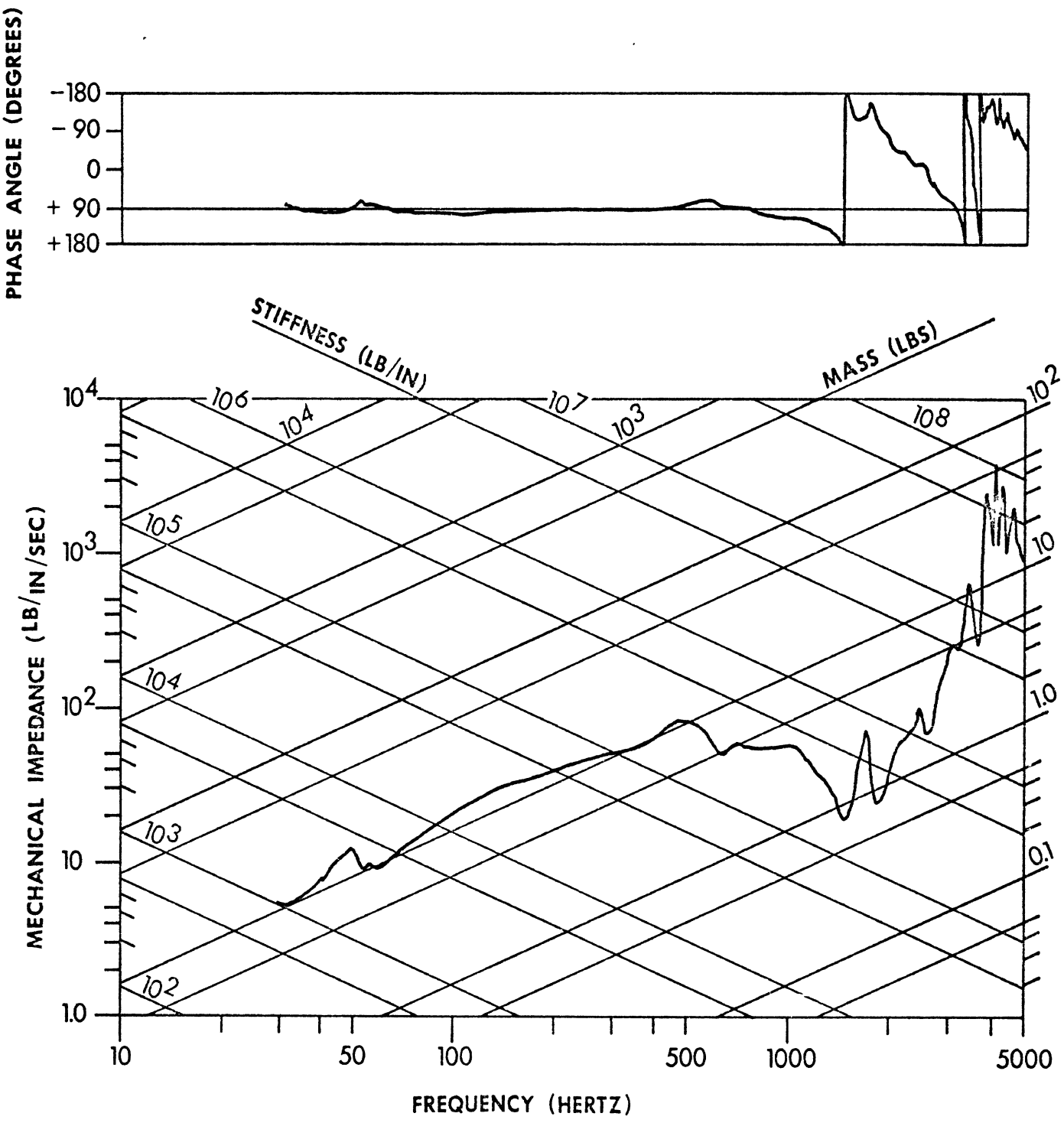

DRIVING POINT: FRONTAL ☐ D.P.I. ☐

OCCIPITAL ☐ T.P.I. (CENTER OF GRAVITY) ☐

PARIETAL ☒ T.P.I. (POINT OPPOSITE D.P.) ☒

Test DHMZ-2 Dummy Head Mechanical Impedance

Figure A-33

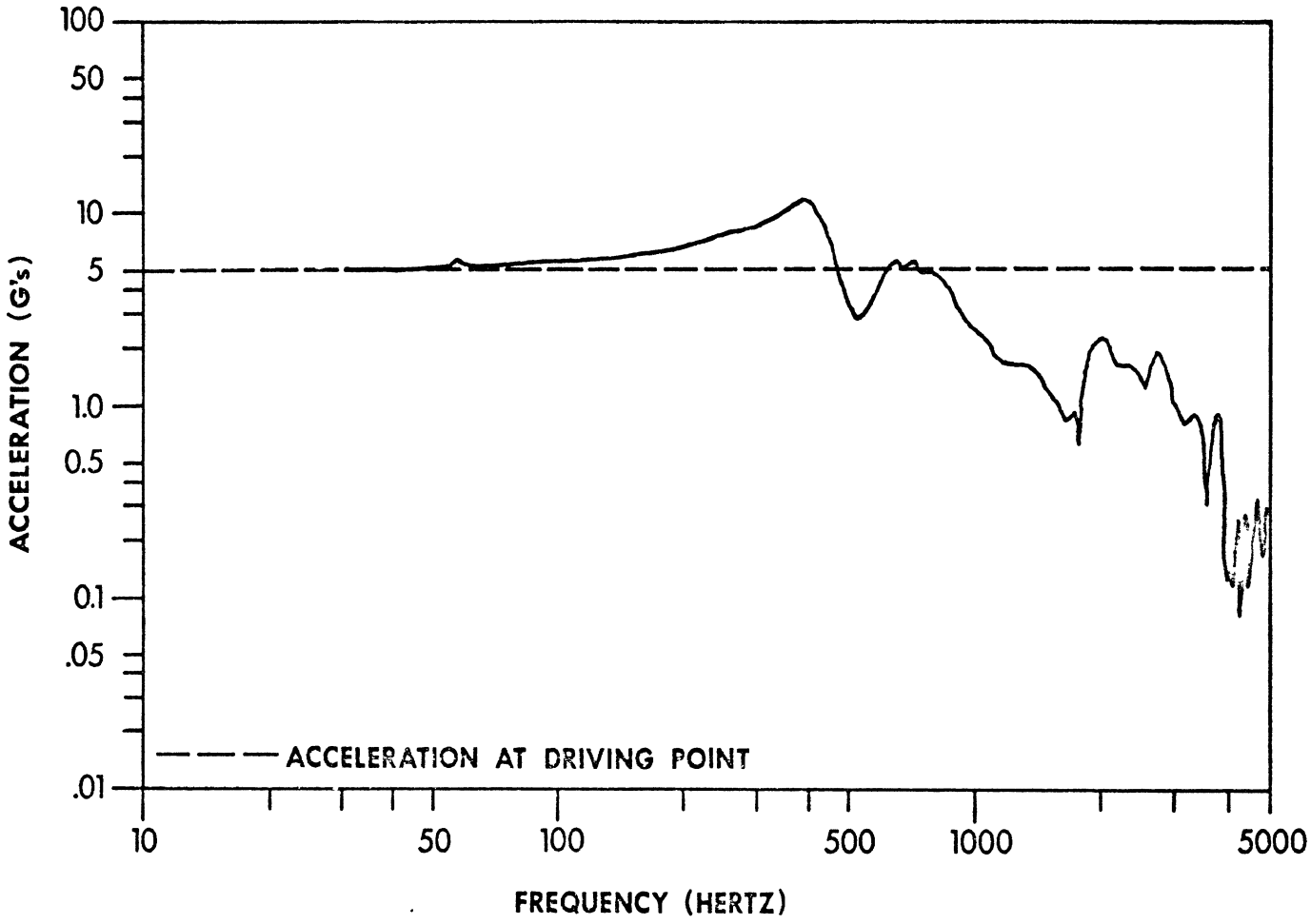

DRIVING POINT: FRONTAL ☐
OCCIPITAL ☐
PARIETAL ☒

TRANSFER POINT ACCELERATION:
CENTER OF GRAVITY ☐
POINT OPPOSITE D.P. ☒

Test DHMZ-2 Dummy Head Accelerations

Figure A-34

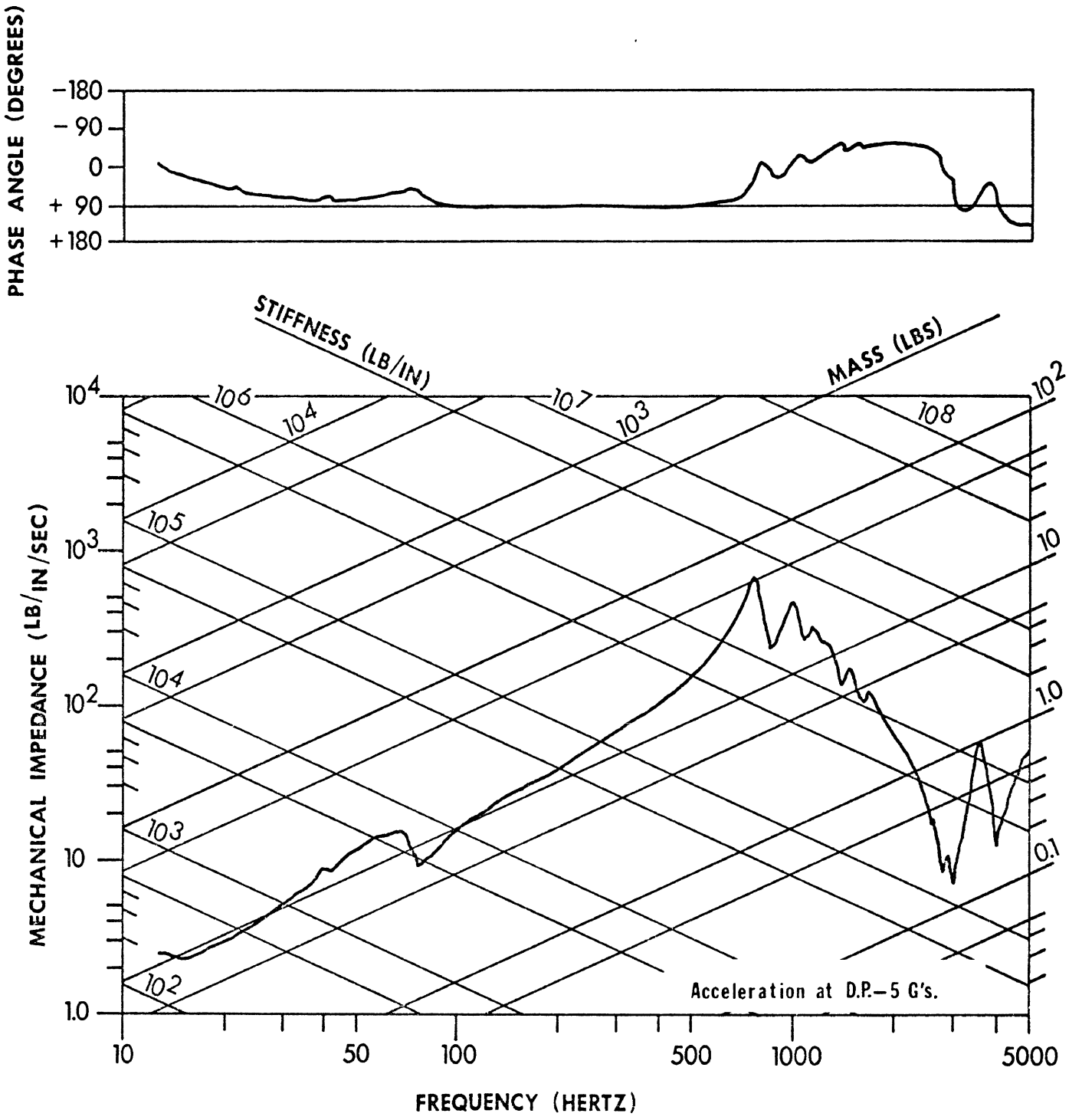

DRIVING POINT:	FRONTAL ☒	D.P.I.	☒
	OCCIPITAL ☐	T.P.I. (CENTER OF GRAVITY)	☐
	PARIETAL ☐	T.P.I. (POINT OPPOSITE D.P.)	☐

Test DHMZ-3 Dummy Head Mechanical Impedance

Figure A-35

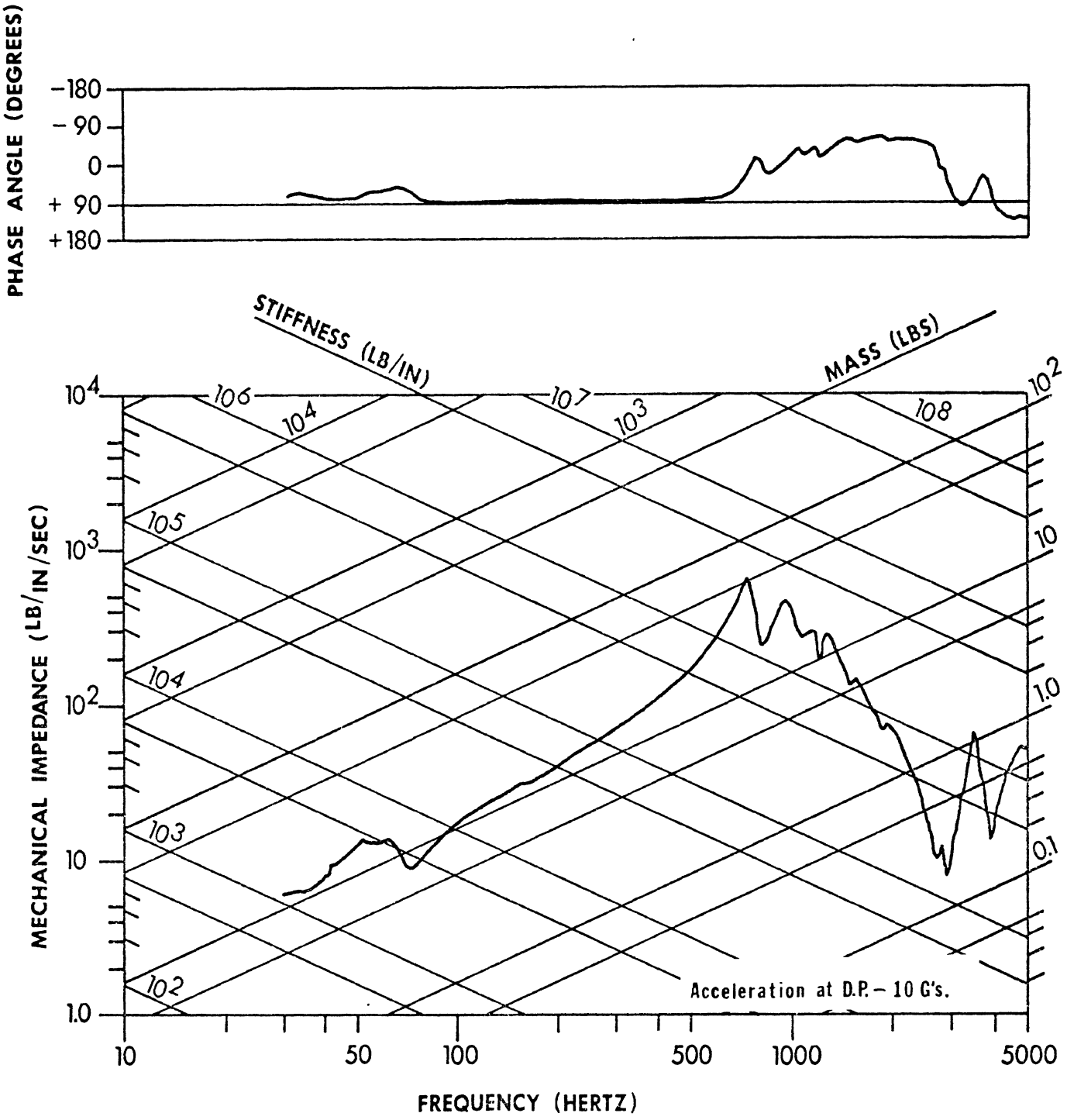

DRIVING POINT:	FRONTAL ☒	D.P.I.	☒
	OCCIPITAL ☐	T.P.I. (CENTER OF GRAVITY)	☐
	PARIETAL ☐	T.P.I. (POINT OPPOSITE D.P.)	☐

Test DHMZ-3 Dummy Head Mechanical Impedance

Figure A-36

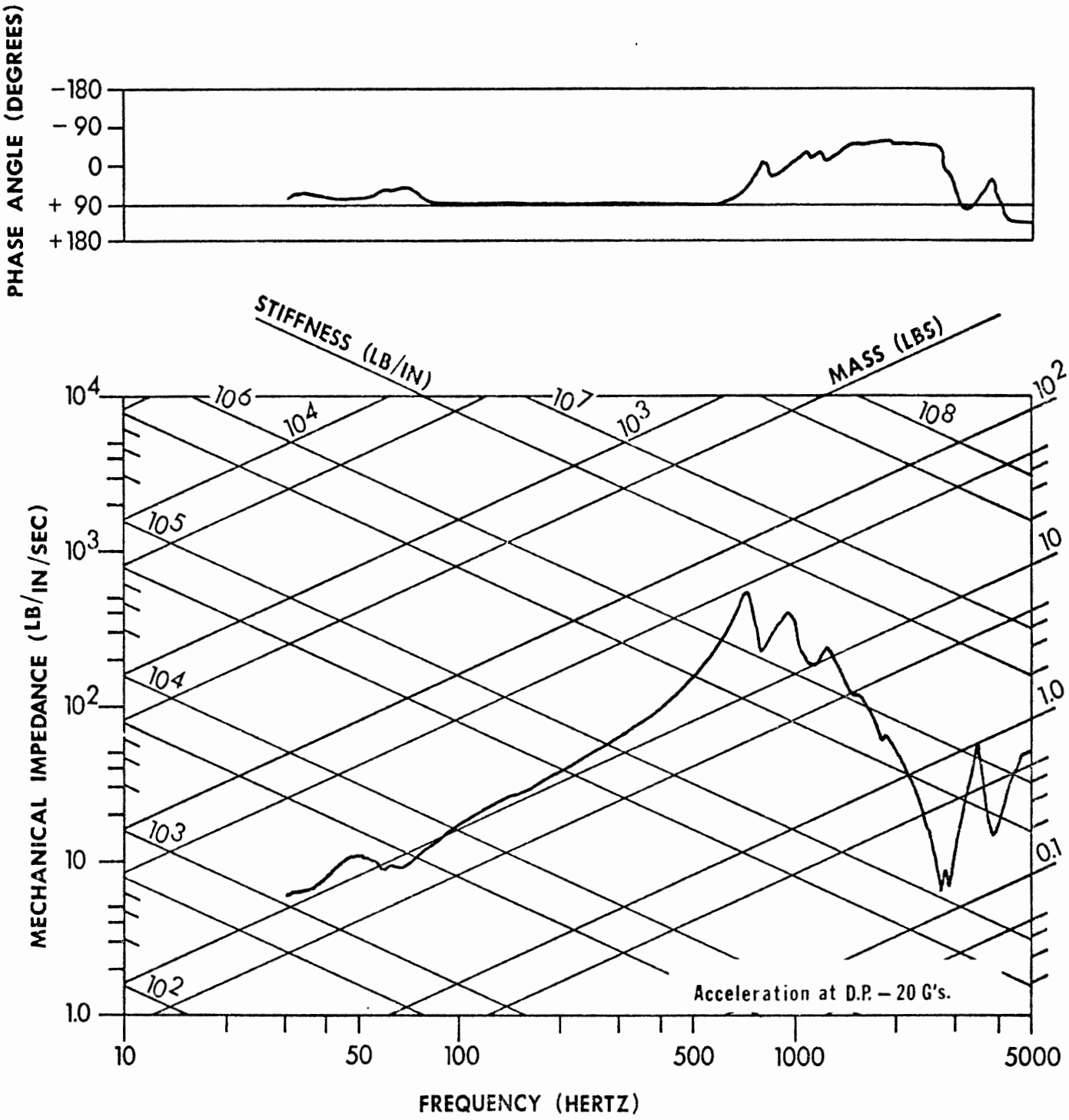

DRIVING POINT:	FRONTAL ☒	D.P.I.	☒
	OCCIPITAL ☐	T.P.I. (CENTER OF GRAVITY)	☐
	PARIETAL ☐	T.P.I. (POINT OPPOSITE D.P.)	☐

Test DHMZ-3 Dummy Head Mechanical Impedance

Figure A-37

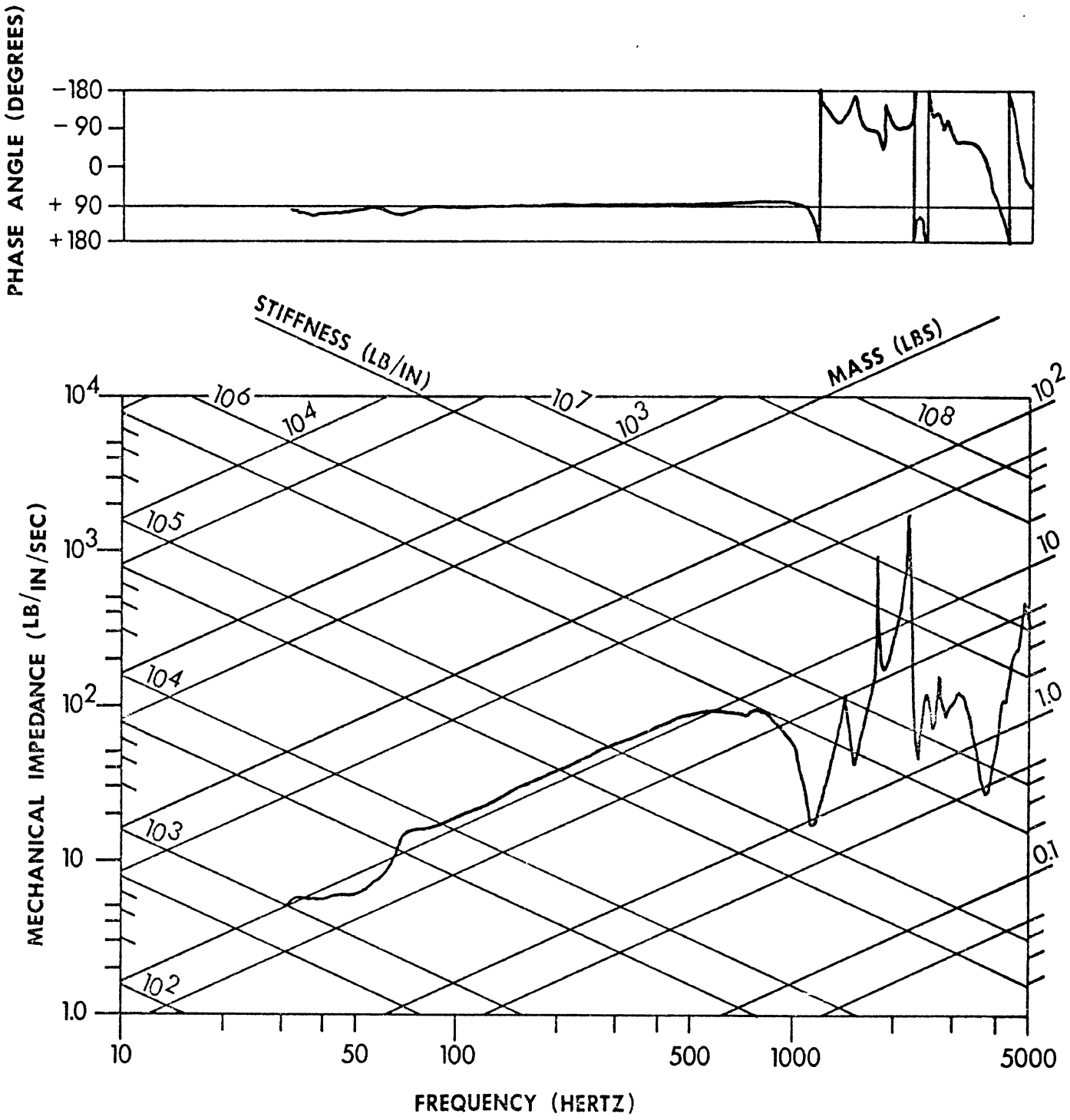

DRIVING POINT: FRONTAL ☒ D.P.I. ☐

OCCIPITAL ☐ T.P.I. (CENTER OF GRAVITY) ☒

PARIETAL ☐ T.P.I. (POINT OPPOSITE D.P.) ☐

Test DHMZ-3 Dummy Head Mechanical Impedance

Figure A-38

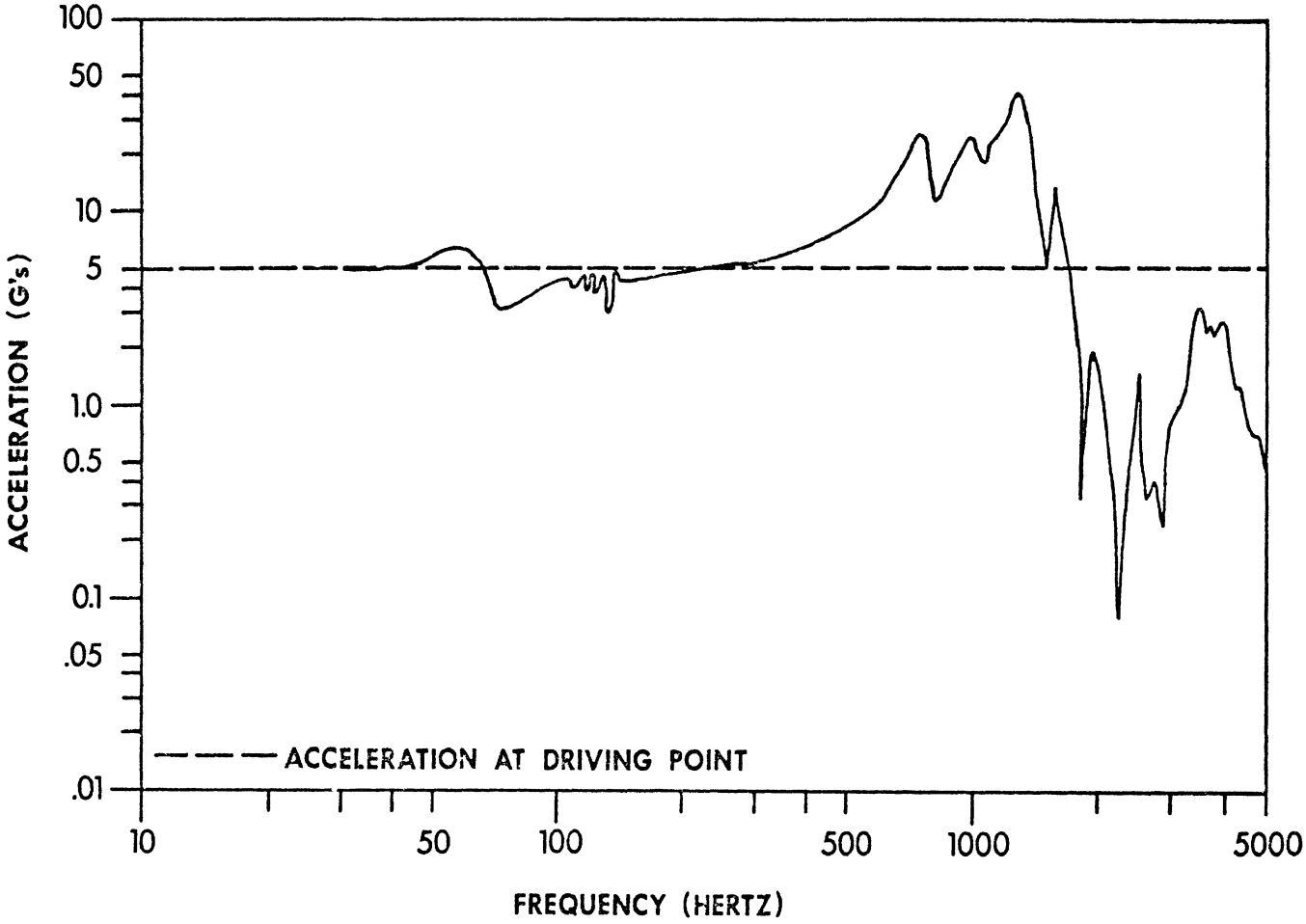

DRIVING POINT: FRONTAL ☒
OCCIPITAL ☐
PARIETAL ☐

TRANSFER POINT ACCELERATION:
CENTER OF GRAVITY ☒
POINT OPPOSITE D.P. ☐

Test DHMZ-3 Dummy Head Accelerations

Figure A-39

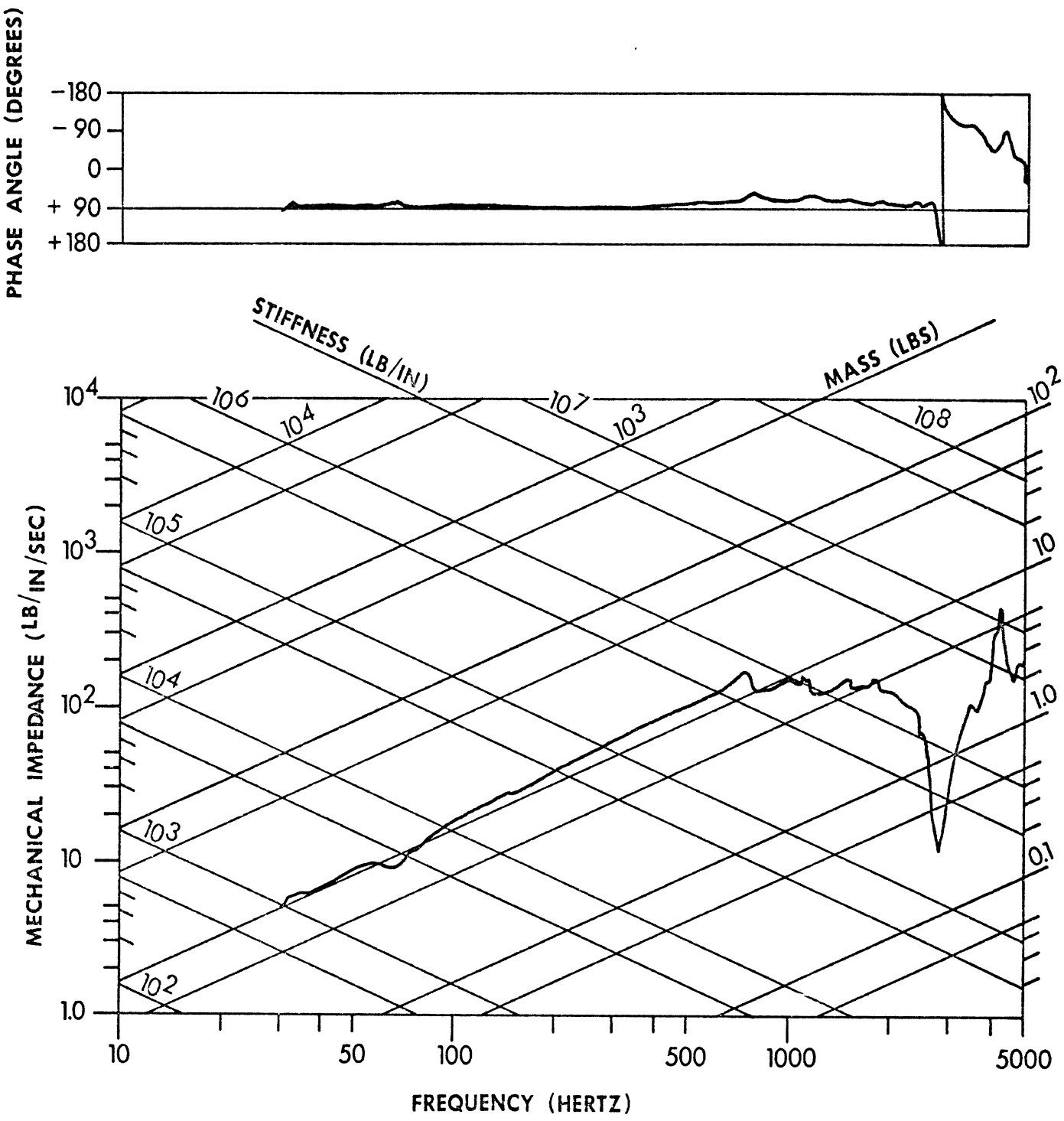

DRIVING POINT: FRONTAL ☒ D.P.I. ☐

OCCIPITAL ☐ T.P.I. (CENTER OF GRAVITY) ☐

PARIETAL ☐ T.P.I. (POINT OPPOSITE D.P.) ☒

Test DHMZ-3 Dummy Head Mechanical Impedance

Figure A-40

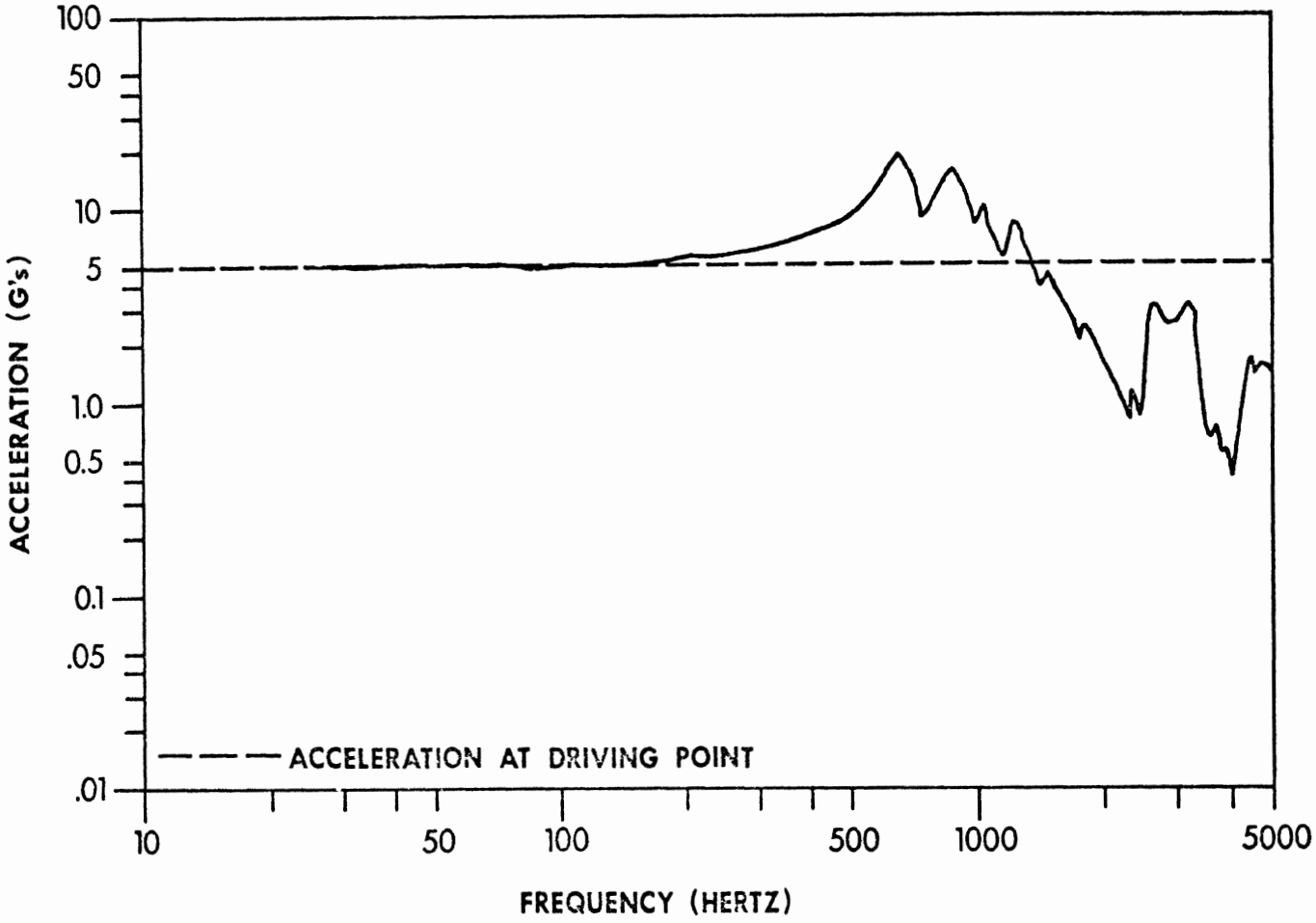

DRIVING POINT: FRONTAL ☒
OCCIPITAL ☐
PARIETAL ☐

TRANSFER POINT ACCELERATION:
CENTER OF GRAVITY ☐
POINT OPPOSITE D.P. ☒

Test DHMZ-3 Dummy Head Accelerations

Figure A-41

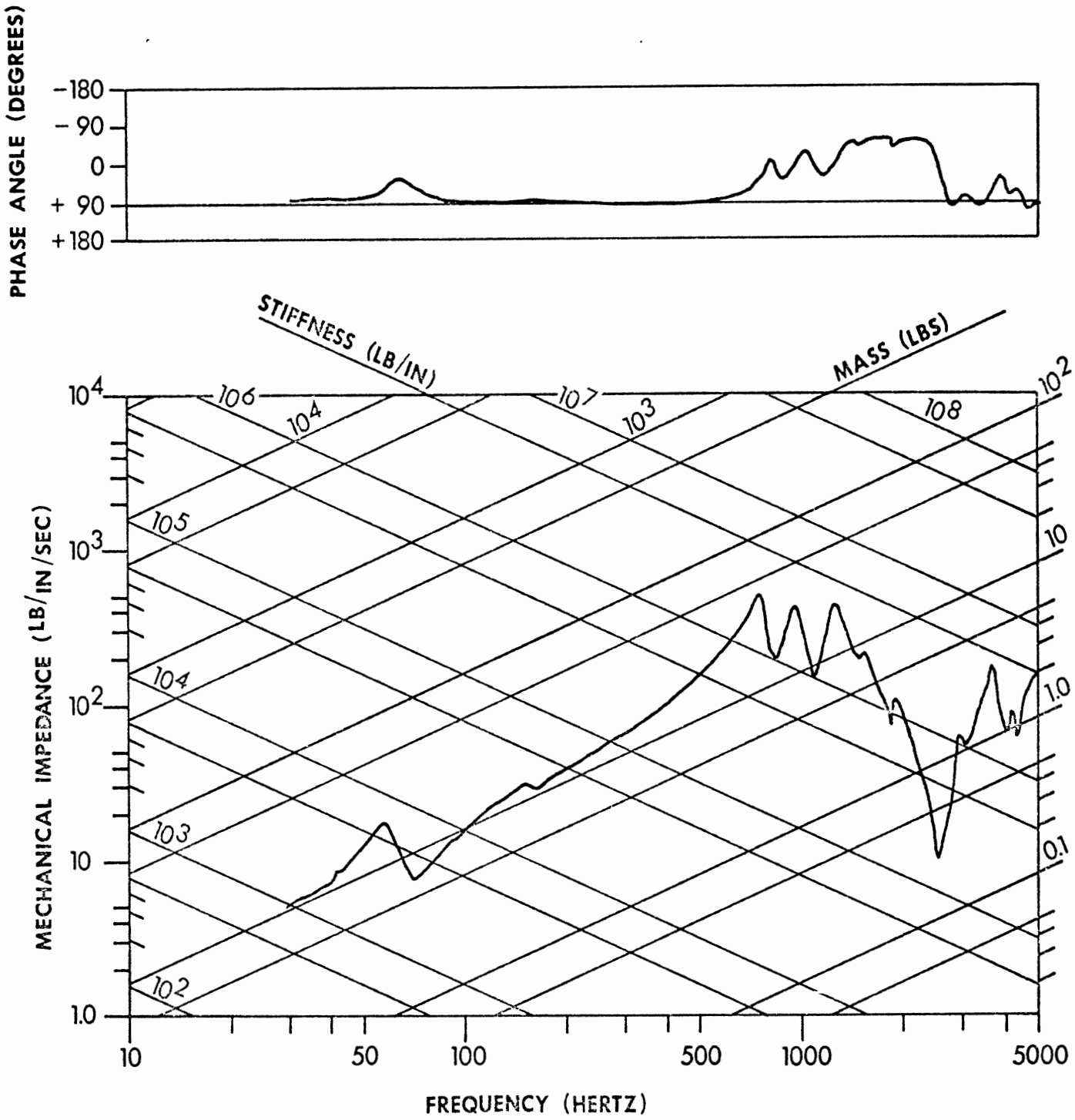

DRIVING POINT:	FRONTAL ☐	D.P.I.	☒
	OCCIPITAL ☒	T.P.I. (CENTER OF GRAVITY)	☐
	PARIETAL ☐	T.P.I. (POINT OPPOSITE D.P.)	☐

Test DHMZ-3 Dummy Head Mechanical Impedance

Figure A-42

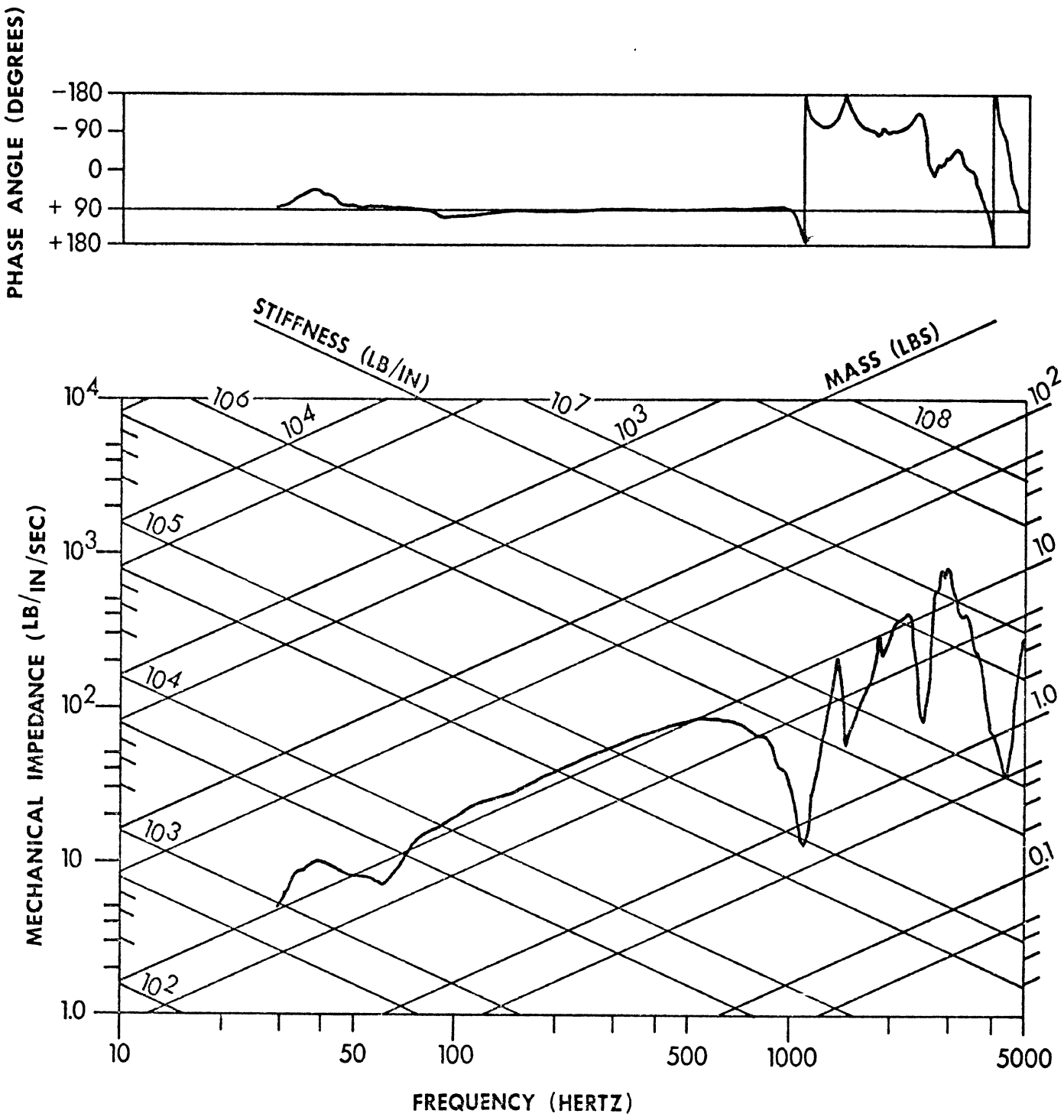

DRIVING POINT: FRONTAL ☐ D.P.I. ☐

OCCIPITAL ☒ T.P.I. (CENTER OF GRAVITY) ☒

PARIETAL ☐ T.P.I. (POINT OPPOSITE D.P.) ☐

Test DHMZ-3 Dummy Head Mechanical Impedance

Figure A-43

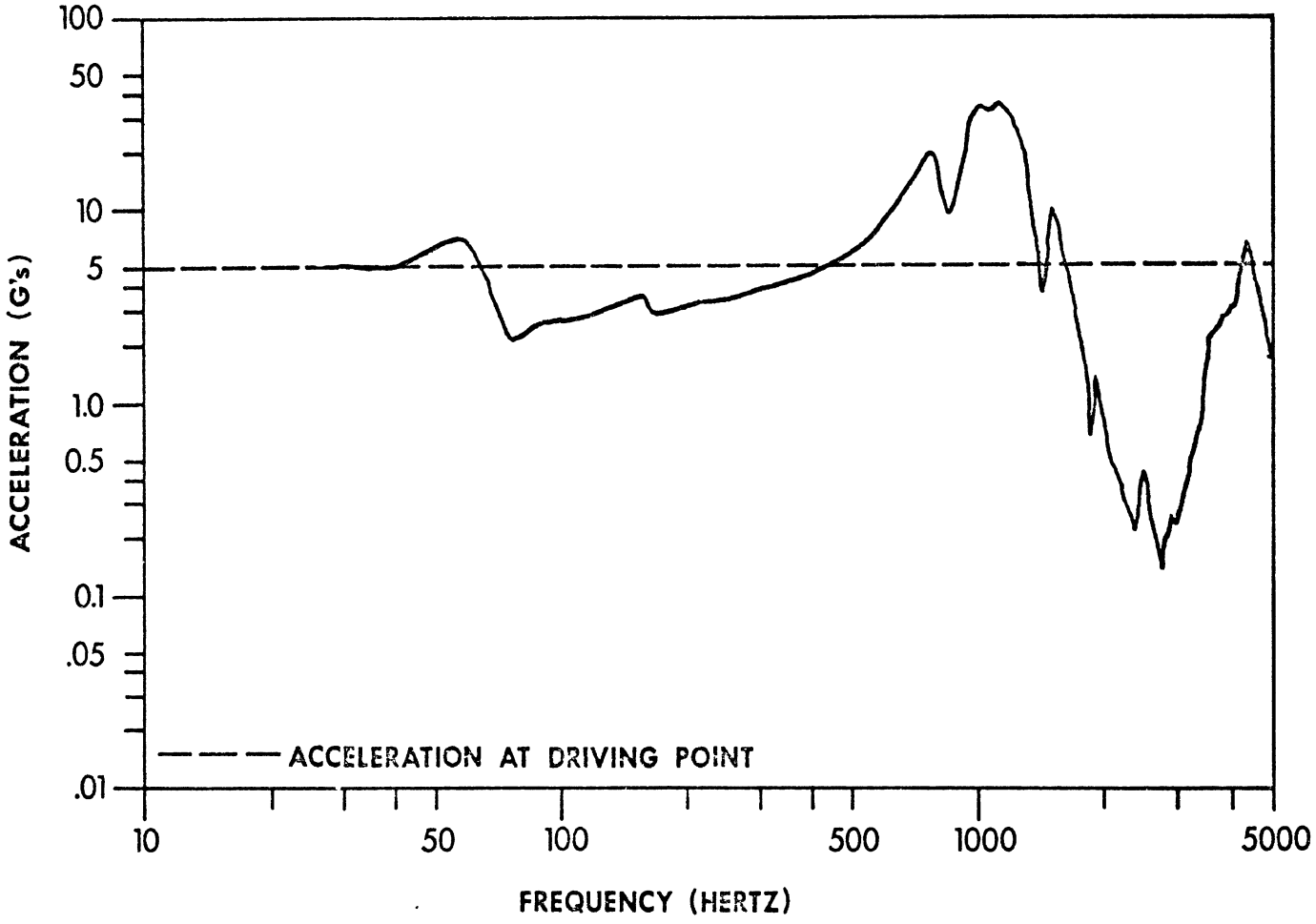

DRIVING POINT: FRONTAL ☐
OCCIPITAL ☒
PARIETAL ☐

TRANSFER POINT ACCELERATION:
CENTER OF GRAVITY ☒
POINT OPPOSITE D.P. ☐

Test DHMZ-3 Dummy Head Accelerations

Figure A-44

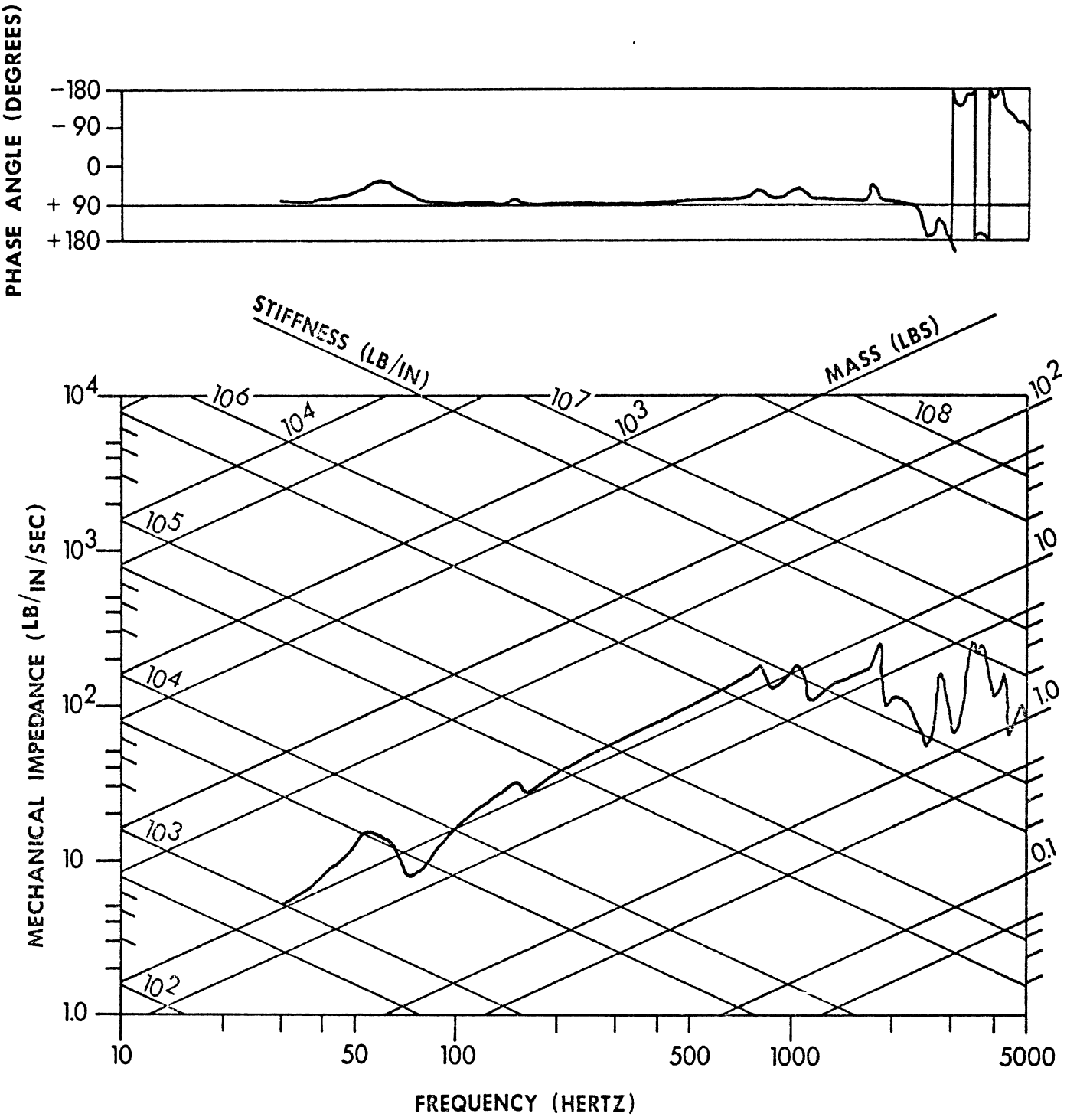

DRIVING POINT: FRONTAL ☐ D.P.I. ☐

OCCIPITAL ☒ T.P.I. (CENTER OF GRAVITY) ☐

PARIETAL ☐ T.P.I. (POINT OPPOSITE D.P.) ☒

Test DHMZ-3 Dummy Head Mechanical Impedance

Figure A-45

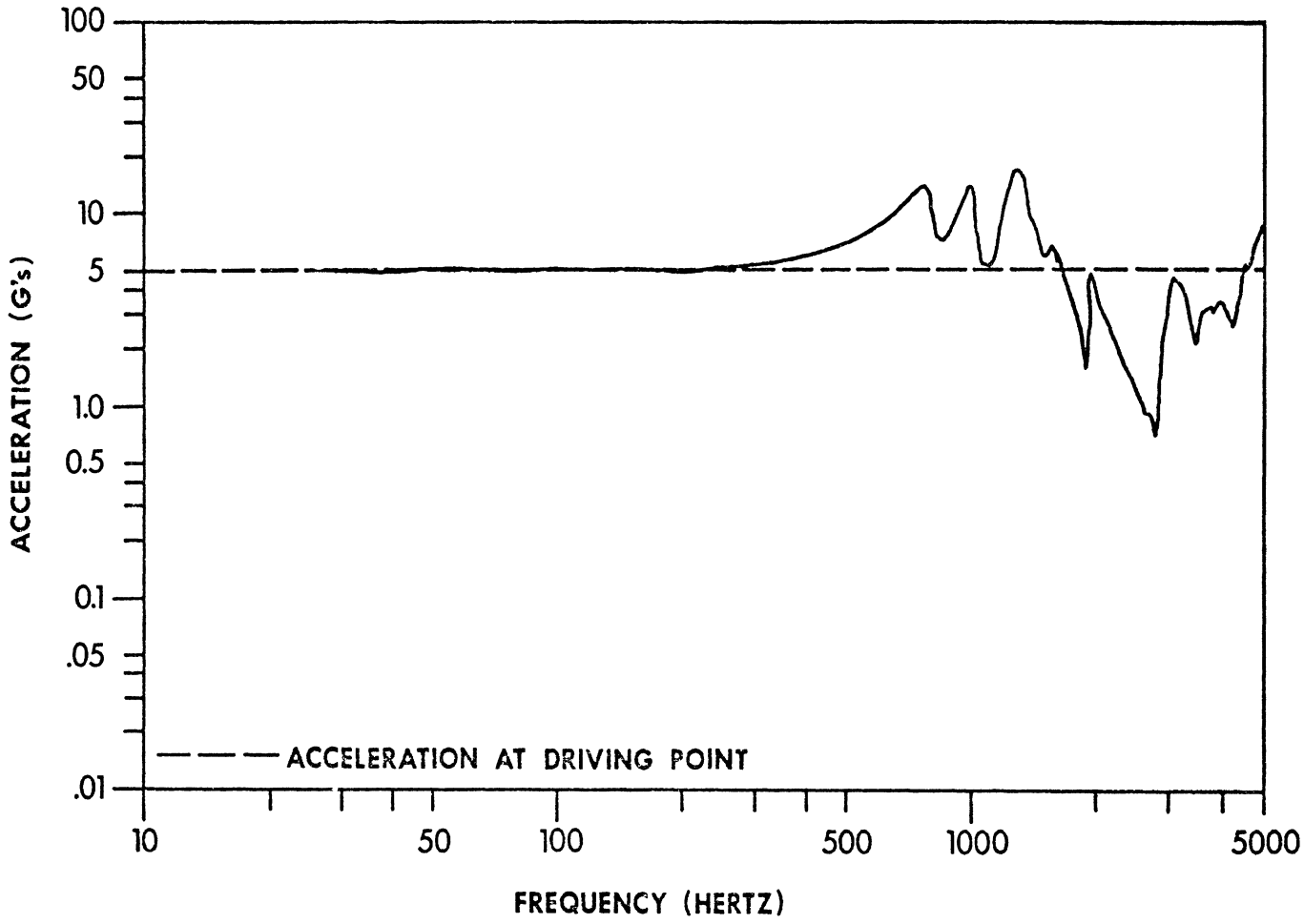

DRIVING POINT: FRONTAL ☐
OCCIPITAL ☒
PARIETAL ☐

TRANSFER POINT ACCELERATION:
CENTER OF GRAVITY ☐
POINT OPPOSITE D.P. ☒

Test DHMZ-3 Dummy Head Accelerations

Figure A-46

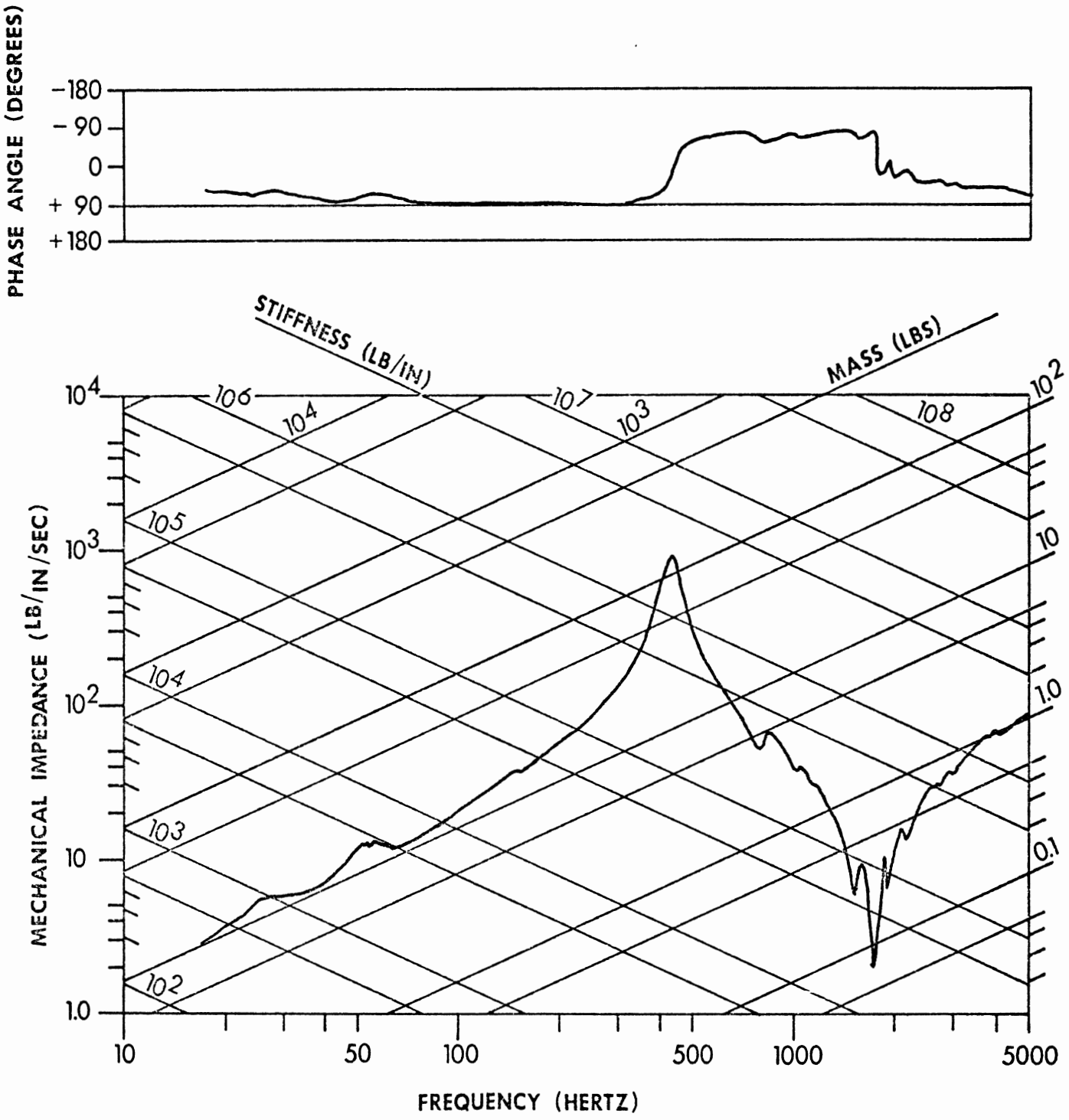

DRIVING POINT: FRONTAL ☐ D.P.I. ☒

OCCIPITAL ☐ T.P.I. (CENTER OF GRAVITY) ☐

PARIETAL ☒ T.P.I. (POINT OPPOSITE D.P.) ☐

Test DHMZ-3 Dummy Head Mechanical Impedance

Figure A-47

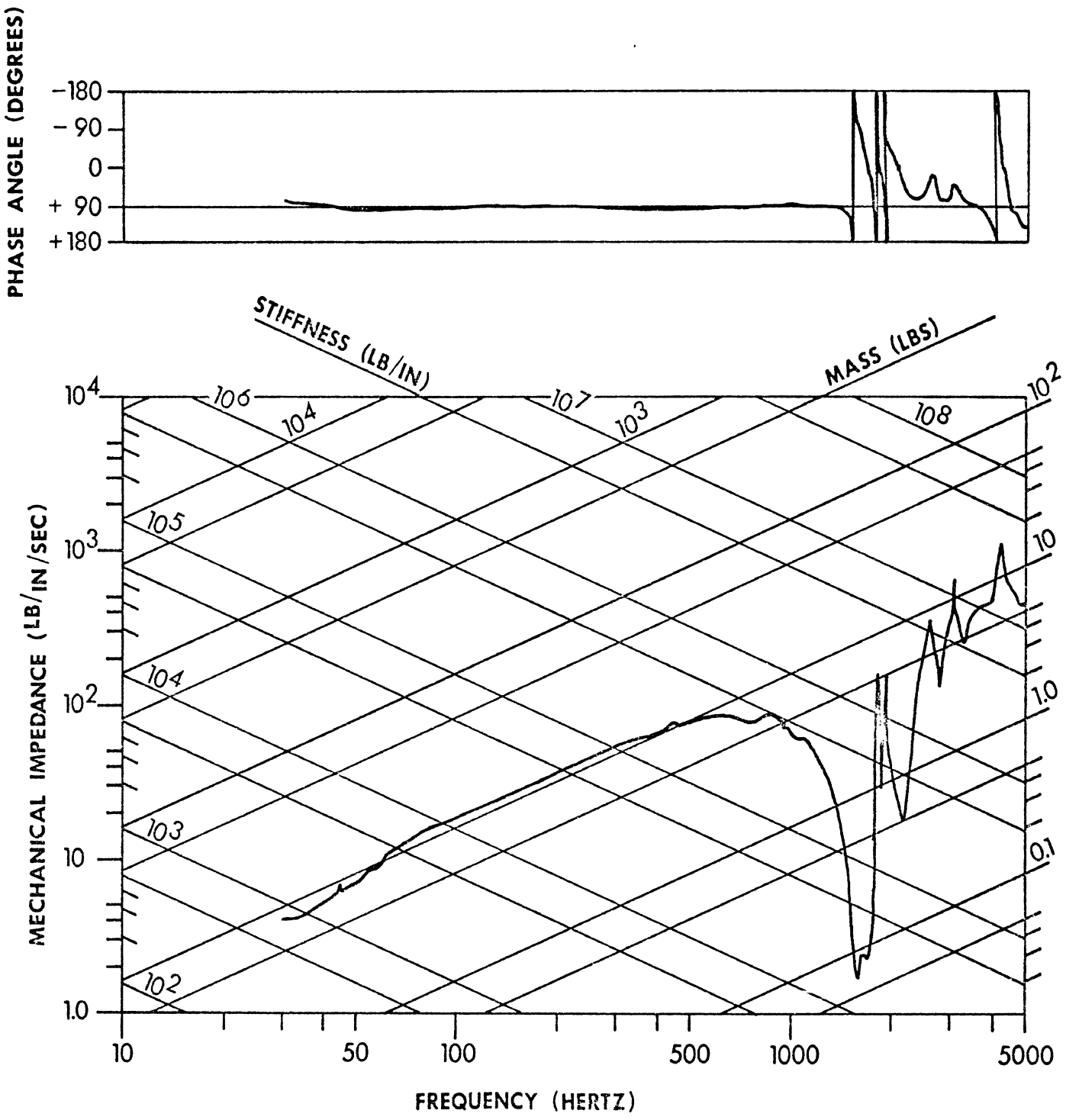

DRIVING POINT: FRONTAL ☐ D.P.I. ☐

OCCIPITAL ☐ T.P.I. (CENTER OF GRAVITY) ☒

PARIETAL ☒ T.P.I. (POINT OPPOSITE D.P.) ☐

Test DHMZ-3 Dummy Head Mechanical Impedance

Figure A-48

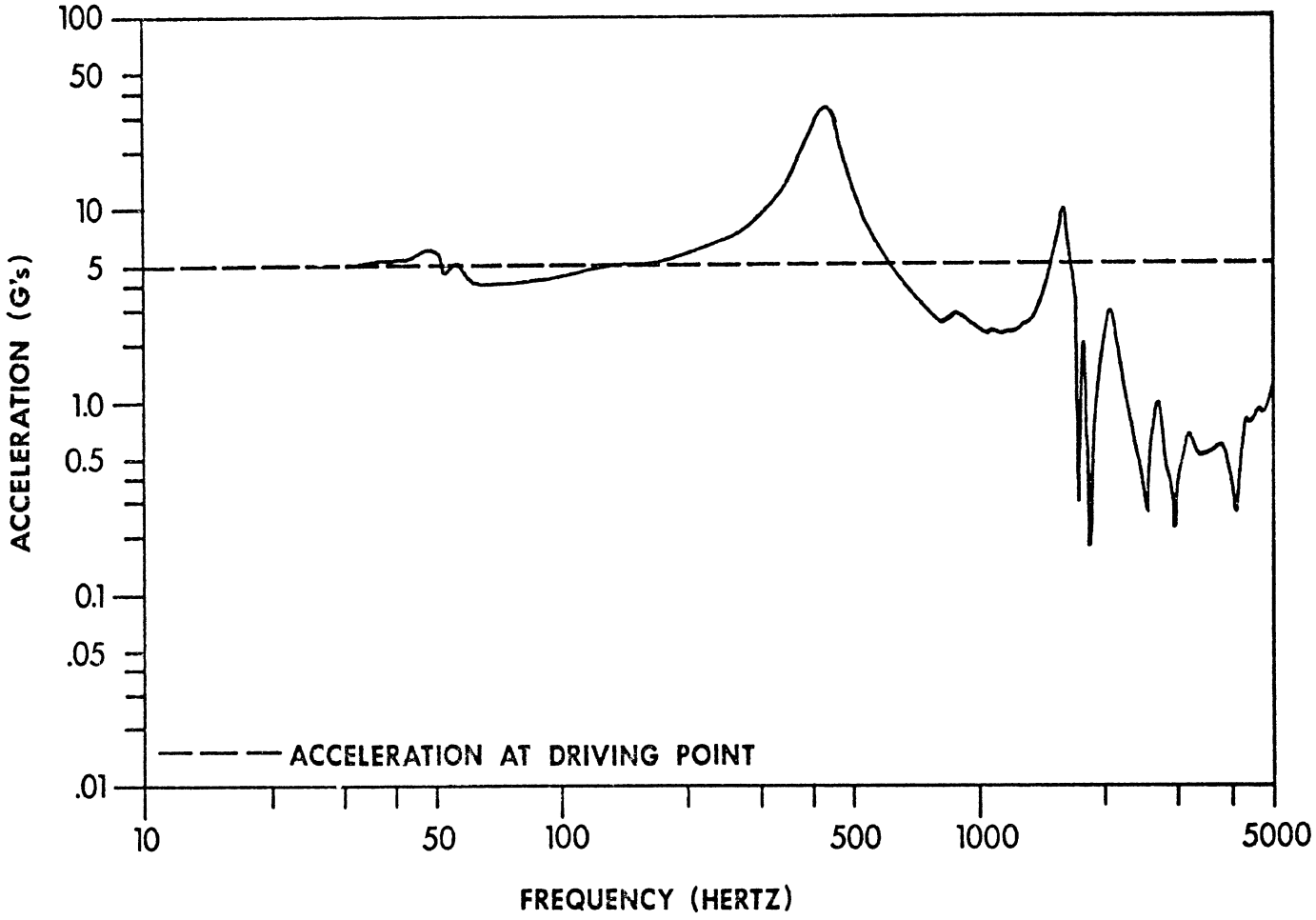

DRIVING POINT: FRONTAL ☐
OCCIPITAL ☐
PARIETAL ☒

TRANSFER POINT ACCELERATION:
CENTER OF GRAVITY ☒
POINT OPPOSITE D.P. ☐

Test DHMZ-3 Dummy Head Accelerations

Figure A-49

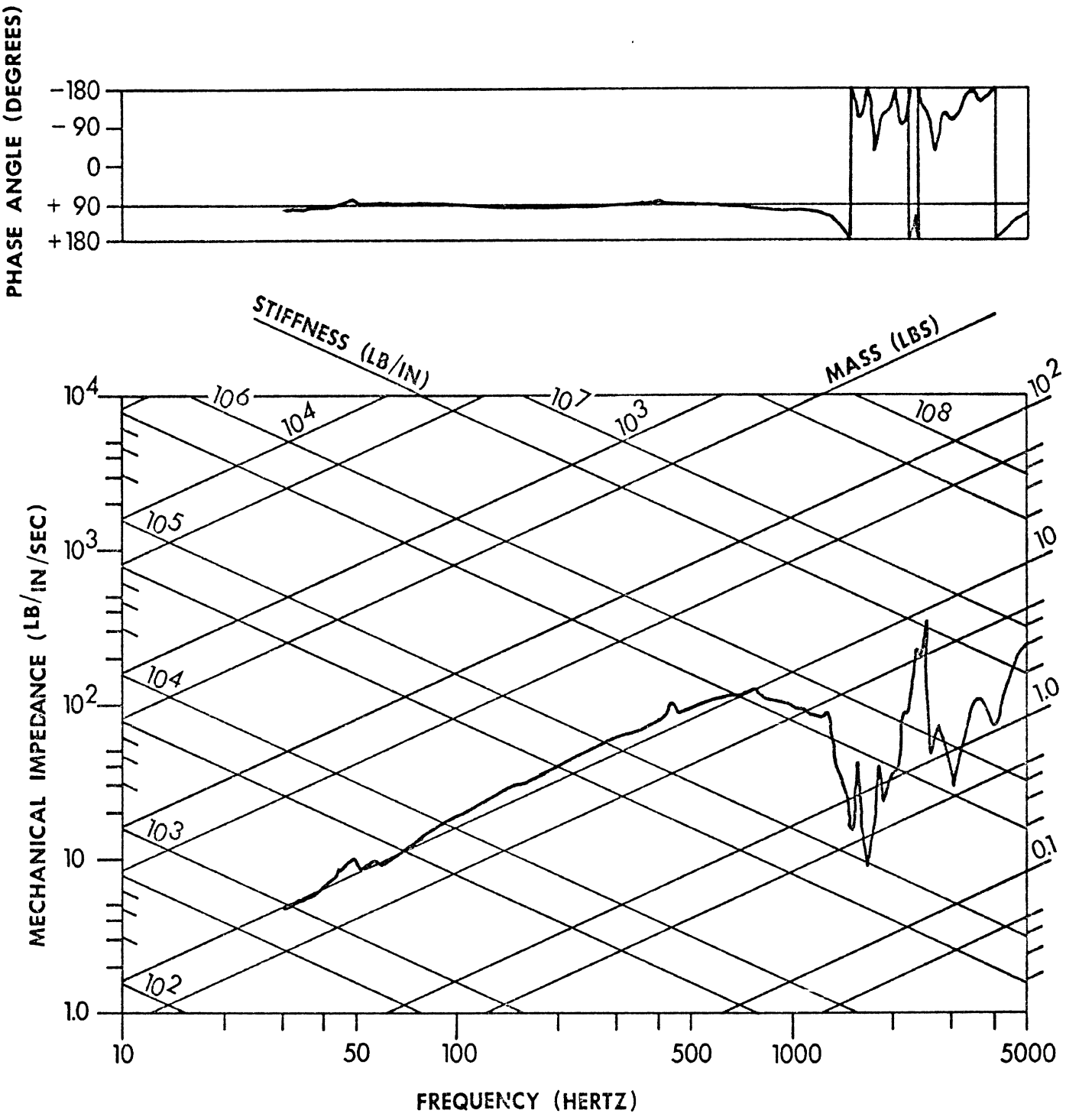

DRIVING POINT: FRONTAL ☐ D.P.I. ☐

OCCIPITAL ☐ T.P.I. (CENTER OF GRAVITY) ☐

PARIETAL ☒ T.P.I. (POINT OPPOSITE D.P.) ☒

Test DHMZ-3 Dummy Head Mechanical Impedance

Figure A-50

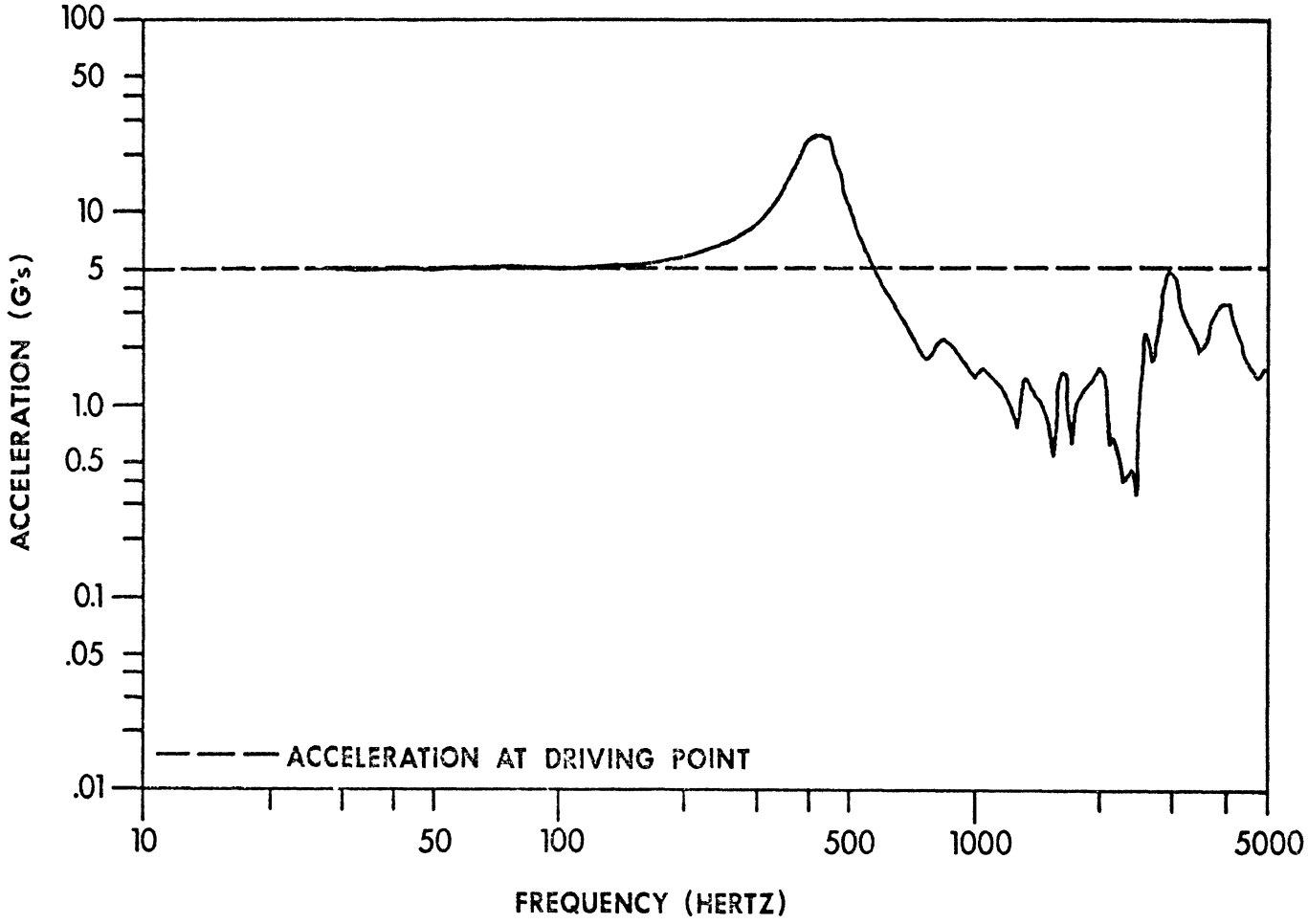

DRIVING POINT: FRONTAL ☐
OCCIPITAL ☐
PARIETAL ☒

TRANSFER POINT ACCELERATION:
CENTER OF GRAVITY ☐
POINT OPPOSITE D.P. ☒

Test DHMZ-3 Dummy Head Accelerations

Figure A-51

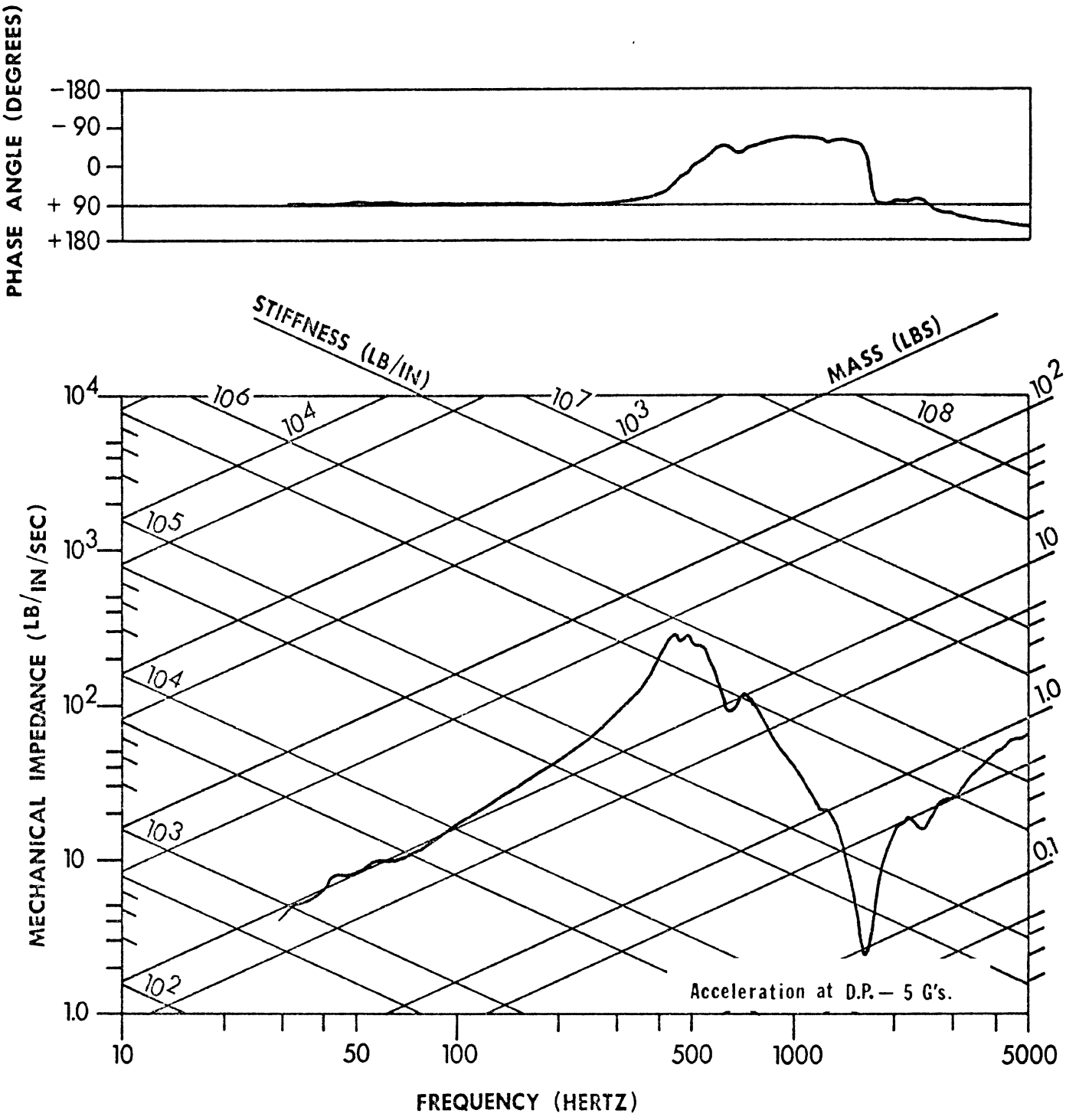

DRIVING POINT: FRONTAL ☒ D.P.I. ☒

OCCIPITAL ☐ T.P.I. (CENTER OF GRAVITY) ☐

PARIETAL ☐ T.P.I. (POINT OPPOSITE D.P.) ☐

Test DHMZ-4 Dummy Head Mechanical Impedance

Figure A-52

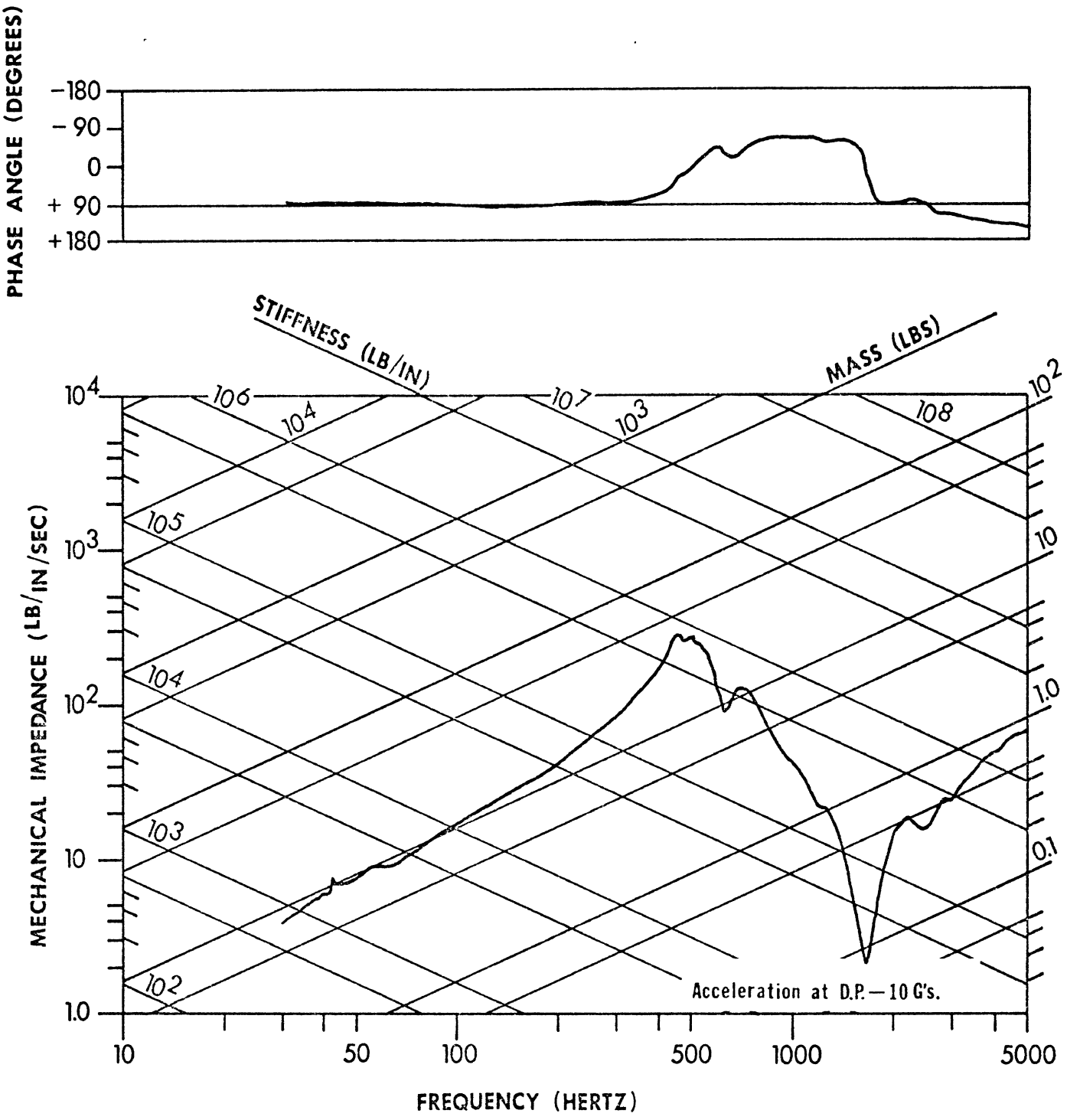

DRIVING POINT:	FRONTAL ☒	D.P.I.	☒
	OCCIPITAL ☐	T.P.I. (CENTER OF GRAVITY)	☐
	PARIETAL ☐	T.P.I. (POINT OPPOSITE D.P.)	☐

Test DHMZ-4 Dummy Head Mechanical Impedance

Figure A-53

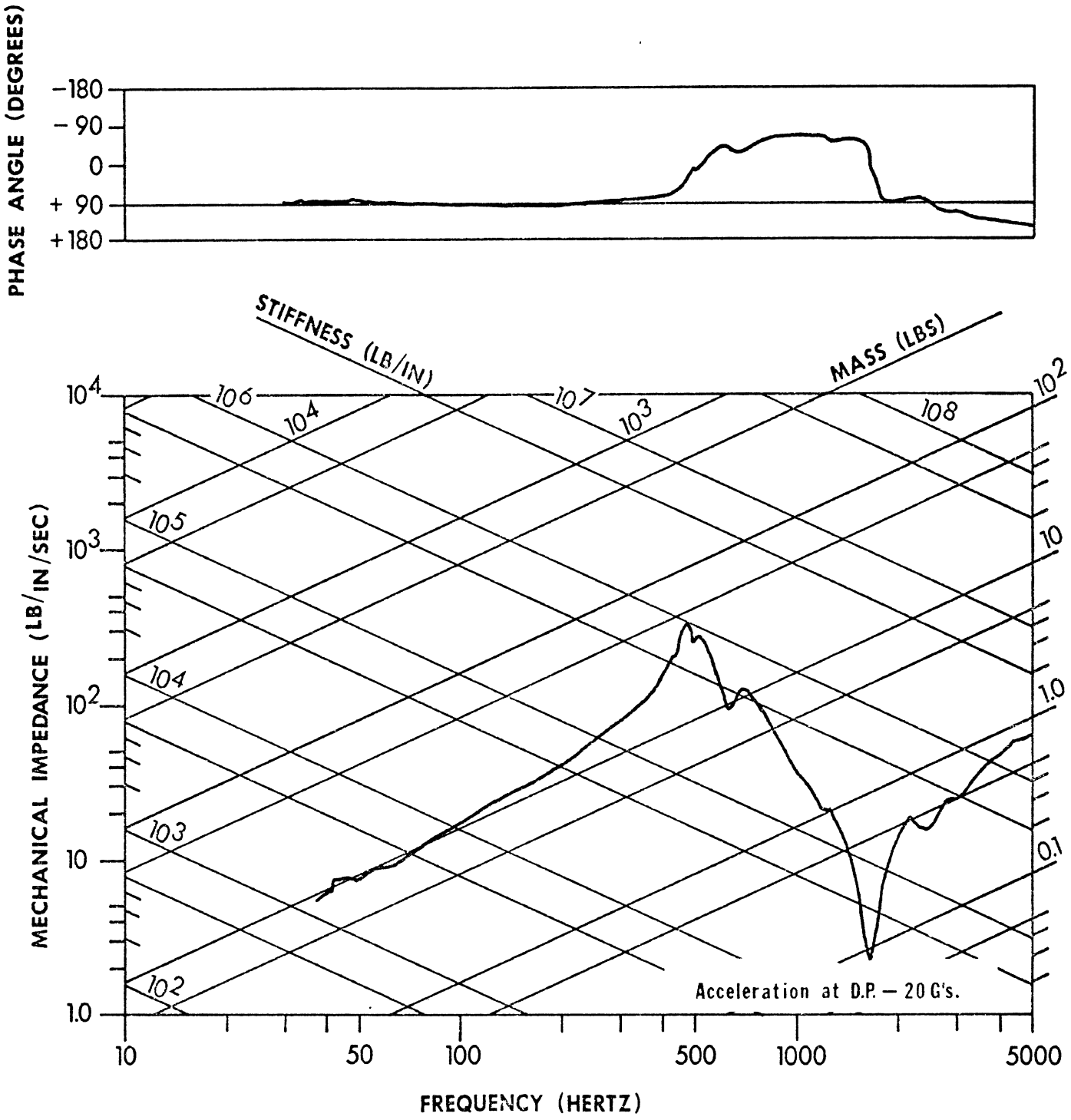

DRIVING POINT: FRONTAL ☒ D.P.I. ☒

OCCIPITAL ☐ T.P.I. (CENTER OF GRAVITY) ☐

PARIETAL ☐ T.P.I. (POINT OPPOSITE D.P.) ☐

Test DHMZ-4 Dummy Head Mechanical Impedance

Figure A-54

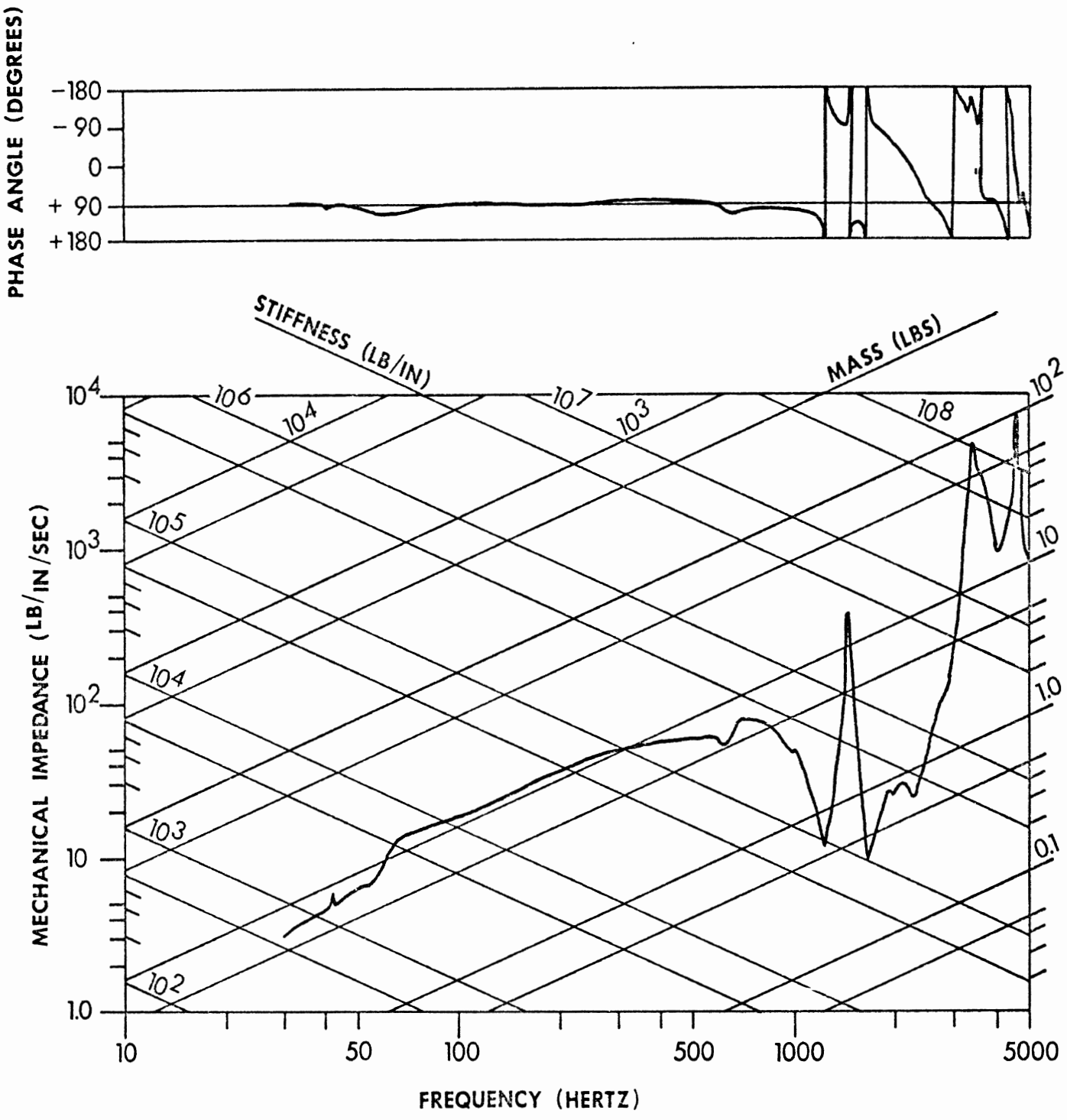

DRIVING POINT: FRONTAL ☒ D.P.I. ☐

OCCIPITAL ☐ T.P.I. (CENTER OF GRAVITY) ☒

PARIETAL ☐ T.P.I. (POINT OPPOSITE D.P.) ☐

Test DHMZ-4 Dummy Head Mechanical Impedance

Figure A-55

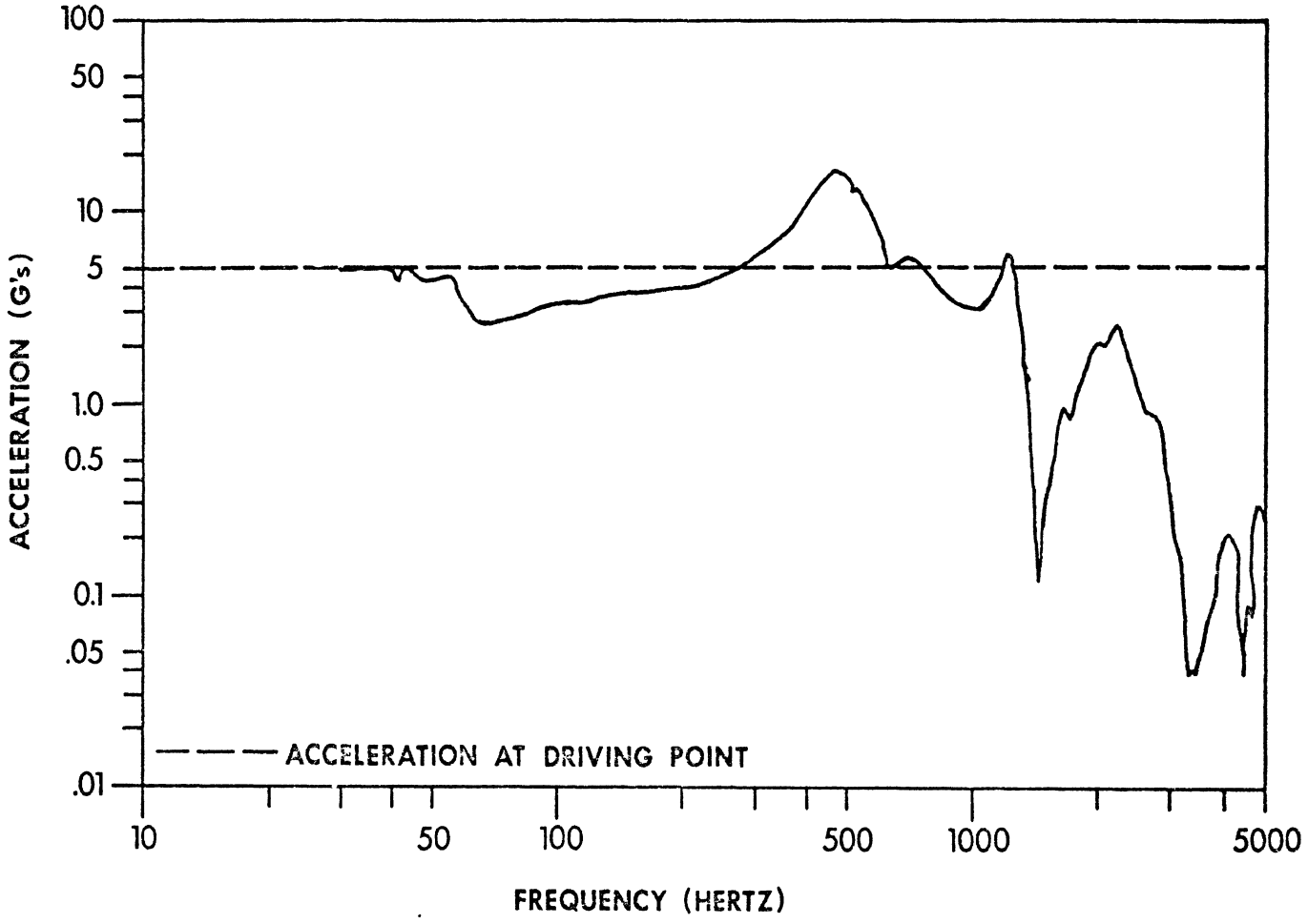

DRIVING POINT: FRONTAL ☒
OCCIPITAL ☐
PARIETAL ☐

TRANSFER POINT ACCELERATION:
CENTER OF GRAVITY ☒
POINT OPPOSITE D.P. ☐

Test DHMZ-4 Dummy Head Accelerations

Figure A-56

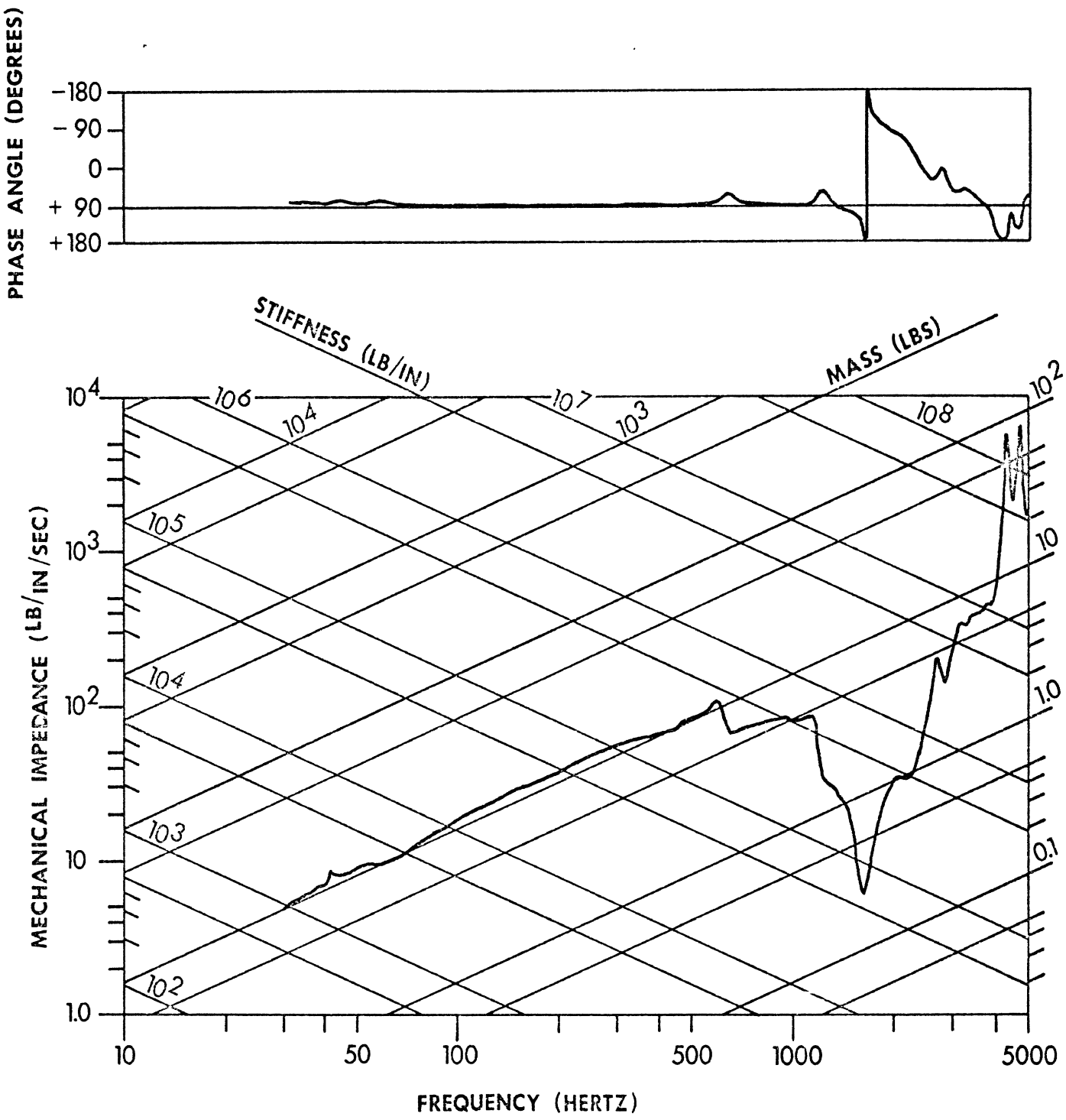

DRIVING POINT: FRONTAL ☒ D.P.I. ☐

OCCIPITAL ☐ T.P.I. (CENTER OF GRAVITY) ☐

PARIETAL ☐ T.P.I. (POINT OPPOSITE D.P.) ☒

Test DHMZ-4 Dummy Head Mechanical Impedance

Figure A-57

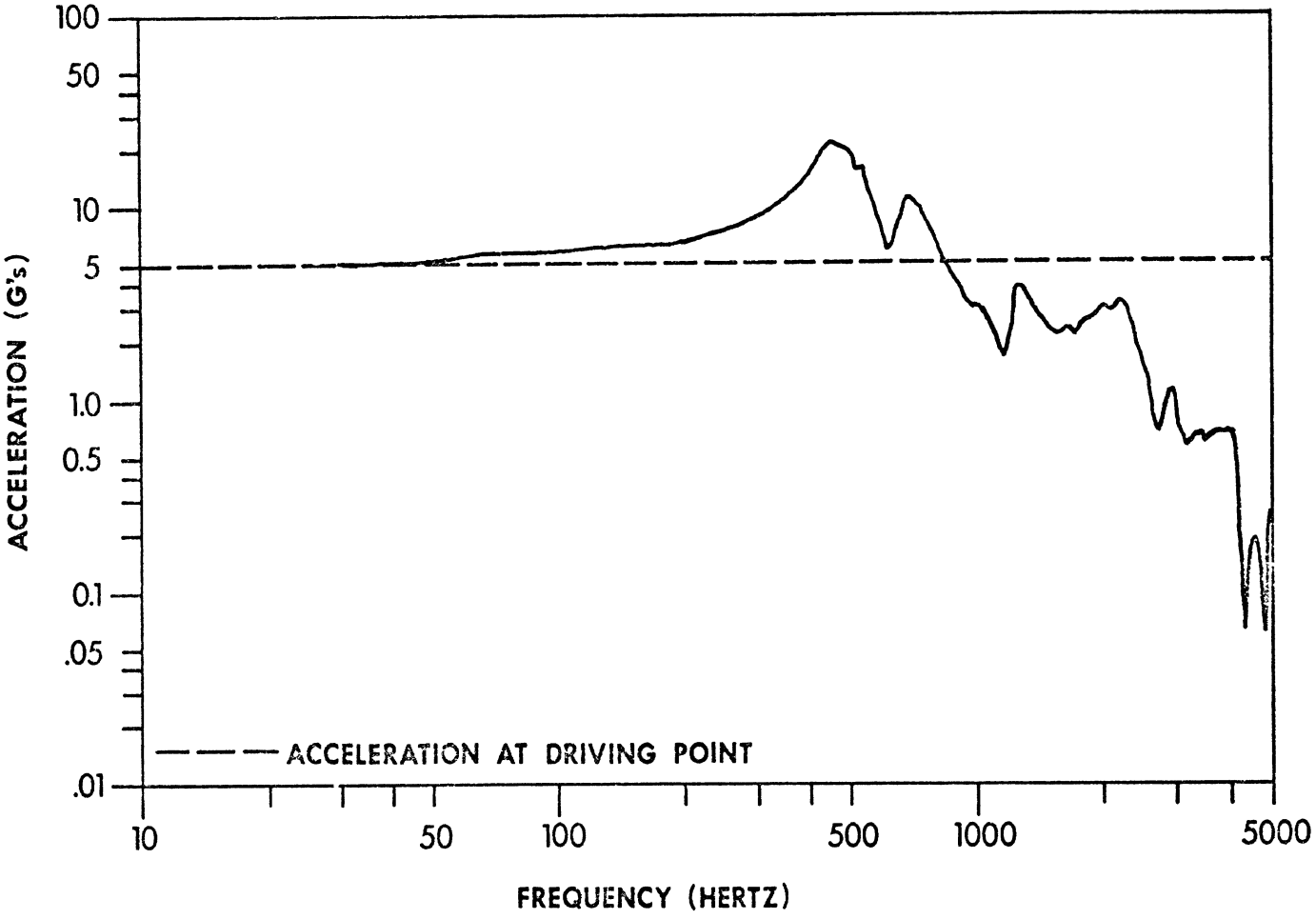

DRIVING POINT: FRONTAL ☒
OCCIPITAL ☐
PARIETAL ☐

TRANSFER POINT ACCELERATION:
CENTER OF GRAVITY ☐
POINT OPPOSITE D.P. ☒

Test DHMZ-4 Dummy Head Accelerations

Figure A-58

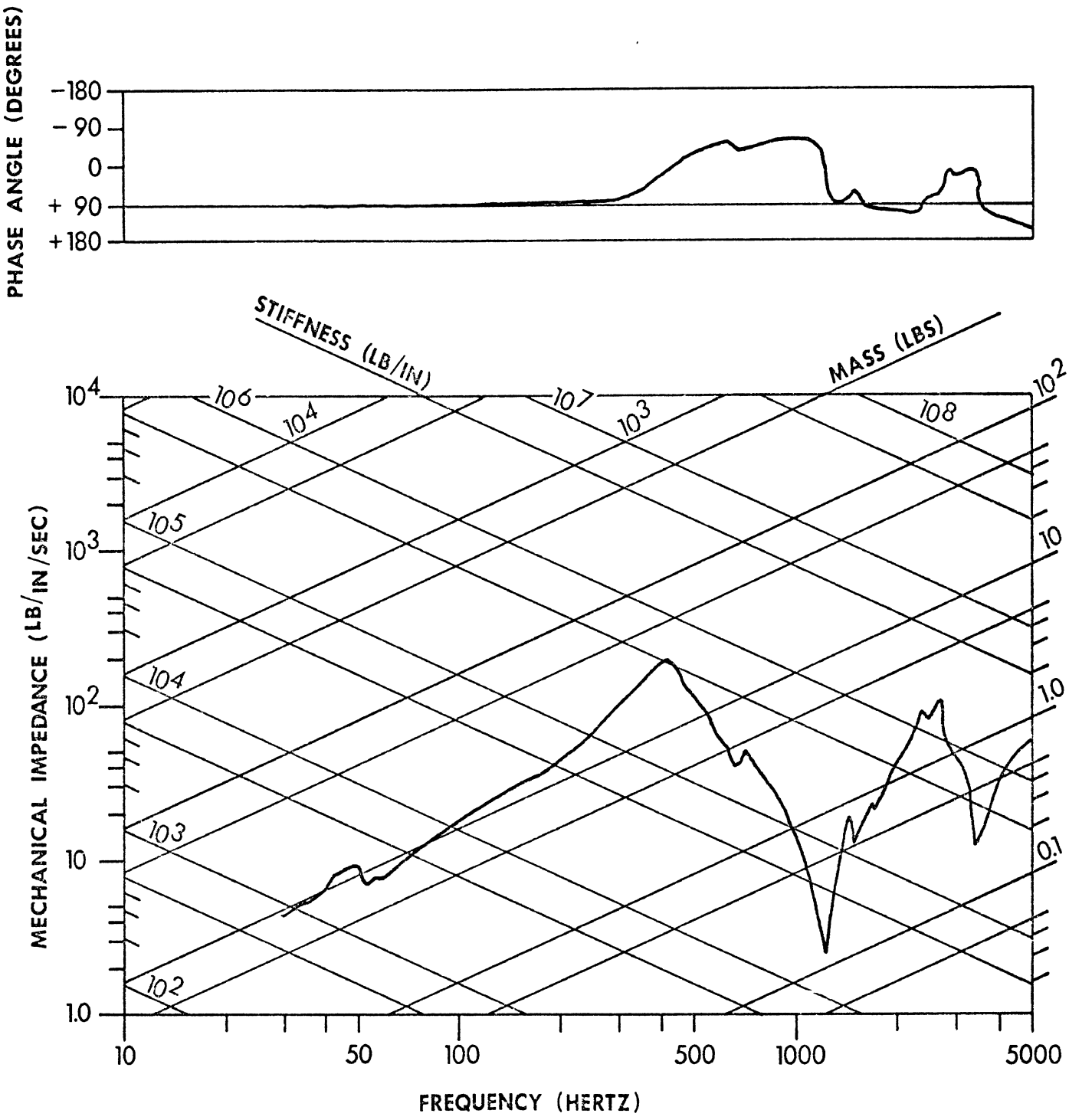

DRIVING POINT: FRONTAL ☐ D.P.I. ☒

OCCIPITAL ☒ T.P.I. (CENTER OF GRAVITY) ☐

PARIETAL ☐ T.P.I. (POINT OPPOSITE D.P.) ☐

Test DHMZ-4 Dummy Head Mechanical Impedance

Figure A-59

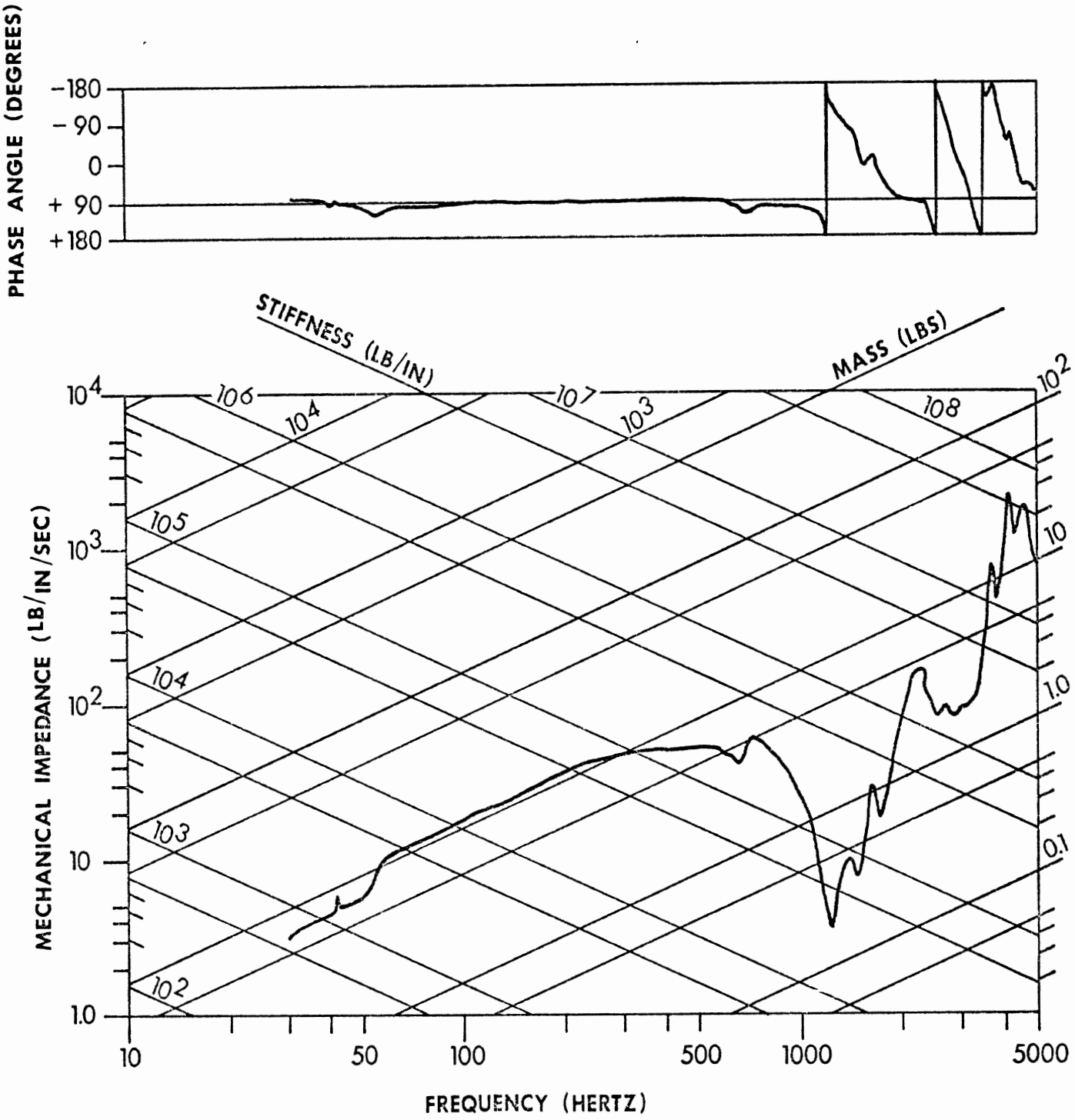

DRIVING POINT:	FRONTAL ☐	D.P.I.	☐
	OCCIPITAL ☒	T.P.I. (CENTER OF GRAVITY)	☒
	PARIETAL ☐	T.P.I. (POINT OPPOSITE D.P.)	☐

Test DHMZ-4 Dummy Head Mechanical Impedance

Figure A-60

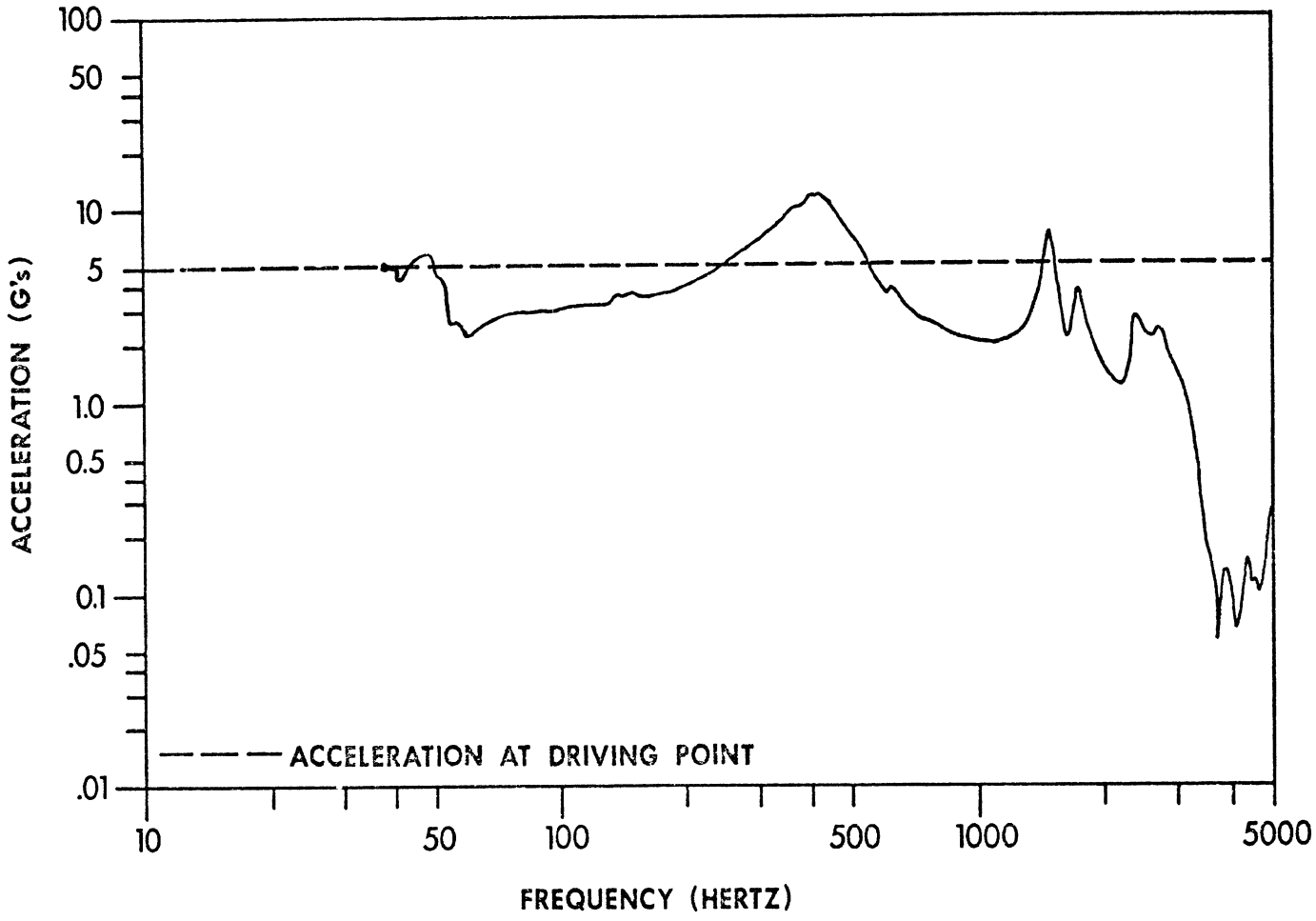

DRIVING POINT: FRONTAL ☐
OCCIPITAL ☒
PARIETAL ☐

TRANSFER POINT ACCELERATION:
CENTER OF GRAVITY ☒
POINT OPPOSITE D.P. ☐

Test DHMZ-4 Dummy Head Accelerations

Figure A-61

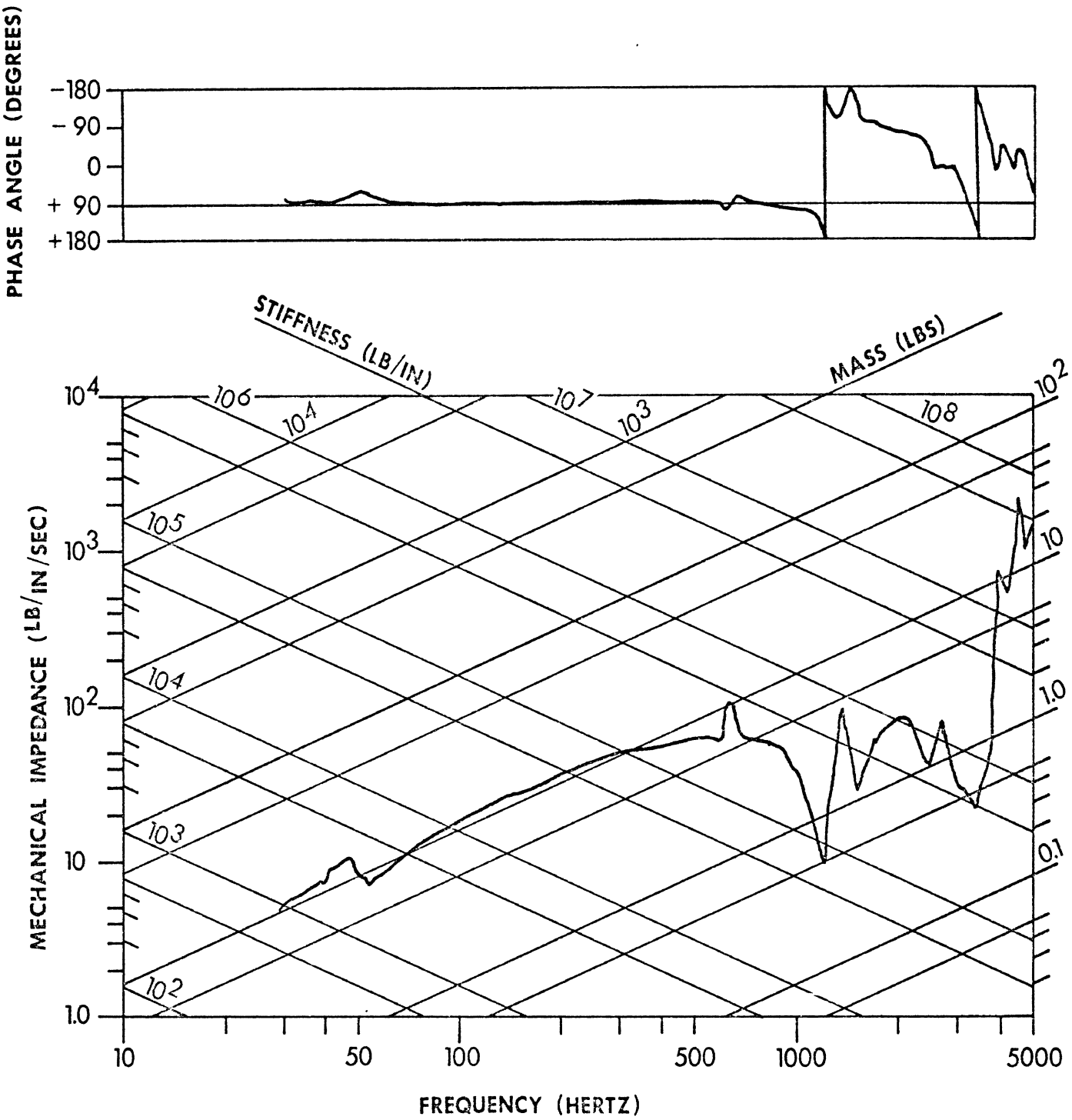

DRIVING POINT: FRONTAL ☐ D.P.I. ☐

OCCIPITAL ☒ T.P.I. (CENTER OF GRAVITY) ☐

PARIETAL ☐ T.P.I. (POINT OPPOSITE D.P.) ☒

Test DHMZ-4 Dummy Head Mechanical Impedance

Figure A-62

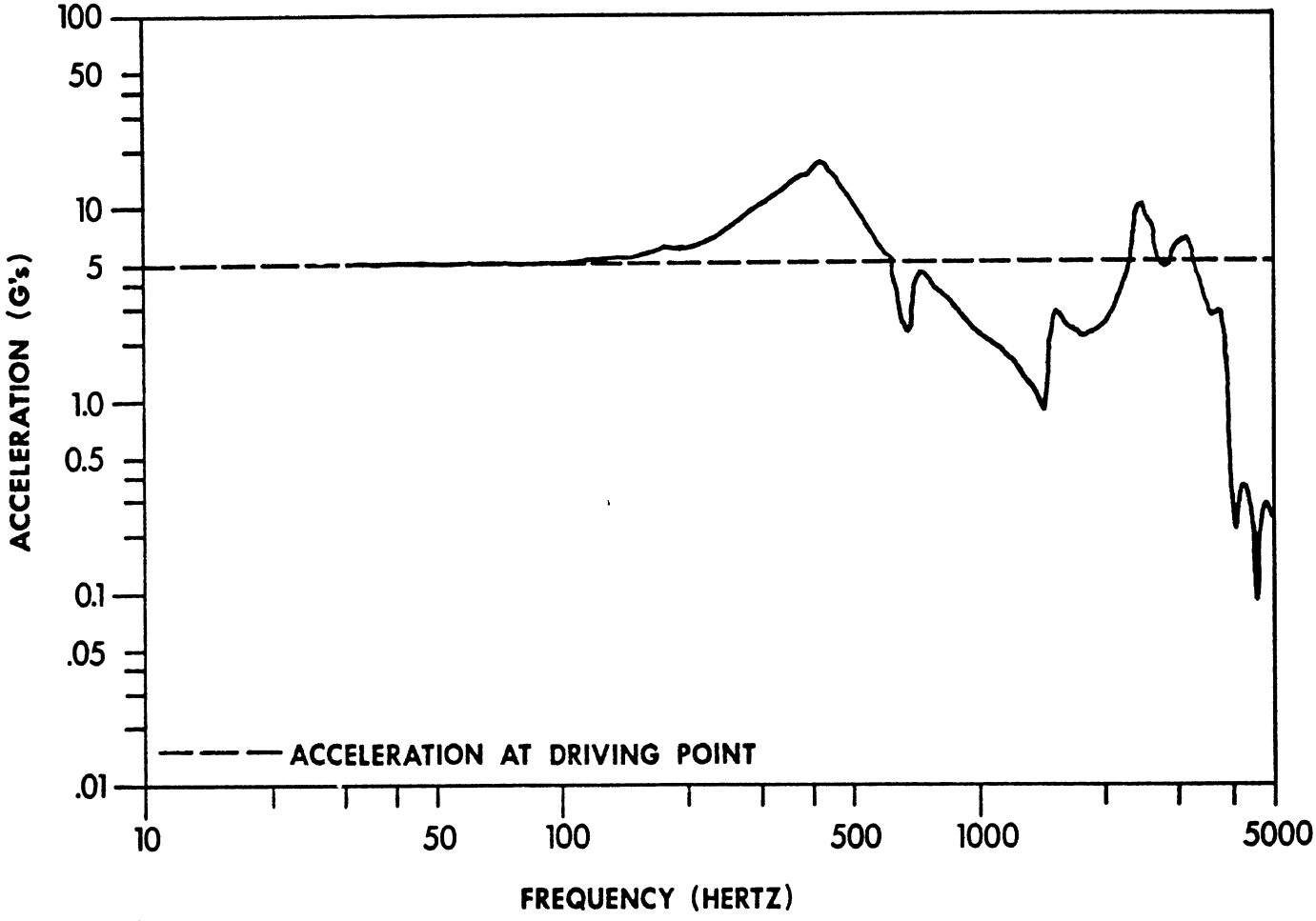

DRIVING POINT: FRONTAL ☐
OCCIPITAL ☒
PARIETAL ☐

TRANSFER POINT ACCELERATION:
CENTER OF GRAVITY ☐
POINT OPPOSITE D.P. ☒

Test DHMZ-4 Dummy Head Accelerations

Figure A-63

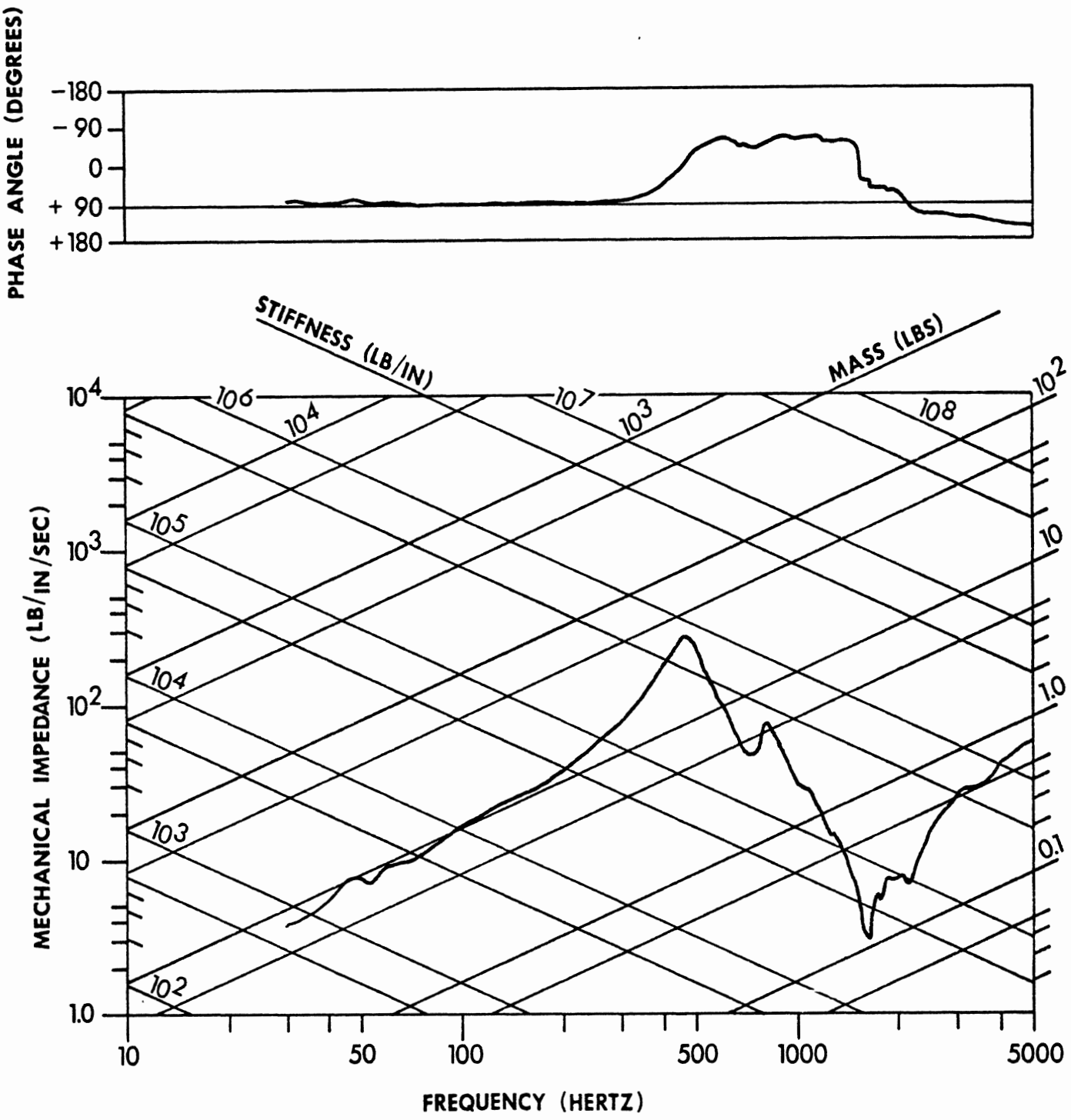

DRIVING POINT: FRONTAL ☐ D.P.I. ☒

OCCIPITAL ☐ T.P.I. (CENTER OF GRAVITY) ☐

PARIETAL ☒ T.P.I. (POINT OPPOSITE D.P.) ☐

Test DHMZ-4 Dummy Head Mechanical Impedance

Figure A-64

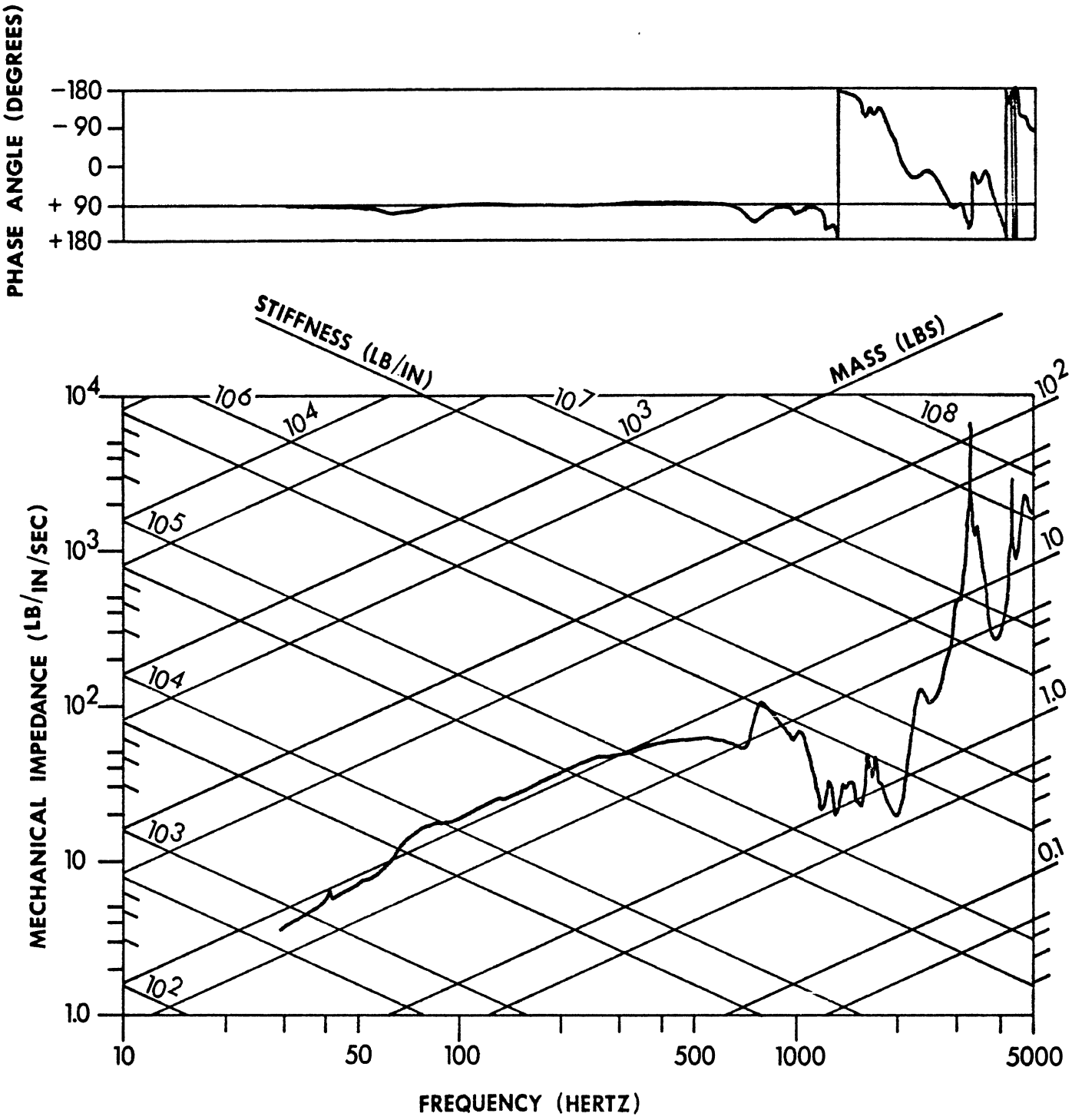

DRIVING POINT: FRONTAL ☐ D.P.I. ☐

OCCIPITAL ☐ T.P.I. (CENTER OF GRAVITY) ☒

PARIETAL ☒ T.P.I. (POINT OPPOSITE D.P.) ☐

Test DHMZ-4 Dummy Head Mechanical Impedance

Figure A-65

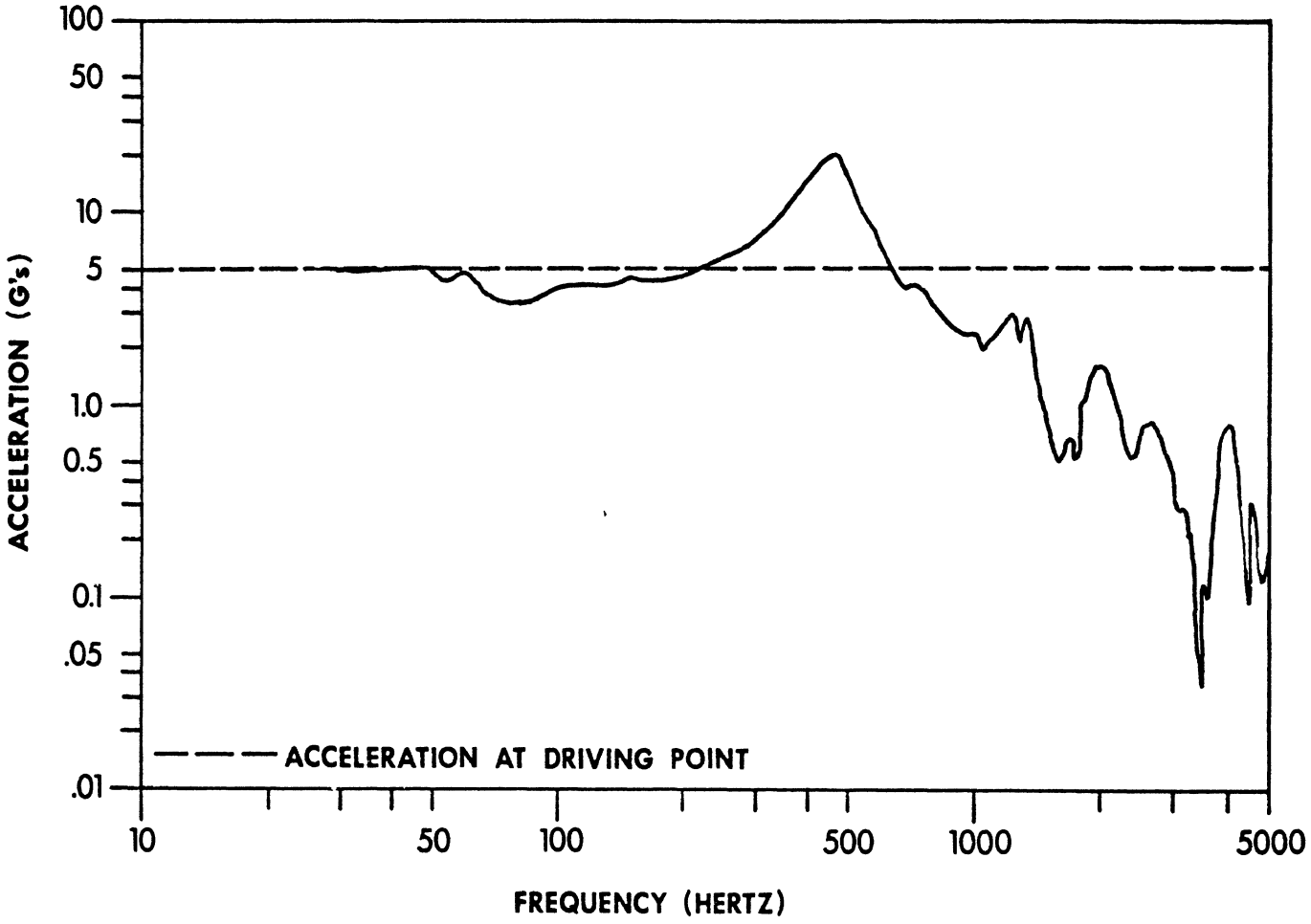

DRIVING POINT: FRONTAL ☐
OCCIPITAL ☐
PARIETAL ☒

TRANSFER POINT ACCELERATION:
CENTER OF GRAVITY ☒
POINT OPPOSITE D.P. ☐

Test DHMZ-4 Dummy Head Accelerations

Figure A-66

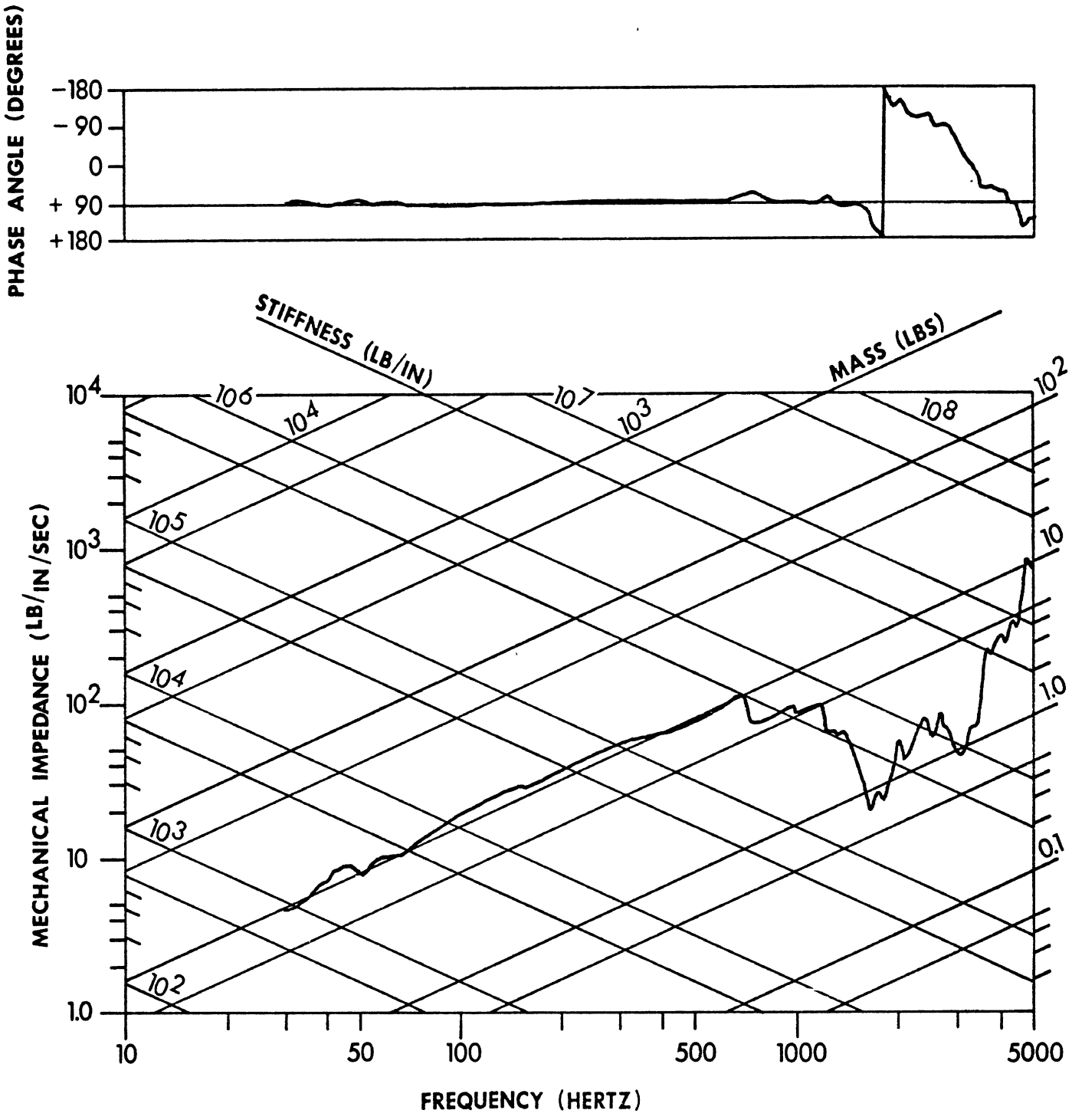

DRIVING POINT: FRONTAL ☐ D.P.I. ☐

OCCIPITAL ☐ T.P.I. (CENTER OF GRAVITY) ☐

PARIETAL ☒ T.P.I. (POINT OPPOSITE D.P.) ☒

Test DHMZ-4 Dummy Head Mechanical Impedance

Figure A-67

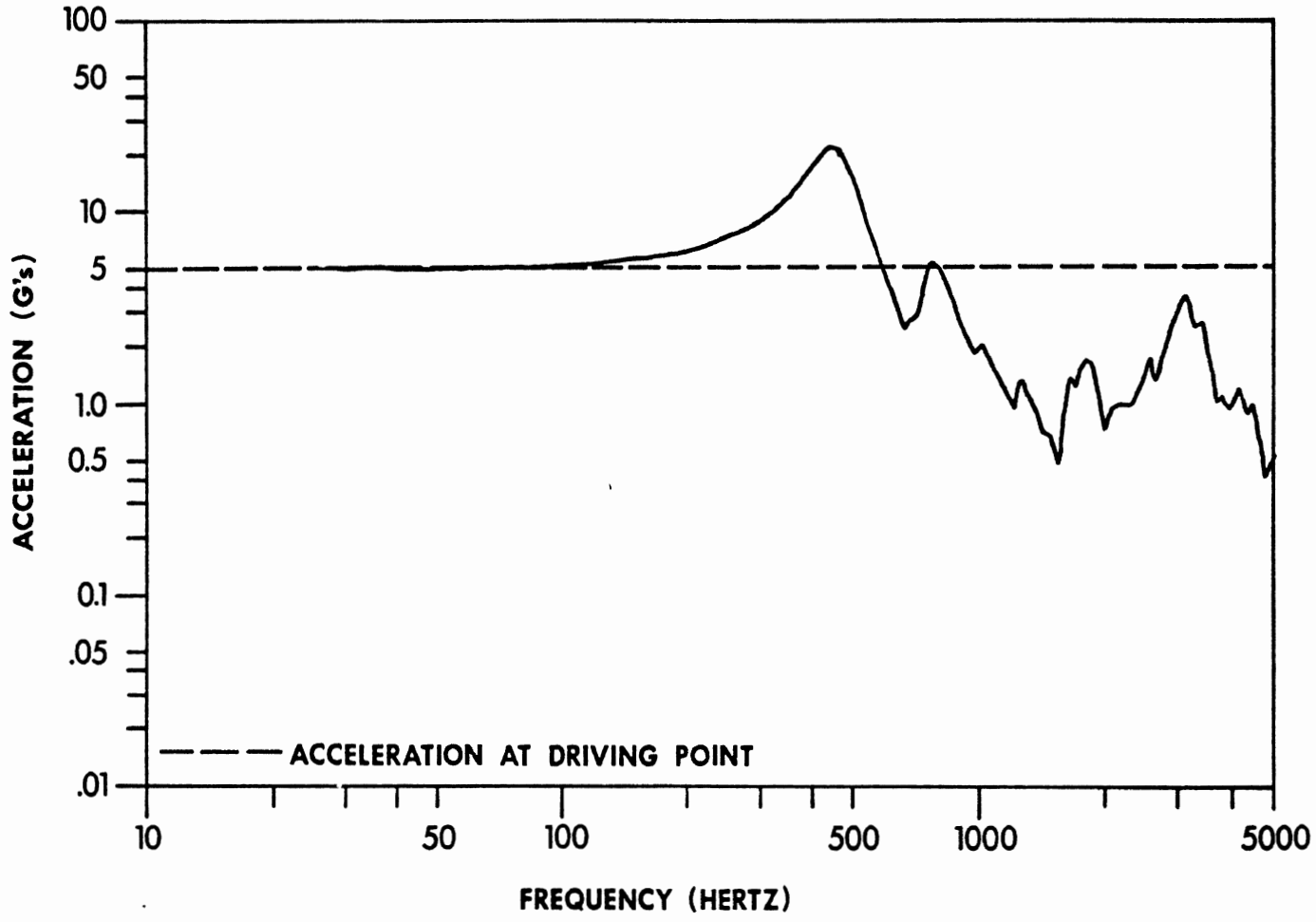

DRIVING POINT: FRONTAL ☐
OCCIPITAL ☐
PARIETAL ☒

TRANSFER POINT ACCELERATION:
CENTER OF GRAVITY ☐
POINT OPPOSITE D.P. ☒

Test DHMZ-4 Dummy Head Accelerations

Figure A-68

APPENDIX B

BIBLIOGRAPHY

Firestone, F. A., "Mobility Method of Computing the Vibration of Linear Mechanical and Acoustical Systems: Mobility-Electrical Analysis," J. Appl. Phys. 9:373-387, 1938.

Franke, E. F., "Response of the Human Skull to Mechanical Vibrations," J. Accoust. Soc. Am., 28, 1277, 1956.

Gurdjian, E. S., V. R. Hodgson and L. M. Thomas, "Studies on Mechanical Impedance of the Human Skull: Preliminary Report," J. Biomechanics, Vol. 3, pp. 239-247, 1970.

Hamme, R. N., "Vibration Damping," Chapter 14 in "Handbook of Noise Control," New York, McGraw-Hill, 1957.

Hixson, E. L. and A. F. Wittenborn, "The Measurement of Mechanical Impedance and its Applications," University of Texas, Defense Research Laboratory, Oct. 1957.

Hodgson, V. R., E. S. Gurdjian and L. M. Thomas, "The Determination of Response Characteristics of the Head with Emphasis on Mechanical Impedance Techniques," Proc. 11th Stapp Car Crash Conference, 1967.

Kemler, E. N. and C. R. Freberg, "Electrical Methods in Teaching and Application of Vibration Theory," J. Eng. Educ., 34:274-281, 1943.

Kennedy, Charles C. and C. D. P. Pancu, "Use of Vectors in Vibration Measurement and Analysis," J. Aeron. Sciences, 11/47.

Kriewall, T. E. and J. C. Johnson, "A Network Approach to Vibration Analysis," University of Michigan, Enginering Research Institute, Final Report, Aug. 1957.

Lewis, Robert C. and Donald L. Wrisley, "A System for the Excitation of Pure Natural Modes of Complex Structure," J. Aeron. Sciences, 11/50.

Manley, R. G., "The Mechanical Impedance of Damped Vibrating Systems," J. Roy. Aeronaut. Soc., 45:342-348, 1941.

McElhaney, J. H., R. L. Stalnaker, V. L. Roberts and R. G. Snyder, "Door Crashworthiness Criteria," Proc. 15th Stapp Car Crash Conference, Nov. 1971.

McElhaney, J. H., V. L. Roberts and R. L. Stalnaker, "The Biomechanical Aspects of Crash Helmet Design," Linear Acceleration (Impact Type) AGARD Conference, Preprint No. 88, 1971.

McGoldrick, R. T., "Method of Mechanical Impedance and the Electrical Analogy," David Taylor Model Basin, Report R-226, Sept. 1947.

Miles, J., "Applications and Limitations of Mechanical-Electrical Analogies, New and Old," J. Acoust. Soc. Am., 14:183-192, 1943.

Remmers, G. M. and R. O. Belsheim, "Effects of Technique on Reliability of Mechanical Impedance Measurement," Shock and Vibration Bulletin, 10/65.

Sharaf, H. M., "A Complex Impedance (Electrical) Recorder," Convention Record of IRE, Vol. 2, Part 6, Audio and Ultrasonics, 59-62, 1954.

Stalnaker, R. L., J. H. McElhaney, V. L. Roberts and R. G. Snyder, "Door Crashworthiness Criteria," Final Report, June 1971.

Stalnaker, R. L. and J. H. McElhaney, "Human Side Impact Tolerances Obtained from Subhuman Primate Scaling Relationships," Proc. 24th Annual Conference on Engineering in Medicine and Biology, 1971.

Stalnaker, R. L., J. H. McElhaney and V. R. Roberts, "A Mechanical Impedance Model for Head Injury Due to Linear Impacts," 1970 Proc. of Symposium on Biodynamic Models and Their Applications, Dayton, 26-28 October 1971.

Stalnaker, R. L., J. H. McElhaney and V. R. Roberts, "MSC Tolerance Curve for Human Head Impacts," ASME Paper No. 71-WA/BHF-10, 1971.

Stalnaker, R. L., J. L. Fogle and J. H. McElhaney, "Driving Point Impedance Characteristics of the Head," J. Biomechanics, Vol. 4, pp. 127-139, Pergamon Press, 1971.